UNIVERSITY OF NAPLES FEDERICO II

DEPARTMENT OF STRUCTURES FOR ENGINEERING AND ARCHITECTURE

PHD PROGRAMME IN

STRUCTURAL, GEOTECHNICAL AND SEISMIC ENGINEERING

XXX CYCLE

COORDINATOR PROF. ING. LUCIANO ROSATI

Donatella de Silva

PHD THESIS

EXPERIMENTAL INVESTIGATION AND NUMERICAL SIMULATIONS ON STEEL ELEMENTS PROTECTED WITH INTUMESCENT COATING

TUTOR

Prof. Ing. Emidio Nigro

CO-TUTOR

Dott. Ing. Antonio Bilotta

To my family…in Heaven and Earth,

with gratitude.

“Sapere aude!”
I.Kant

Abstract

Intumescent coatings (IC) have long been used as effective methods for long-term passive fire protection for buildings. However, much is still unknown about these coatings.

IC react under the influence of fire and swell to many times their original thickness, producing an insulating char that protects the substrate from the effects of the fire (damage or excessive deformation). Its role is also to provide a smooth, aesthetically pleasing finish, which is durable and easy to maintain.

In the current international framework for designing of structures in case of fire, the performance based approach is provided (Fire Safety Engineering, FSE). The performance based approach consists of detailed analysis of the fire, considering natural fire curves, which combine more sophisticated calculation (advanced methods) for structural models.

In order to perform rigorous and realistic analyses on structures protected with IC, thermal properties of IC should be known. Nevertheless, the thermal characterization of these systems is not available. Hence, experimental tests at high temperature should be performed.

The aim of this work is to provide a thermal characterization of reactive protective (IC), which can be used in advanced calculations. This aspect is important to predict the behaviour of IC , to optimize the experimental tests and to increase reliability. Moreover the thermal characterization of IC is useful to design an intervention of IC fire protection with performance-based approach and not only with prescriptive-based approach.

So, in order to investigate the different fire phenomena that can affect the IC performance and their behaviour under different fire conditions, two sets of experiments representing different types of heating exposure were conducted for different water based IC.

In the first set of experiments, in furnace, steel plates were exposed to ISO834 and Smouldering fire curves with different initial heating rates. The steel specimens were steel plates with three different section factors protected by 500 µm, 1000 µm, 1500 µm and 2000 µm of dry film thickness (d_{IC}) of IC.

In the second set of experiments, steel plate samples protected by 3 different IC and by two different d_{IC}s (1000 μm, 1500 μm) were tested in a cone calorimeter. The steel specimens were exposed to different heat fluxes: 50 and 30 kW/m^2.

Moreover, the IC performance was quantitatively assessed according to two different parameters: the thermal conductivity based on the Eurocode formula for insulated steel sections and the IC swelling (directly measured during the test using the digital image correlation technique).

The results underlined that many IC characteristics, such as the IC expansion and the equivalent thermal conductivity, are dependent on the section factor and on d_{IC}; these two parameters depend also on the type of heating (e.g. furnace and cone calorimeter). However, other aspects like the paint activation temperature or the temperature at which the minimum value of thermal conductivity is reached, are intrinsic characteristics and they seems to be independent of the fire conditions.

One of the main goals of this work was to find a thermal conductivity law of the IC, based on a series of experimental data, which can also be applied to cases of real structures, in order to model them.

In particular, starting from the typical development of the IC equivalent conductivity, calculated according the Eurocode formula, a standard segmented multivariate linear regression analysis was applied to the data gathered in the previous phase at significant temperatures, depending on the two factors that have been seen to have a greater influence on IC behavior: the section factor and initial thickness of IC.

In order to validate the calibrated regression laws of the equivalent IC conductivity, several real scale tests were also simulated. In particular, starting from experimental data (on the same IC tested in small scale), that are easily accessible by the current state-of-the-art testing procedures, several section of different type and protected with different IC thickness were modeled: hollow circular section, H shape sections and I shape section were considered. In all the cases the numerical/analytical results are in good agreement with the experimental temperatures.

Indeed modeling the whole structure in advanced calculation method (e.g. FEM), knowing IC thermal properties, allows one side to optimize the IC thickness to be applied for reaching a certain safety level overcoming the usual design approach based on tables; on the other hand, it is possible to take into account the indirect actions that may arise in the event of fire (e.g. redundancy actions due to thermal expansion), that cannot be taken into account applying simplified methods (e.g. analytical method for single members). In other words, we could have the opportunity to design a steel structure protected by intumescent coatings applying a modern fire design according to Fire Safety Engineering approach.

Acknowledgements

This dissertation represents the result of the last three years of work at the Department of Structure for Engineering and Architecture as PhD student.
I would like to thank many people for their support, without whose help this work would never have been possible.
First of all, I would like to thank my supervisor, professor Emidio Nigro, for his support and his precious advice, I am particularly grateful to him for his precious scientific support, for his constant inspiration, guidance, encouragement and valuable advice throughout the project…I also really appreciated that he was a precious friend for me as well.
I'd like to express my sincere thanks to the doctor Antonio Bilotta for his constant scientific contribution to this work and especially because he was always present in overcoming all the difficulties encountered during this three years.
Moreover, this research was made possible by Amonn Fire Italian company and by the Fire Safety Engineering Research and Technology Centre (FireSERT) for offering their laboratories; so, I'd like to thank Giovanni Nava, Mauro Banfi, Thomas Ollapally, Denise Fiorina and all the other people of the company.
A special thank goes to the professor Ali Nadjai, for his precious scientific support and because during my time in Belfast he always made me feel like at home.
I would also like to thank with the rest of the students I met in Ulster, laboratory assistants and technicians in the FireSERT for their assistance and useful advice during this research project.
I am grateful also to my friend and colleague Naveed Alam for his help and friendly company throughout the project, in particular in preparing and conducting the experiments in Belfast.
My heartfelt thanks to all my Italian colleagues Anna, Alberto, Andrea, Marco, Mariano, Romeo, Paolino…with all of them I shared a lot of moments during my PhD period and everyone contributed to this my success.

I’m going to write the rest of the thanks in Italian language...I want them to arrive directly to the heart of the readers, without any translation...

Ringrazio con tutto il cuore i miei genitori, perché passo dopo passo, sacrificio dopo sacrificio, sono sempre stati per me un esempio di forza e perseveranza…permettendomi di non arrendermi mai. Ringrazio anche mia sorella che ha rappresentato più volte la mia spalla forte, sopportandomi e supportandomi in ogni momento difficile di questo percorso.
Il ringraziamento più grande va sicuramente a mio marito, perché soprattutto in questi ultimi due anni tutte le “mie” soddisfazioni e tutte le “mie” privazioni sono diventate le “nostre”, amplificando la gioia condivisa dei miei successi, ma allo stesso tempo alleviando il peso delle rinunce e delle sconfitte.
Chiudo con un ringraziamento speciale…quello che arriverà, spero, più in alto di tutti…grazie miei “angeli custodi” perché non mi avete lasciato la mano neanche per un istante.

Table of Contents

List of figures

List of Tables

Chapter 1

INTRODUCTION

Fire is a phenomenon that can be useful but is also dangerous. Learning to control it, prevent it, and understand its behaviour is at the core of the fire protection engineering discipline. Desire to learn more about the role fire protection engineering plays in safeguarding people, homes, and buildings against the threat of fire.

The field of fire protection engineering, which utilizes principles from all the engineering disciplines, is largely about understanding fire behaviour, prevention, and safety.

Fire protection engineers seek to learn more about how humans react to and behave around the threat of fire and they play a vital role in the research and development of ways to protect people, property, and the environment from fire dangers. The history of fire protection engineering is based on a series of catastrophic conflagrations.

The first recorded example is the huge fire in 64 AD which devastated Rome (Fig. 1.1). Emperor Nero, in response to a catastrophic fire, ordered to rebuild the city implementing passive fire protection techniques, such as fireproof materials for external walls. After the collapse of the Roman Empire and the onset of the Middle Age, a new technical approach for fire protection emerged after the Great London Fire of 1666 (Figure 1.1). The English city adopted its first building regulations requiring fire-resisting wall separations and design fire-suppression equipment [1][2].


Figure 1.1 Two of the greatest destructive fires in history: on the left "The Fire of Rome"; on the right "The Great Fire of London", unknown artists.

During the Industrial Revolution, the introduction of huge factories and material storage practices resulted in a greater fire risks and a number of disastrous building fires occurred during this period. Once again, this pointed out the need for structural fire solutions and the necessity of new fire-fighting measurements, manual up to that time. In this period, the installation of manually operated perforated pipes at the ceiling represents the first fixed fire-suppression system in the history. Also, the number of conflagrations dropped as conventional timber structures were generally replaced by masonry [1][2].

During the 19th century, many organisations and insurance companies were established to reduce the loss of life and property from destructive fire. Fire protection engineering became a profession and principles of science and engineering were applied to develop research aimed to find new structural fire solution and fire-extinguishing systems. Anyway, many of the advances in fire protection were brought about as a reason to catastrophic fires with consequent loss of life and property [3].

During the 20th century, building and fire codes and standards became primary means of applying fire protection engineering for life safety and property protection. Lessons learned from catastrophic fires, especially in new tall steel-framed buildings, were applied to revise codes and standards and improve the fire regulations [4], generally based on the traditional prescriptive approach.

Subsequently, a number of new fire protection systems were developed for use by the engineers: new fire-suppression, smoke control and insulation systems

were created, also thanks to a new research approach, mainly based on real fire experiments and full-scale fire testing [5]. Finally, the computational power of modern computers has resulted in computational methods for determining the quantitative evaluation of fire protection and fire resistance. The performance-based design is currently used primarily for unique structures that cannot be adequately protected utilising the existing prescriptive building and fire codes, or to determine engineering alternatives to prescriptive code requirements [2]. Still the fear of uncontrolled fires and the desire to avoid their consequences have remained as a primary human reaction and as an important human objective: fires cause indirect and consequential losses arising from loss of production, of profits, of employment and of exports and thus destroy a significant percentage of the economic wealth of a country. Because the consequences of a fire are disastrous and the risk is always high, fire protection measures have to be adopted. Fire protection involves the study of behaviour, suppression and investigation of fire and related emergencies. It also includes research and development, production, testing and application of suitable fire protection systems [6]. The primary goal of fire protection is to limit the levels of casualties and injuries and of property losses in a fire event [7].

1.1 FIRE PROTECTION SYSTEMS

Fire protection engineering is usually divided in active and passive fire protection systems. This division is based on how the systems work in order to contrast the fire and guarantee a good level of safety.

Active fire protection systems involve automatic devices and human direct actions to control and extinguish the fire [8]. These systems are divided into two categories according to their purpose: fire control and fire suppression. Striking examples of such active systems are automatic sprinkler systems and fire ventilation systems.

On the other hand, passive fire protection systems are built as a part of the whole building. They do not require operation by people or automatic controls, but they can be considered as an on-site fire resistance measure to prolong the longevity of load-bearing structures during fire. Their primary reason is life

safety and this goal is mainly accomplished by maintaining structural integrity during the fire and limiting the spread of fire and its damaging effects [8]. Passive fire protection systems are usually divided into two types, non-reactive, of which the most common types are boards and sprays, and reactive, of which intumescent coatings are the most common example. In turn, intumescent coatings can be either divided into on-site or off-site applied paints.

1.1.1 PASSIVE FIRE PROTECTION MATERIALS

The consequences of a fire are usually disastrous and the risk is always high for this kind of dangerous events. The division between active and passive fire protection is also related to the influence that these systems have on the frequency and the consequences of a fire event. The probability of occurrence of a fire is already low and difficult to decrease further. So, to limit the consequences is fundamental. Passive fire protection systems have a key role on the limitation of human and material losses. For example, structural fire protection materials are applied to avoid catastrophic consequences, such as the building collapse during a conflagration.

The application of insulation materials is one of the most common measures to protect the structure from direct fire exposure. Traditionally the most adopted way of achieving a good level of structural fire safety is to cover or wrap the steel elements with conventional fire protection products. The most common passive fire insulation materials (boards, sprays, flexible blankets and concrete encasement) are shown in Figure 1.2.

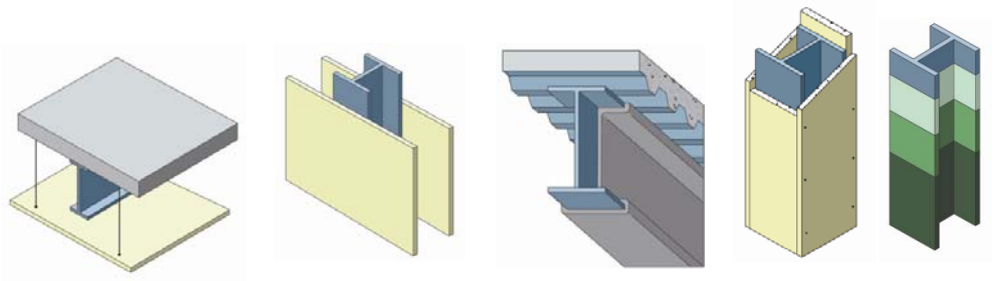

Figure 1.2 Common passive fire protection materials [9].

Board systems are one of the most popular type of fire protection. They are usually based on ex-foliated vermiculite, which is a hydrous silicate material characterised by non-combustibility and low conductivity. They are widely used both where the protection system is in full view and where it is hidden. They offer the specifier a clean, boxed appearance and have the additional advantage that application is a dry trade and may not have a significant impact on other activities. Also, boards are factory manufactured and their thicknesses can be guaranteed. Furthermore, boards can be applied on unpainted steelwork. On the other hand, a board system could be relatively expensive because of its difficulty of fitting around complex details and its long application procedure. Moreover, they have durability problems in a corrosive environment and they are subjected to loss of integrity in long-term service and applying them the skeleton structure is hidden.

Spray applied fireproofing materials, such as cementitious formulations or mineral fibre products, are extensively used in the United States. Despite being one of the cheapest forms of fire protection in terms of application costs and applicability to complex shapes and details, they have decreased in popularity in the last decades. Mainly it is because they are not suitable for aesthetic purposes and their application is a wet trade: drying time needs to be accounted for in the construction program and this may have impacts on other site operations. Furthermore, some of the earliest spray protections contained asbestos, which is no longer allowed due to health issues.

Another solution for the passive fire protection of steelworks is the application of flexible blanket systems: the steel structure is wrapped with low conductivity material, usually made by mineral wool. They have been developed as a response to the need for a cheap and easily applied fire protection material which can be applied with a dry trade on complex shapes and details.

Until the late 1970s, concrete was by far the most common form of fire protection for structural steelwork. However, the introduction of lightweight, conventional systems such as boards and sprays have seen a dramatic reduction in their use. Nevertheless, concrete encasement still has its place and it continues to have a small percentage of the fire protection market with other traditional methods. The principal advantage of concrete is an excellent

durability in corrosive conditions: it performs well where resistance to impacts, abrasion, weather exposure and corrosive agents is significant. On the other hand, concrete is heavy and expensive compared to the lightweight systems and it often requires large space utilisation and time-consuming application procedure [10].

1.2 INTUMESCENT COATING

The previously described conventional methods for fire protection engineering can be easily installed in many different situations, but they are usually deemed to be aesthetically unpleasant and, therefore, they do not represent the best desirable choice for slender and light buildings with visible steelwork.

For this reason, the trend in structural fire protection for steel over the past two decades has been the rise in popularity of thin intumescent coatings. This option definitely seems a preferable alternative for fire protection of visible steel structures.

The past decade has seen a huge swing towards the use of thin film intumescent coatings in new buildings (news on the line magazine of Paint and Coating – PCI). Once a niche product, these accounted for more than 70% of the market in 2010, according to the Construction Markets survey carried out each year on behalf of the steel construction sector (see Figure 1.3). This was followed by board (25%) with a relatively small percentage of spray and other niche products. According to new research by Global Market Insights Inc., the market for intumescent coatings is forecast to be worth $1.16 billion by 2022. Increasing applications in the energy sector coupled with stringent government regulations pertaining to health and safety standardization are likely to drive demand over the forecast period. Features such as fireproofing and heat resistance are anticipated to be among key factors to drive intumescent coatings market growth. The strong landscape for shale gas production is also likely to positively impact the industry. The cellulosic intumescent coatings market size was over $400 million in 2014, with revenue expectation of over $570 million by 2022. Growth in the construction sector and increasing demand for thin-film

coatings in marine and automobile applications are expected to boost growth. Hydrocarbon coatings market size is likely to grow faster than the global average to exceed $580 million by 2022.

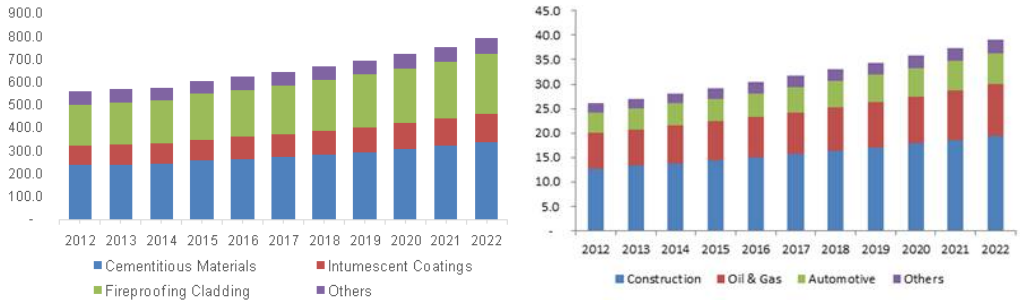

Figure 1.3 Europe intumescent coatings market size by end-use, 2012 - 2022 (Kilo tons) [11].

Most intumescent coatings are applied on site, although off-site application has increased in popularity in recent years and now accounts for about a third of total use. Intumescent coatings are paint-like materials that expand when heated to form a char with excellent insulating properties. They can be water based, which is mostly used on site, or solvent based, which dominates the off-site market. If applied on site, these coatings can be used to create decorative finishes - although this may cost more. Aesthetic finishes are also possible when applying a coating off site, however this is more problematic because of the difficulty of repairing any damage on site to the same standard. Off-site application of intumescent coatings can be more expensive in terms of up-front costs than on-site alternatives, but can have benefits where site access is difficult or restricted and may save costs in the long run. It has also other advantages like quicker construction, improved quality control, reduction in site disruption, cleaner sites, improved site safety, easier servicing installation.

Intumescent coatings are paint-like substances which are inert at low temperatures. Under thermal exposure, the coating swells up when it reaches a temperature threshold (about 250°C). The swelling reactive layer keeps growing until the underlying ablative paint is totally consumed, but it stops if heating is interrupted. Finally, if the aggression process is maintained, a solidified char

layer appears on top of the system. The final structure is a porous stratified layer with high insulating properties [15]. The first commercial patent for a foaming fire retardant system was issued to H.Tramm in 1938 [16]. A variety of coating formulations, in the forms of paints and mastics, have been developed and put into commercial use starting in the 1950s. However, the implementation of intumescent products in the building industry remained very limited until the mid-1980s [15]. Over the past decades intumescent coatings have been considerably improved and now they dominate the fire protection market. Their great success is due to the possibility to easily cover complex details with an attractive and decorative finishes: thin coating allows to express the shape of underlying steel (Figure 1.4).

Figure 1.4 King's Cross Station, London, UK- Application of IC [18].

Apart from the attractive architectural appearance, intumescent coatings are thin and lightweight and they do not change the intrinsic properties of the protected material.

On the other hand, intumescent coating application costs are usually higher than sprays, although costs have decreased in recent years. Furthermore, their application is a wet trade which requires suitable atmospheric conditions during application and precautions against over-spray. Another drawback of adopting

this fire protection system is the limited fire resistance period: most intumescent coatings can traditionally
provide up to 60 minutes fire resistance in an economic way. Improvements in the technology of application and production in recent years have reduced coating thicknesses considerably and intumescent paints are competitive in the 90 minutes market as well. Nevertheless, nowadays an increasing number of intumescent coatings can achieve 120 minutes fire resistance. This aspect has revolutionized fire protection engineering because intumescent coatings are now designed for structures with 120 minutes fire resistance requirements, such as high-rise buildings.

Intumescent coatings can be divided into two broad families: thin film and thick film. Thin film intumescent coatings are either solvent-based or water-based and are mainly used for cellulosic fire conditions. Thick film intumescent coatings were originally developed for the off-shore and hydrocarbon industries, but have been modified for use in buildings.

Today, intumescent coatings are not used only as fire protection in the building industry, but they are applied and adopted for several purposes. First of all, their versatility makes them useful and efficient on many kinds of substrates, not exclusively metals. Intumescent paints can be used on polymers, on textiles or even on wood [15]. Furthermore, intumescent coatings could be used in place of fire insulation and provide equal protection to shipboard structures (interior wall and doors) during a fire [21]. Moreover, intumescent paints can be adopted for military applications. Military structures, devices and vehicles are likely to be exposed to extreme heat on battlefields and this kind of coatings can provide protection to elevated temperatures for a wide range of devices, such as munitions and vehicles [21]. Intumescent coatings can be applied also as passive fire protection system to protect off-shore and on-shore facilities against the effects of fire, for example in oil and gas industries [22]. Another possible application is in the protection of fuel tanks against heat exposure, which can cause to rupture (cracks) and potentially explode [15].

Indeed, intumescent paints can be divided into three categories [23]:

- Single part solvent-based

- Single part water-based
- Two-part epoxy solvent free or solvent-based

The solvent-based can be used for exterior and interior application and are tested against weather and temperature variations. The water-based intumescent have less odor, but they are less tolerant of humidity and low temperatures. The two-part epoxy systems are used in the chemical industry and offshore operations. They are used in areas that may be difficult to access for maintenance or where high levels of impact damage may occur. [8]

1.2.1 DESCRIPTION OF INTUMESCENCE PROCESS

The intumescent coatings are thermally reactive fire protection materials. According to Vandersall, an intumescent system consists of four main chemical components: an acid source, a carbon source, a nitrogenous source, and a blowing agent [24]. Also, some pigments are present in the intumescent coatings: not only for its decorative properties, but they provide better weather proofing ability and improved mechanical stability [26]. All these ingredients are bound together in a polymer matrix [27][28].

Commonly used inorganic acid sources are ammonium salts, amine/amide phosphate and organophosphorus compounds. Compounds such urea, melanine and dicyandiamide of urea-formaldehyde resins are often introduced into the intumescent formulations to act as blowing agent. Ammonium polyphosphate (APP) and pentaerythritol (PER) are the most typical carbon-rich polyhydric compounds, the main cause of formation of black carbonaceous compact foam [30]. Finally, titanium dioxide and silica are the most commonly used inorganic pigment fillers in the intumescent coatings.

When the paint is exposed to flames or to a thermal radiation and it reaches a critical temperature, usually around 250°C, the inorganic acid source undergoes a thermal decomposition, yielding acid. Then the blowing agent is activated at a temperature of 300°C-350°C, causing an endothermic reaction which absorbs heat from the substrate and decomposes to release a large amount of gaseous products. Thus, gas production is triggered by this reaction: the gas bubbles are trapped in the coating to cause the molten carbon matrix to

swell, forming an expanding multi-cellular system. The expansion continues until the blowing agent is finished or the carbon matrix is not viscous enough; moreover, as the temperature increases, the mixture is solidified.

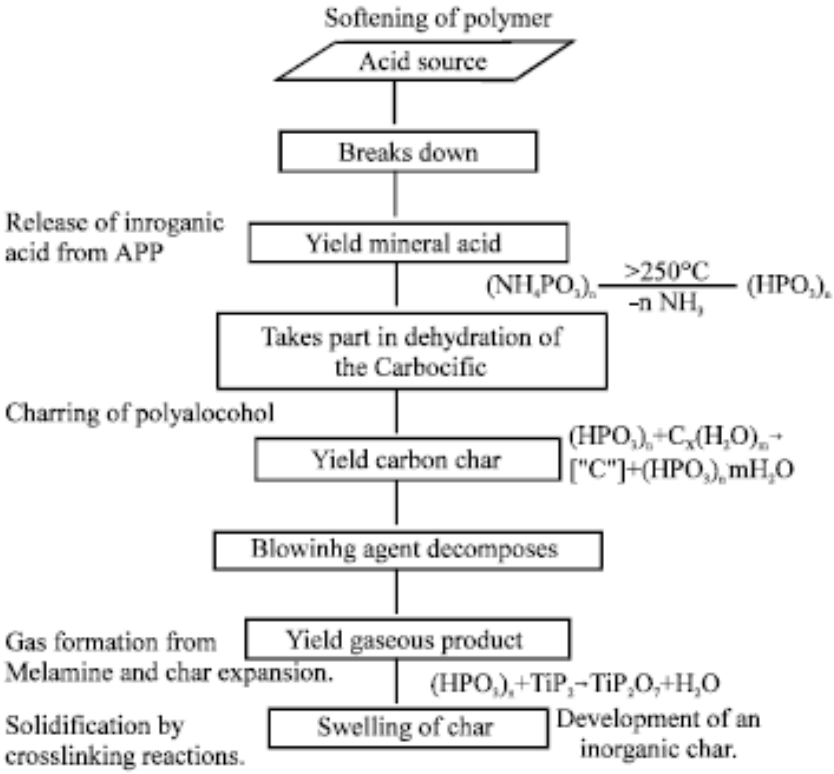

Figure 1.5 Intumescent coating mechanisms in a fire[29].

Finally, the carbon char further oxidizes leaving a residual protective multi-cellular insulation char structure, characterized by a high porosity and negligible self-weight. It appears as a soft white foam and it behaves as a low-conductivity thermal barrier, which decreases the speed of temperature penetration inside the substrate [31][32][33][34]. In this way, the intumescent process causes the coating to bubble, foam and swell up to 100 times its original thickness to produce a porous charred thermal barrier against heat transmission and oxygen diffusion [35].

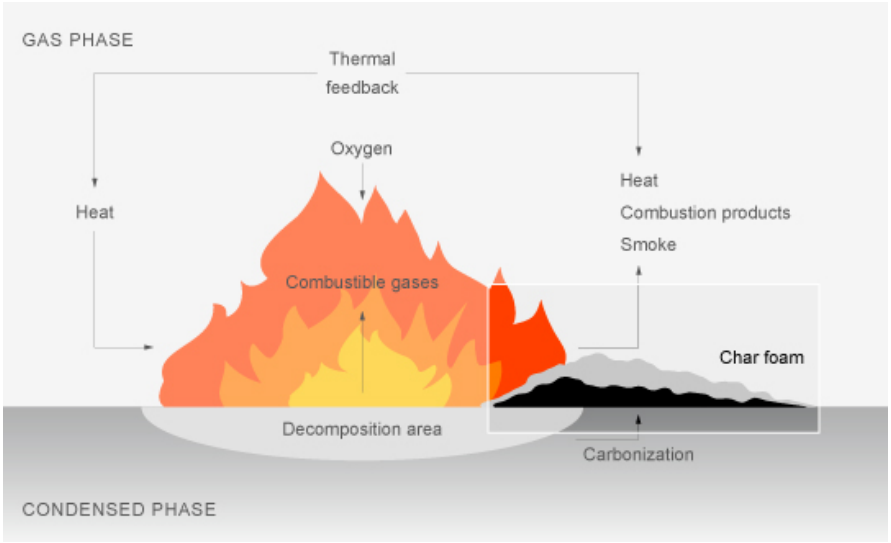

Figure 1.6 Intumescence process [35].

As shown in Figure 1.6, four reaction steps can describe the intumescent process when the coating is exposed to flames or to a thermal radiation:

1. In the early stage of heating, an endothermic process starts and a large amount of thermal energy is absorbed by the intumescent coating, whose temperature increases quickly;
2. At a critical temperature, the polymer matrix melts and degrades to form a viscous liquid: the inorganic acid source in the coating undergoes normally thermal decomposition at temperatures between 100°C and 250°C;
3. At temperatures between 280°C and 350°C, the blowing agent with the coating decomposes to release a large amount of gas, a fraction of which is trapped within the molten matrix;
4. the molten fluid hardens and releases residual volatile to form a char structure.

These four reaction steps could happen in sequence or together and with different time intervals: this fact mainly depends on the composition of the chemical and their mixture. In an intumescent paint, it is fundamental that the different chemical sources in the mixture show a suitable matching thermal

behavior. Moreover, the order and timing of the chemical and physical processes are critical, as they must happen in an appropriate sequence. For instance, if gasification takes place when the molten polymer is too viscous, bubble growth will be strongly opposed and the gas will tend to diffuse through the mixture without generating bubbles: if that happens when the polymer melt is too fluid, the bubbles will be too large, resulting in a fragile and ineffective char [33].

This reactions have a consequential change also of the IC thermal properties.

1.3 STATE OF THE ART

Recently, many researchers have been involved in the study of intumescent coatings behavior and also the national and international standards about intumescent coating are constantly evolving

1.3.1 RELEVANT STUDIES

Some researchers were interested in the chemical composition and they tried to define the best mixture for an efficient intumescent coating. Vandersall [41] firstly reviewed intumescent chemistry in 1971 and he described the general categories of its chemical components. In the 1980s, Camino et al. [25][42][43] worked on a detailed mechanism of intumescence and published a series of papers to give a general overview of the chemical aspects and of the main intumescent coating components. More recently, Le Bras [44][45] and Bourbigot [46][47] have carried out more investigations regarding the intumescence chemistry and physics. Their studies were focused on how intumescent coatings behave with different chemical components and how these components influence the different aspects of the intumescent behaviour, considering also additives inside the compositions.

Beyond the chemical composition, many numerical and mathematical models of various complexities have been developed in order to study the intumescent process and the heat transfer behavior of intumescent systems. An innovative model was developed by Cagliostro et al. [48]: the model took into

account the fundamental chemical reaction kinetics, mass and heat transfer profiles in order to evaluate the temperature of the substrate material.

The model estimates the insulating efficiency by considering the effective thermal conductivity, evaluated as the ratio between the thermal conductivity and the expansion factor of the intumescent layer. Anderson et al. [49] developed a procedure to estimate the effective thermal conductivity of the intumescent char and, in particular, he focused on the effect of material expansion on the thermal response of an intumescent coating.

Also Di Biasi et al.[53] studied a 1-D transient mathematical model for a composite system consisting of a substrate (steel) and an intumescent coating exposed to radiative heating. By applying a simple heat conduction equation for the first material, a general model proposes the coating consisting of three components, which degrade according to independent finite-rate reactions. Mass and heat transfer take place across a variable volume medium, including a simplified mechanism for bubble dynamics and material swelling.

Many others models have been developed, but most of them were based on simplified one-dimensional heat transfer through the intumescent layer and on semi-empirical formulas.

On the contrary, Butler et all. [15][50] have developed several models at a very complex level, including 1-dimensional and 3-dimensional heat transfers in order to study intumescence in great detail.

In the literature, many research studies based on these intumescent models can be found. Various approaches and methodologies have been proposed to analyses the performance of intumescent coatings exposed to different fire conditions. Anderson et al. [49] adopted his own model to evaluate the effective thermal conductivity of the intumescent layer. The procedure was based on a heat transfer analysis of temperature-time data from one-dimensionally designed experiments of coated steel coupons exposed to aviation-type fuel fires exposures. Jimenez et al. [23] studied the performance of an intumescent coating subjected to a hydrocarbon fire. Both aviation-type fuel fires and hydrocarbon fires are more severe than standard fires in that they will reach very high temperatures with rather rapid growth. Li et al. [27] proposed a simple approach to assess the equivalent thermal resistance of intumescent

coatings subjected to the ISO 834 cellulosic fire [32]. Bartholmai et al. [51] investigated the influence of external heat flux and coating thickness on the thermal insulating properties of intumescent coatings. In a mass loss cone heater set-up, the intumescent paint was exposed to several radiant heat fluxes, providing temperature-time curves similar to the standard fire one [32].

Dai et al. [52] carried out some experiments on steel joints partially protected by intumescent coatings and subjected to standard fires. The efficiency of the fire protection was evaluated through the effecting thermal conductivity by inverting formula 4.2.5.2 reported in the Eurocode [11] for calculating the temperature of insulated steel members.

Wang et al. [28] performed some furnace tests on steel plates protected by intumescent coatings and exposed to three non-standard fire curves in a furnace. The effective thermal conductivities were evaluated based on the measured steel and furnace temperatures by using the Eurocode inverted equation [11]. Andersen in [26] identified four different phases in the variation of the thermal resistance of intumescent coatings exposed to non-standard fire curves and highlighted how the duration of the phases and the corresponding values of the thermal resistance also depend on the heating rate and on the type of steel profile.

Shaumann et al.[55] studies the thermal performance of a solvent-borne intumescent coating in case of natural fires. The intumescent coating is originally designed to protect steel members in case of ISO-standard fire. In the first part of the study the thermal performance of the coating is evaluated for various heating rates using thermogravimetric analyses. It is demonstrated that the mass loss of the coating shows a clear dependency on the heating rate during the reaction step of intumescence. In the second part of the study the thermal insulation efficiency of the coating is investigated using small scale furnace tests with an innovative test setup.

However, even if the progress made in these studies, the intumescent process is still not completely understood. More research is needed in order to properly describe the thermal properties and the performance of intumescent coatings subjected to different fire scenarios. A strong support for this research must necessarily be given by experimental evidence, starting from lab-scale test

1.3.2 CURRENT DESIGN PRACTICE FOR INTUMESCENT COATINGS AND CURRENT REGULATIONS

In the current design practice, intumescent coatings manufactures usually provide design tables to structural engineers. These tables report the minimum required dry film thickness (DFT) of intumescent coating needed to ensure that the temperature of a structural steel member is kept under a specified design temperature in a specified amount of time during which the structural bearing capacity must be ensured.

To design a proper fire protection, structural fire engineers choose the best intumescent coating thickness from the provided design tables, based on many input parameters: critical temperature, section factor, profile type (open or closed sections) and element type (mainly beams or columns).

However, this method of designing a proper passive fire protection is problematic for several reasons.

Firstly these design thicknesses are typically determined on the basis of standard fire conditions, in particular on results achieved by a cellulosic standard fire exposure [36][37], in a prescriptive designing approach.

Then standard fire results are extended to all the other fire scenarios without deeply investigating the behavior of the intumescent coatings under different fire conditions.

This fact leads to the assumption that the thermal properties of the intumescent coatings are independent of the fire condition. On the contrary, intumescent coatings are reactive materials and their thermal properties are dependent not only on temperature, but also on the heating condition and the type of fire exposure. Therefore, the thermal properties of intumescent coatings, particularly thermal resistance and thermal conductivity, obtained by standard fire tests are not consistent and reliable under different sets of fire conditions [33]. The thermal properties of other conventional fire protection materials are mainly temperature dependent and they can be described by simple empirical property-temperature relationships. On the contrary, the performance of intumescent paints is complex and the coatings behave differently according to

the applied heating condition, coating thickness and protected member [36][37][47].

Moreover, the design tables provided by the intumescent coating producer companies only clearly state the fire resistance class and the design temperature: mainly they define the time necessary for a structural element subjected to standard fire exposure to reach a certain fixed temperature.

This leaves out completely the temperature evolution in the structural element during the fire exposure. As a consequence, the only possible methods which can be adopted for the structural fire design according to Eurocode [12] are simplified procedures, such as the method of critical temperatures.

In this method, the structural fire design is performed member by member, ignoring the overall behavior of the structure structural system. Thus, the design of structural fire protection does not investigate the overall stability of the structure during the fire and this could be a dangerous simplification [48].

Finally, many different types of intumescent coatings are produced worldwide: there are many mixtures of components and additives which provide really different performances in the different fire scenarios.

Therefore, in recent years researchers have been mainly concerned with developing new intumescent coatings products. However, there is a severe shortcoming in these research studies based on the expected performance and the testing procedures.

Intumescent coatings, in order to be marketed, must be tested according to standard fire exposures and standard fire resistance tests and consequently industry aims at developing new intumescent coating products to pass these types of tests, in which the fire exposure is fixed [63][64][65][68].

As already stated, the fire protection performance of intumescent coatings is unfortunately highly dependent on the heating condition and hence the type of fire exposure. Therefore, since the frontier of structural fire engineering is pushed to include fire conditions different from the standard ones, it is crucial to characterize the fire performance of intumescent coatings in different fire exposures and structural design [10].

In addition to the dependence of thermal response (reaction of the paint) under different fires, among the main problems for intumescent coatings there

are the adhesion to the steel profile during fire exposure. In particular, the dissolution of the coating, resulting in a reduction of performance, can occur for heating curves with thermal gradients lower than Standard fire curve ISO 834 close to the coating initiation temperature. For this reason, in [63] a slow heating curve (smouldering curve) is also defined.

Hence, the prescriptive approach provides a set of simplified rules and requirements to be fulfilled if you want to guarantee a fixed capacity with immediacy and simplicity of calculation (tabular methods, analytical and experimental).

On the other hand, in the last decades, codes of practice for Fire Safety in the design, management and use of buildings based on performance-based approach (also known as Fire Safety Engineering) are alternative to the prescriptive regulations.

The performance approach is based on the definition of possible fire scenarios in the construction, on more detailed analysis of the fire phenomenon, with adoption of fire models that lead to "natural fire curves", and on more accurate calculation procedures (advanced methods) for thermo-structural modelling. They seek to allow the development of solutions based on an understanding of the causes of risk to life and how these can be mitigated.

Therefore, in the current regulatory framework the prescriptive and the performance-based approach are provided.

Prescriptive methods generally corresponds to a lower depth level compared with the performance methods. Thus, the design choices that are obtained with the application of the prescriptive methods are generally more protective and expensive than those that could be done by means of a performance approach, simulating the real evolution of the fire through natural fire curves. However, the accuracy level reached by the performance-based approach overall involves a rise in safety level against fire, due to the greater reliability than prescriptive. For this reason, for particularly complex construction or public buildings, new codes expressly recommend using the performance-based approach, which allows taking into account the fire resistance of the structure, the propagation of hot gases and the movement of people during the evacuation, in order to achieve an appropriate level of fire-protection.

The ongoing regulatory updates, in all European countries, give evidence to the high social impact of the issue of safety in fire conditions of the newly developed facilities, both industrial and commercial destination and for civilian use. On the other hand, a strong socio-economic interest also characterized the safety of existing structures. In fact, the presence of more and more critical activities from the fire protection point of view and the considerable urbanization that characterizes the modern urban centers led to an increased awareness of the importance to intervene on the built enviroment. Although it is not always possible to apply expeditiously national fire regulations to existing buildings, it is clear that the performance approach is particularly suitable for the evaluation of fire safety of steel structures, possibly equipped with passive or active protection systems. Obviously, the more complex the structure, the more useful in depth fire risk analysis can be.

Also the durability and reliability of the coatings is, however, important as the products are expected to have a long lifetime and perform in case of fire so that lives are saved. Intumescent coatings are sometimes used without a topcoat or damage may occur to the topcoat over the lifetime of the coating system so it is important that the durability of the intumescent coating is taken into account.

Intumescent coatings that are not as durable as other intumescent coatings may require more frequent maintenance and have a shorter lifetime. Damages to the coating may also influence the fire performance of the coating.

Several tests on samples with accelerated exposure to UV and extreme temperature changes must be conducted in accordance with the tests described in ETAG18-2[68] for X-conditions (Intumescent coating systems for outdoor use). Tests must be conducted on panels with non-topcoated intumescent with standard compatible primer as a preceding coat. X-condition tests, according to ETAG18-2 are designed to simulate resistance to outdoor exposure for intumescent coating systems (including topcoat).

1.3.3 THERMAL EQUIVALENT CONDUCTIVITY OF THE INTUMESCENT COATINGS

Apart from the externally visible properties, the main results are series of temperatures, evaluated by using thermocouples placed at particular locations. Using this data, it is possible to analyze the IC characteristics, using the method described in paragraph 2.1.2.

In a more detailed research focused on setting up precise numerical models of the intumescent process, the temperature of the intumescent paint and char structure is of higher significance. However, since this research mainly focuses on the efficiency of the IC under different fire conditions and from the structural point of view, measurements of the steel temperature were made, inasmuch the temperature of the steelwork beneath the intumescent coating is of main practical significance. When necessary, the IC temperature was considered to be simplified, as an average of the steel temperature and the gas temperature.

The temperature measurements were used to calculate the corresponding thermal equivalent conductivity of the IC, according to [12], point by point.

By collecting all the punctual values of thermal conductivity throughout the time, a common trend was observed for all the samples: the general shape is shown in Figure 1.7a. A corresponding trend was also observed in the development of increase in thickness of the IC (Figure 1.7b).

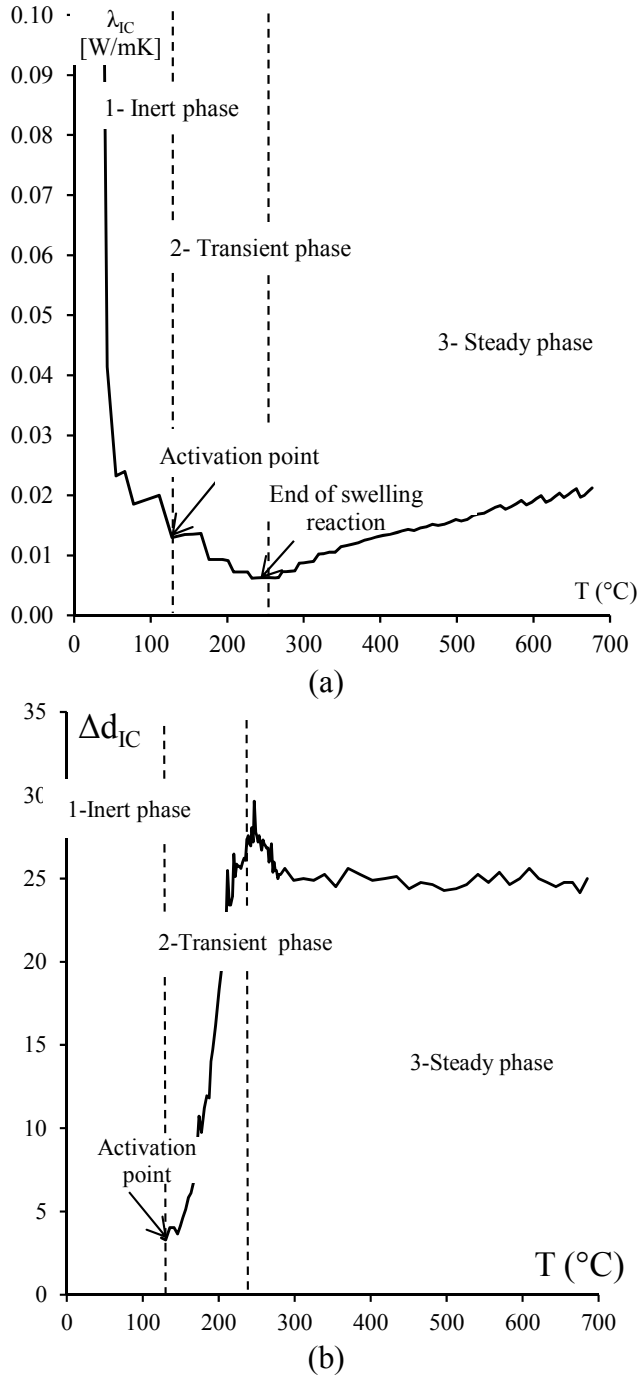

Figure 1.7 Common trend of the thermal equivalent conductivity(a) and of IC swelling (b) of IC and definition of the four general phases in their development.

Andersen [31], proposed the development of the thermal resistance throughout the time can be divided into four general phases. However, the previous term "decay phase" suggested by Andersen [26] was changed in "post-austenitization phase" since the intumescent coating behavior at really high temperatures is still not completely known[14]. Further experiments should be performed in order to understand better this characteristic. Thus the four phases of the development of the thermal resistance throughout the time are inert phase, transient phase, steady phase and “post austenitization phase”. The same phases were identified in this work for the equivalent thermal conductivity.

Inert phase

Before the IC reaches its reaction temperature, the dry coating is inert to the temperature and its thickness is kept to the initial value. During the inert phase the IC is slowly melting and increasing its viscosity considerably. The thermal resistance provided to the steel is minimal and the measured protected temperature is similar to the unprotected one. However it produces a little insulation to the steel. Unlike the unprotected case, the paint provides to the steel a thin layer of material characterised by a thermal capacity and thermal resistance, even if they are really small. Moreover, the intumescent paint changes the colour of the steel profile specimen (because generally the IC color is white) and consequently it changes completely its radiative characteristics, e.g. emissivity.

Transient phase

The transient phase is mainly composed by two branches: a growing branch and a declining branch, which can be separated at the "end of reaction" critical point. The first branch begins when the intumescent paint reaches its activation temperature: the blowing agent present in the coating is activated and an endothermic gas-producing reaction starts. At this point the melted layer of intumescent coating is viscous enough to be penetrated by the gas bubbles produced during the reaction.

The IC starts swelling and rapidly increases its volume. When all the virgin material is consumed and the blowing agent is exhausted, the paint looks like an expanded black multicellular char structure. This point corresponds to the minimum value of thermal IC conductivity within the transient phase and the

intumescent char is considered as fully developed. In addition, at this point the char structure is characterized by a black color due to the high concentration of carbon binder.

Afterwards, the gradual increase of the thermal IC conductivity is related to the gradual consumption of the carbon binder, which is the main component constituting the char structure. During this phase also the char color changes, starting from black/grey and becoming white. Furthermore, the consistency of the char structure changes during this stage: from a cohesive and compact material towards a brittle and lightweight material. This aspect confirms the fact that the main responsible for the cohesion and the dark color is the carbon binder, which is combusted during the declining branch of the transient phase.

Steady phase

When the endothermic reaction is exhausted because all the combustibles have been burned, the IC enters into the so-called steady phase. At this stage the only contribution to the thermal conductivity is provided by the white expanded char structure. During this phase the thermal IC conductivity is kept to a constant value or sometimes it slightly increses.

Post-austenitization phase

After the austenitization point the char structure looks like an extremely brittle and inconsistent material, characterised by a light white colour. At this stage the carbon binder is completely combusted and with that the char structure is degraded and, in particular, it has lost its cohesion. During the post-austenitization phase and at high temperatures, the cracks begins to occur in the char structure. The thermal IC conductivity starts increasing from the steady value and an increment in the steel temperature is recorded. The cracks act as thermal bridges and the char structure does not provide a good insulation to the steel anymore.

1.3.4 FIRE PERFORMANCE-BASED APPROACH WITH INTUMESCENT COATING

As stated above, the performance-based approach is more accurate and it allows optimizing the design of protection systems in order to reduce costs, to improve the performances and to increase the safety [50]. To properly apply the

performance-based approach to steel structures protected with intumescent coatings (IC), characterizing the thermal properties of the protective is necessary but not sufficient [45][40][44][58]. Indeed, the flows around this type of products can change their behavior until to complete ineffectiveness. Therefore, for approaching to a performance-based design of steel structures with regard to fire hazard, elaborating an engineering robust tool is of paramount importance. Indeed, to apply a performance-based method, the knowledge of thermal transient during fire is required, but the product data normally provided by the manufacturers are not enough to achieve this scope. Hence, the design tables provided by the producers for the IC dry film thickness, required according to a prescriptive approach, do not allow to design steel structures according to analytical approaches. Moreover, the large number of cases to be covered in a performance-based approach would result in a large number of tests to certify products, and therefore in very high and unacceptable costs for manufacturers. For this reason, the performance-based methods are not used for IC protected steel structures, even if they are now well established and already being applied worldwide to practical engineering problems.

1.4 PROJECT GOALS AND THESIS ITEMS

The safety of buildings against fire can be considered a strategic target at European and worldwide level. The steel structures are vulnerable to high temperatures but the huge amount of studies conducted on the performance of steel in fire have allowed finding numerous and effective solutions to ensure its resistance even under extreme conditions.

Intumescent paints represent the protective solution less invasive, overall for existing structures, and the market interest in the product has grown a lot in recent years. Indeed, the amount of marketed products is huge. In general, these products are certified according to standard procedures and within the so-called prescriptive approach. Such procedures generally consider as thermal input (fire curves) nominal curves, which often are very different from the real fire curves (natural curves). Although the use of nominal curves in the prescriptive approach is often on the safe side compared to the natural ones to be used in a

performance-based approach, in the case of intumescent paints the swelling process can be particularly influenced by the heating input. Therefore, the performance of the paint may become dependent on the temperature evolution.

Furthermore, several studies have highlighted how the behavior of the intumescent coatings does not depend only on temperature evolution, but is also affected by other properties of the fire, such as flame exposure, heat flux and fire growth rate. In particular, it has been demonstrated that the current procedure of assessing intumescent coating thermal properties under standard fire condition could not be applied to other fire conditions due to the fire-dependent nature of organic materials such as intumescent coatings.

This input-dependant behaviour of IC represents a limitation of the current procedures of product certifications, but also a very strong limitation for the application of the performance-based approaches (Fire Safety Engineering-FSE) for assessing the performance of structural elements in fire. The negative effects are for:

- Lawmakers, which are not yet able to provide uniformity in the safety levels of structures protected with different systems,
- and Steel Producers, which are strongly limited in the promotion of structures protected with intumescent paint, where it is considered appropriate or necessary to take the FSE.

As said before, several researchers and some international research projects have already dealt with the subject, but they did not yet identify a solution to the problem of application of the FSE on the structures protected with IC.

Since fire prevention plays a strategic role in civil defence, and since the regulatory updates are continuous and tend to the fire performance approach (FSE), alternatives to prescriptive one, the proposed research activity focuses on the guidelines and calculation methods to apply the FSE to structures protected with IC in a rigorous and safe way.

The current study went beyond the results of a previous project presented in [50] and aimed at further investigating the different aspects that affect the thermal conductivity of the intumescent coatings and their behavior in different conditions, in order to help the development of new design rules allowing the

application of cost-effective construction solutions by steel construction industry.

A better understanding of the different phases in the variation of the thermal behavior of the coatings was achieved, by investigating the role played by several characteristics, such as the fire heating rate, the activation temperature, the variation of thermal conductivity as well to other relevant parameters of the intumescent coating such as expansion ratio.

Attention was also paid to the influence of the dry film thickness (DFT) of the intumescent coating and the section factor of the plate.

Furthermore, FE analysis were performed in order to model the behavior of IC protected structures with advanced approaches (e.g. performance based design) and in order to define the ideal thickness of the coatings, both regards efficiency and the cost optimization.

In order to fulfil the project objective, two different sets of experiments were conducted, representing different types of heating exposure. Moreover, several commercial water-based intumescent coatings were tested in order to highlight common aspects in the behavior of this passive fire protection material.

In the first set of experiments, a gas furnace was used to expose the steel samples to ISO834 fire curve and to smouldering curve [65].

The specimens used in this experimental set-up were about 50 steel plates with different section factors and with different DFT of a fixed water-based commercial IC. In these experimental set-ups the application of the intumescent coatings was carried out by a professional workshop.

In the second set of experiments four different commercial water-based IC characteristics were investigated using the cone calorimeter: 100x100x10 mm steel plate samples were exposed to pure radiation. The cone heater generated different heat fluxes at the specimen level, providing temperature-time curves. The steel plate samples were coated by two different dry film thicknesses of the four intumescent paints in order to understand its influence. Attention was also paid to the radiation properties (emissivity) of the intumescent paints.

Figure 1.8 presents a schematic overview of the thesis. It describes the main problem statement and the applied methods in order to fulfil the project objective by implementing different experimental set-ups.

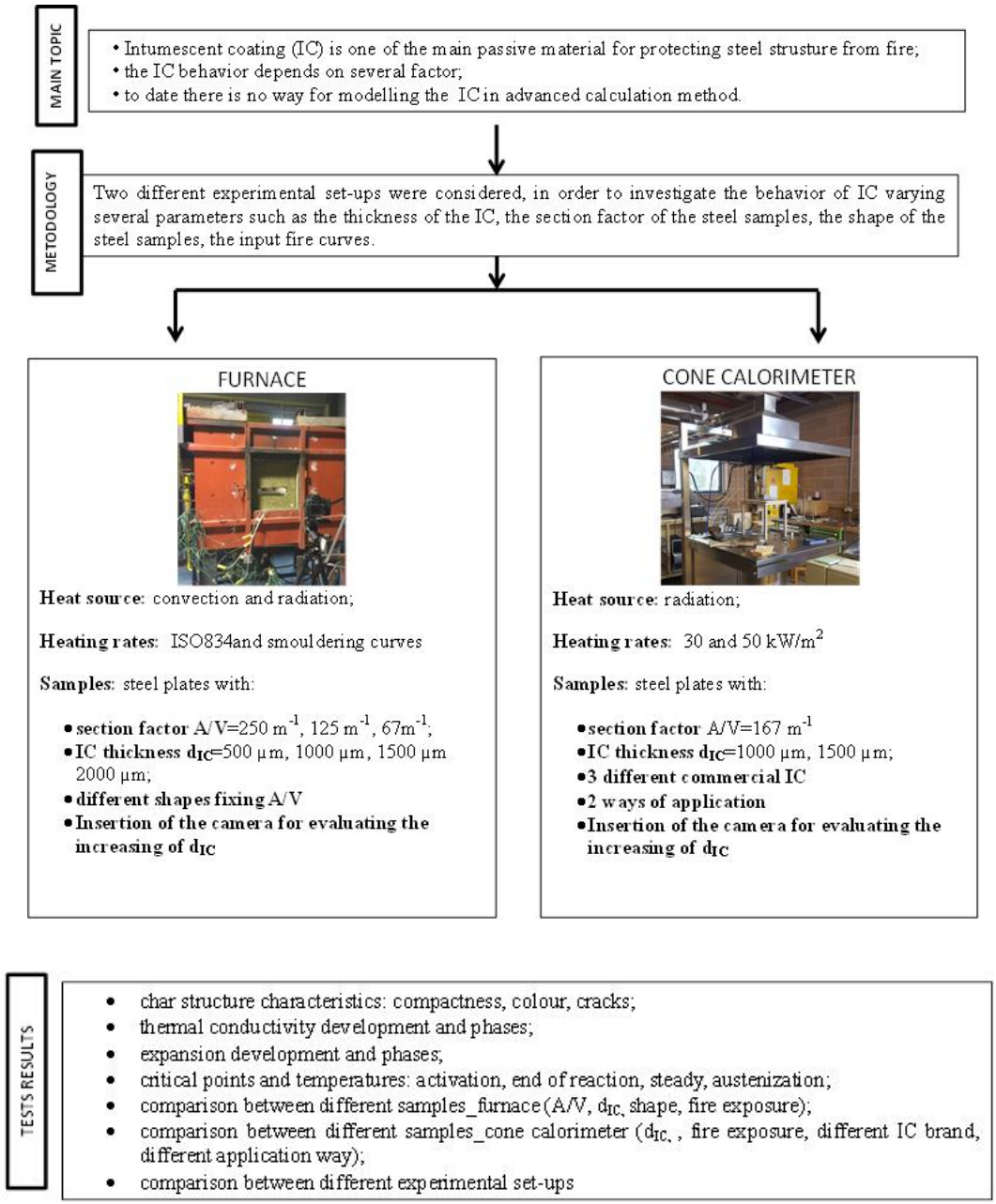

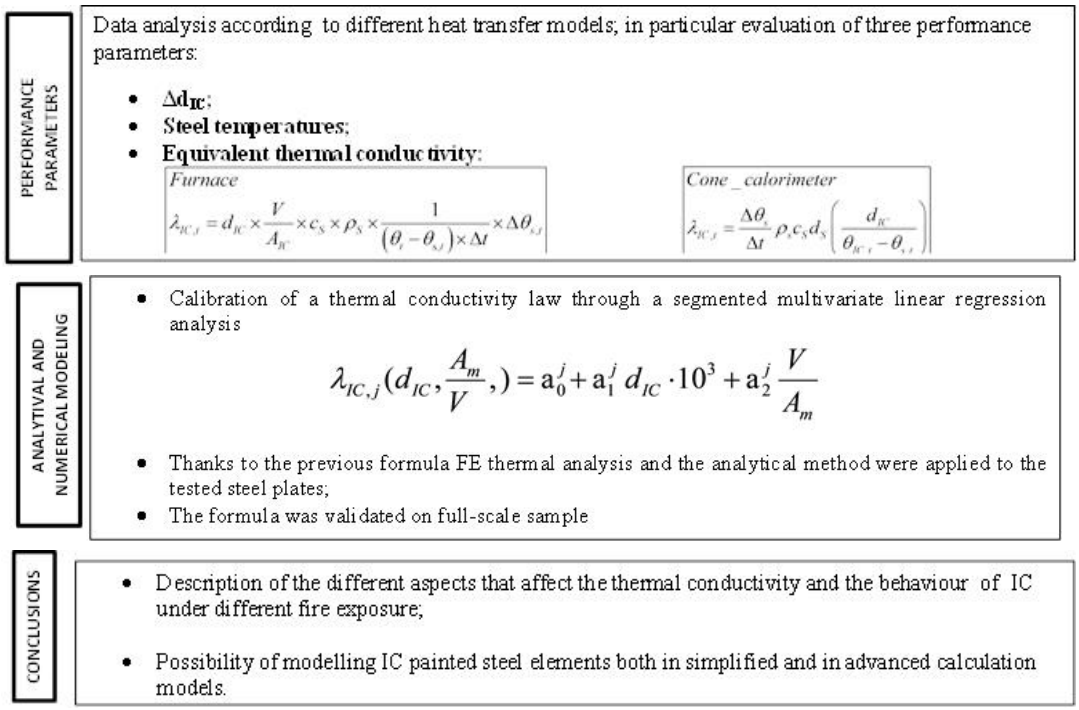

Figure 1.8 schematic overview of the thesis.

Chapter 2

EXPERIMENTAL TESTS

This chapter provides the description of the experimental tests, both in terms of set-ups arranged during the tests and in terms of results. The aim is to design and build an apparatus to collect many different types of data all at once from a single test and to perform tests on different samples to gain a better understanding of intumescent coatings.

This chapter presents and discusses the results achieved during the experimental campaign both in furnace and in cone calorimeter as well.

The two different sets of experiments took place at two different locations: the gas furnace at the Fire Laboratory of Amonn Company, in the north part of Italy, while the cone calorimeter test at Fire Safety Engineering Research and Technology Centre (FireSERT), at Ulster University.

2.1 HEAT TRANSFER MODELS OF PROTECTED STEEL ELEMENTS

The heat transfer models were established for the experimental set-ups, both in the furnace and in the cone, where the steel is protected by intumescent coatings, which react in case of high temperatures, developing thermal insulating properties[14].

2.1.1 HEAT TRANSFER MODELS FOR GAS FURNACE

The heat transfer mechanism between the hot gasses and the protected steel, well-known in the literature [40] can be simplified as the one in Figure 2.1: the samples are subjected to both convective heat transfer from the hot air present in the furnace chamber and radiative heat transfer from the heating source.

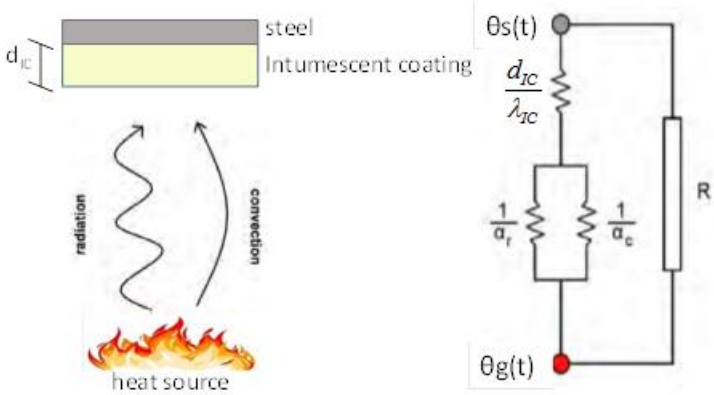

Figure 2.1 Schematic illustration of the heat transfer model for steel protected by intumescent coating [14].

Obviously, in this case the presence of intumescent coating decreases the speed of temperature penetration through the steel substrate. At the surface, the heat transfer is simplified by two parallel heat transfer coefficients, which stand for convection α_c and radiation α_r , placed in series to a conduction thermal resistance d_{IC} / λ_{IC}, which represents the insulation material (intumescent coating in this case).

This model is based on the assumption that the temperature gradient is linear and the quantity of energy needed to heat the insulation is negligible. The intumescent coating has usually a small thickness (about few millimeters) and thus this assumption is usually valid. The derivation of this heat transfer model is based also on other two assumptions. The heat flow in the steel and the insulation material is unidimensional and the validity of this assumption is greater when there are minimal corner effects.

Also, at every point of time the steel temperature is uniformly distributed over the cross section of the steel member: this means that the thinner the parts of cross-section, the greater validity of this assumption [40]\.

The heat transfer model is derived by simple heat balance equations: at the steel boundaries, the quantity of heat passing through the combustion gasses to the steel section is equal to the quantity of heat that is absorbed by the steel in order to increase its temperature (increment in the thermal energy).

Based on that, the quantity of heat ΔQ [J/m] per meter length passing through the combustion gasses to the insulated steel section during the time interval Δt can be expressed as:

$$\Delta Q = \frac{1}{1/\alpha + d_{IC}/\lambda_{IC}} A_s(\theta_g - \theta_s)\Delta t \qquad \text{Eq. 2-1}$$

where:

- α: combined heat transfer coefficient (convection + radiation) [W/m^{2}K]
- d_{IC}: insulation material thickness [m]
- λ_{IC}: thermal conductivity of the insulation material [W/mK]
- A_s: exposed steel surface area per meter length [m^2/m]
- θ_g: oven/furnace temperature [°C]
- θ_s: steel temperature [°C]
- Δt: time increment [s]

On the other hand, the quantity of thermal energy ΔU [J/m] per meter length absorbed by the protected steel in order to increase its temperature by ΔTs can be written as:

$$\Delta U = c_s \Delta\theta_s V_s \rho_s \qquad \text{Eq. 2-2}$$

where:

- c_s: steel specific heat capacity [J/kgK]
- $\Delta\theta_s$: temperature increment in the steel [°C]
- Vs: steel volume per meter length [m3/m]
- ρ_s: steel density (7850 kg/m3 [95])

At high temperatures, the thermal heat resistance related to convection and radiation can be normally ignored in comparison with the thermal resistance d_{IC}/λ_{IC} of the insulating material. Furthermore, in comparison to the heat capacity of the steel section, the heat capacity of the intumescent coating and, in general, lightweight insulation materials is very small. Therefore, it is generally

justifiable to ignore completely the heat capacity of the insulation. In addition, this leads in approximated solutions on the safe side [35].

Considering these assumptions, the rise in steel temperature ΔTs [°C] can be derived by equating the two expressions: at the steel boundaries the quantity of heat ΔQ passing through the combustion gasses to the steel section during the time interval Δt is equal to the quantity of thermal energy ΔU absorbed by the steel substrate:

$$\Delta\theta_s = \frac{A_p}{V}\frac{\lambda_{IC}}{d_{IC}}\frac{1}{\rho_s c_s}\left(\theta_g - \theta_s\right)\Delta t \qquad \text{Eq. 2-3}$$

which can be rewritten in order to obtain the temperature of the insulated steel θ_s^i at step i, which can be expressed as:

$$\theta_s^i = \theta_s^{i-1} + \frac{\lambda_{IC}}{d_{IC}}\frac{1}{\rho_s^{i-1} c_s^{i-1}}\frac{A_s}{V_s}\left(\theta_g^{i-1} - \theta_s^{i-1}\right)\Delta t \qquad \text{Eq. 2-4}$$

where:

- θ_s^{i-1} : temperature of the protected steel at previous step i -1 [°C];
- c_s^{i-1} : steel specific heat capacity at step i -1 [J/kgK];
- ρ_s^{i-1} : steel density at step i -1 [kg/m^3]
- T_g: average furnace temperature between the steps i and i -1 [°C]:
- A_P/V: section factor [m^{-1}]

In the case of intumescent coating $A_P/V = A_S/V_S$ because this kind of protection is applied in adhesion to the steel profile.

Eq. 2-4 is really similar to formula reported in the Eurocode [63] for steel sections protected by intumescent coating.

Indeed inverting this equation the thermal conductivity (λ_{IC}) of the intumescent coating can be obtained: it represents the ability of a given thickness of an insulation material to permit the heat penetration.

In this particular scenario, the intumescent coating, with its low thermal conductivity offers resistance to the heat transfer between the hot gasses and the steel substrate and its thermal resistance varies with time, depending on several aspects.

2.1.2 VARIABLE "Λ" METHOD

Because the response of reactive coatings to heating is complicated by the various chemical reactions, phase transitions, thermal expansion, and charring phenomena, developing holistic models which account for all relevant parameters to predict their thermal insulating properties under different heating regimes is fraught with complications.

As a result, it is typical to treat the thermal conductivity of reactive coatings using an empirically informed procedure called the "Variable λ Method" which is set out in Annex E of [63].

Based on the heat transfer models described in the previous paragraph, this method is intended for evaluating the equivalent thermal conductivity of fire protection systems and is defined by the following expression:

$$\lambda_{p,t} = d_p \times \frac{V}{A_p} \times c_a \times \rho_a \times \frac{1}{\left(\theta_t - \theta_{a,t}\right) \times \Delta t} \times \Delta\theta_{a,t} \qquad \text{Eq. 2-5}$$

where:

d_p= dry film thickness of reactive product, in metres;

V/A_p= inverse of the steel section factor, in metres;

c_a= temperature dependant specific heat capacity of steel at θ_a, in J/kgK;

ρ_a= density of the steel, in kg/m^3;

θ_t= furnace temperature, in Celsius degrees;

$\theta_{a,t}$= steel temperature, in Celsius degrees;

Δt = time step, in seconds;

$\Delta\theta_{a,t}$= steel temperature rise over time step Δ_t, in Kelvin degrees.

As also said before, Eq. 2-5 derives from an energy balance taken during a given time interval during heating for unidirectional heat flux conditions.

So, in this project, it was applied to the tested "big" plates (only in this case the flux is unidirectional), and as such it assumes an adiabatic condition between the furnace gases and the surface char.

2.1.3 HEAT TRANSFER MODELS FOR CONE CALORIMETER

While the heat transfer model adopted for the electric oven and gas furnace experimental set-ups is a widely known and applied analytical method, this one-dimensional model was recently proposed by Wang et al. [39] and it is valid for steel samples protected by intumescent coatings in the mass loss cone heater set-up.

The heat transfer mechanism between the cone heater and the protected steel can be simplified as the one in Fig. 2.5. As the case of the unprotected steel, the samples are exposed to a heat flux at the surface level. Unlike the previous heat transfer model for the cone heater, the presence of an insulation material (intumescent coating) decreases the speed of temperature penetration through the steel substrate.

Moreover, in the study by Wang et al. [39] three different kinds of heat losses between the heat source and the steel sample are included in the heat transfer model. As the steel heats up, it transfers heat to the surrounding environment in the form of convection (convective heat transfer coefficient α_c) and re-radiation (steel emissivity ε_s).

Furthermore, a small amount of energy is dissipated from the bottom of the steel plate specimen, through the insulation material.

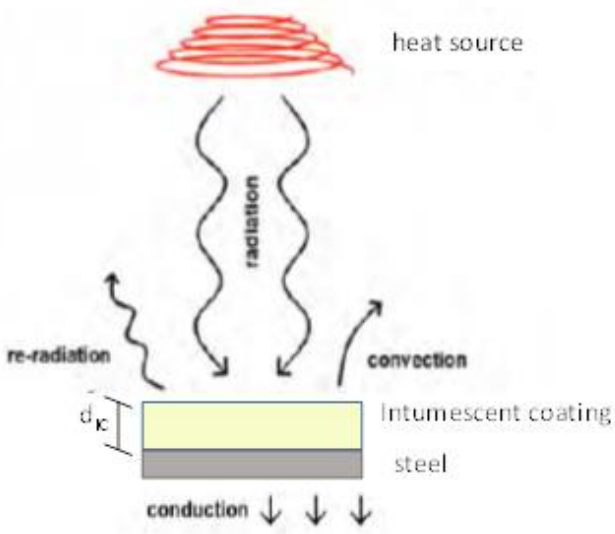

Figure 2.2 Schematic illustration of the heat transfer model for steel protected by intumescent coating in cone calorimeter [14].

The derivation of the model is based on the assumption that the heat flow is unidimensional and the cone heater and the protected steel sample are considered as two infinitely parallel grey planes, neglecting edge effects and local boundary conditions. In this model also the intumescent paint emissivity and absorptivity are considered constant, even if these parameters are most likely dependent on temperature. Omrane et all. [57] have verified that good results are obtained considering a constant emissivity equal to 0.92, a value close to the ones suggested by two other previous research studies [51][58]. Moreover, the intumescent coating is assumed to have a nominal density of 1000 kg/m^3 and specific heat of 1000 J/kgK. Since the heat stored in the intumescent coating is extremely small, it is not necessary to use very accurate values of intumescent coating temperature, density and specific heat [44].

The heat transfer model is derived by simple heat balance equations: at the steel boundaries the net quantity of heat passing through the cone heater to the steel section is equal to the re-emitted quantity of heat by the steel through convection and radiation plus the quantity of heat absorbed by the intumescent

paint and the steel in order to increase their temperatures (increment in the thermal energies).

Based on that, the net quantity of heat ΔQ [J] passing through the cone heater to the insulated steel section during the time interval Δt can be expressed as:

$$\Delta Q = \alpha_{IC} q_r A_s \Delta t - \dot{Q}_{loss} \Delta t \qquad \text{Eq. 2-6}$$

where:

- q_r: heat flux from the cone heater to the protected steel surface [W/m2]
- α_{IC}: intumescent paint absorptivity [-]
- A_s: exposed steel surface area [m2]
- Δt: time increment [s]
- ΔQ loss: conductive heat loss from the backside of the steel plate [J/s]

On the other hand, the quantity of thermal energy ΔU [J] released and absorbed by the protected steel sample can be written as:

$$\Delta U = \left[\varepsilon_{IC} \sigma \theta_{IC}^4 + h_c \left(\theta_{IC} - \theta_a \right) \right] A_s \Delta t + \frac{\Delta \theta_{IC} + \Delta \theta_s}{2} \rho_{IC} c_{IC} A_{IC} d_{IC} + \Delta \theta_s \rho_s c_s A_s d_s \qquad \text{Eq. 2-7}$$

where:

- ε_{IC}: intumescent paint emissivity (0.95)
- σ: Stefan-Boltzmann constant (5.67 x10^{-8} W/m^2K^4)
- θ_{IC}: intumescent paint surface temperature [K]
- h_c: convective heat transfer coefficient (20 W/m^2K)
- θT_a: ambient temperature [K]
- A_s: exposed steel surface area [m^2]
- Δt: time increment [s]
- $\Delta\theta_s$: temperature increment in the steel [°C]
- $\Delta\theta_{IC}$: temperature increment in the intumescent paint surface [°C]
- ρ_{IC}: intumescent paint density (1000 kg/m^3)
- c_{IC}: intumescent paint specific heat capacity (1000 J/kgK)
- A_{IC}: intumescent paint surface [m^2]
- d_{IC}: intumescent paint dry film paint thickness [m]
- ρ_s: steel density (7850 kg/m^3)

- c_s: steel specific heat capacity [J/kgK])
- d_s: steel plate thickness [m]

Considering these assumptions, a heat transfer model for protected steel specimens can be derived by equating the two expressions: at the steel boundaries the net quantity of heat ΔQ passing through the cone heater to the steel section during the time interval Δt is equal to the total quantity of thermal energy ΔU released and absorbed by the steel substrate:

$$a_{IC}q_r - \frac{\dot{Q}_{loss}}{A_s} = \varepsilon_{IC}\sigma\theta_{IC}^4 + h_c\left(\theta_{IC} - \theta_a\right) + \frac{\Delta\theta_{IC} + \Delta\theta_s}{2\Delta t}\rho_{IC}c_{IC}d_{IC} + \frac{\Delta\theta_s}{\Delta t}\rho_S c_S d_S \qquad \text{Eq. 2-8}$$

Eq. 2-8 contains three undetermined variables: the intumescent paint absorptivity α_{IC}, the conductive heat loss ΔQ_{loss} from the backside of the steel plate through the mineral wool and the intumescent coating surface temperature θ_{IC}.

However, several studies [44][59][97][76] have shown that some previously mentioned terms of Eq. 2-8 are less significant than others. In particular, the heat stored in the intumescent coating is very small quantity when the intumescent paint has reached its full expansion, so it can be neglected [44].

Moreover, the heat stored in the steel plate substrate is a relatively small quantity when the steel plate has reached a quasi-steady state. Thus, it can be stated that after achieving quasi-state conditions, the intumescent coating surface temperature should be approaching a constant value, mainly depending on the level of radiation. As a consequence, the cone heater incident irradiance is much greater than the other three terms and they can be neglected.

Nevertheless, the intumescent coating surface temperature θ_{IC} is really difficult to evaluate and it can be estimated by adopting sophisticated equipment, for instance a thermographic phosphor technique. Thus, without this information it is not possible to derive precisely the intumescent coating thermal conductivity for this specific experimental setup.

Following the previous approach, the thermal conductivity of the intumescent coating material may be obtained from the following equation:

$$K_{IC}\left(\frac{\theta_{IC}-\theta_s}{d_{IC}}\right)-Q_{loss}=\frac{\Delta\theta_s}{\Delta t}\rho_S c_S d_S \qquad \text{Eq. 2-9}$$

Since Q_{loss} is negligible, in order to calculate , T_{IC} is necessary to calculate from Eq. 2-8, which can be finally written as:

$$\varepsilon_{IC}\sigma\theta_{IC}^4+h_c\left(\theta_{IC}-\theta_a\right)=Q_e \qquad \text{Eq. 2-10}$$

where Q_e is the external heat flux of the cone.

So, fixing $\varepsilon_{IC},\sigma,h_c,\theta_\alpha$ and Q_e the intumescent coating surface temperature θIC can be calculated and from k_{IC} (that in the following will be indicated with λ_{IC}) can be calculated as well[44].

2.2 PRELIMINARY TESTS

Even if an experience in the field of testing on steel elements protected with IC had already been acquired as shown in [49][50], during the initial phase of the experimental tests both in furnace and in cone calorimeter, a range of preliminary experiments was conducted before the main ones.

This practice is always advisable in order to identify the problems related to the experimental work in terms of practical issues. Conducting trial experiments helped to understand the test peculiarities and how to focus on a specific result.

Moreover, some practical issues were faced in order to fully understand the experiments and to find the best experimental set-ups, according to the project goal. The preliminary experiments also underlined the advantages and disadvantages of a certain test respect to another one, with its specific defects, lacks and weaknesses. For example, the thermocouples represented a key topic in the preliminary experiments.

By conducting trial tests, it was possible to fully understand their operation principle and characteristics. Based on that experience, serviceable thermocouples were assembled and used in the different experimental set-ups in

the proper way. Another important aspect was the placement and fixation of them to the samples: several tests were conducted in order to define the best way to fix them to the steel specimen and, in particular, to avoid their ejection during the tests. Furthermore, special attention was paid on furnace controller and the real possibility of defining and obtaining an accurate temperature-fire curve according to the standard ones. The same principle was also applied on the cone calorimeter, where the cone was calibrated in order to obtain precise heat fluxes at the exact distance requested by the standard, although in some cases this distance was increased to measure the swelled thickness of the IC. Few preliminary tests were always conducted prior to the main experiments. This range of experiments is useful to find a suitable experimental set-up for each specific case and to give a first impression on the behavior of the intumescent coating. Moreover, unprotected steel samples were heated in each different experimental setup and the steel temperature measurements were verified by means of analytical heat transfer models. This was performed in order to make sure that the heat exposure was fully understood for all the different tests, prior to the heating of the coated specimens.

2.3 INTUMESCENT COATING TESTED

Four commercial intumescent coatings available in the market were investigated, in order to highlight eventual common aspects in the behavior.

In this project they are identified as IC_A, IC_B, IC_C, IC_C*. All of them are water-based emulsion and they are not flammable.

All the IC created a compact and hard film on the samples: this is also confirmed by the fact that the coating is water-based and an initial steel oxidation takes place during the drying procedure.

Anyway, all the necessary information about the intumescent coatings and also about the application instructions, the consumptions were found in the technical data sheets provided by the manufactures.

2.4 EXPERIMENTS IN THE GAS FURNACE

This section describes the experiments conducted in a gas furnace on a commercial water based coating (IC_B), varying different parameters such as input fire curve, coating thickness, plate thickness and shape of the sample, measuring temperature and expansion of IC with Digital Image Correlation technique.

By elaborating the tests results, a better understanding of how the intumescent reacts was able to be seen along with different trends and behaviour patterns of different samples. This detailed characterization also helped in finite element numerical model of protected steel elements, exploiting thermal conductivity formulations of European code [63].

2.4.1 TEST INSTRUMENTATION: GAS FURNACE

The fire resistance properties of a material can be used to consider its behaviour when subjected to specific heating conditions and the gas furnace is used for performing fire tests on structural element or on several materials.

It can reproduce really severe fire scenarios, characterised by high temperatures and high heating rates.

The gas furnace at Amonn Fire Laboratory can reach maximum temperatures around 1400°C. The gas furnace heating chamber has a volume of 1 m^3; 1m wide and 1m long).

Four sides of the walls are lined with special high temperature insulating fire bricks on the hot face and pre-cast refractory castables at the edges exposed to the specimen restraint frame as well as mineral boards on the cold face.

A refractory lined Blank-Out Wall with lifting hooks is also supplied; this enables the user to close one side of the furnace wall when either a vertical or a horizontal test specimen is mounted for testing.

Two burners, based on an upright furnace position are installed on the opposite side of the furnace wall. Each burner is designed to use liquefied petroleum gas and all necessary flame safety systems, intermittent pilot systems, and temperature sensors are incorporated.

The fossil fuel is burned and the heat created is then pushed into the heat exchanger, where the air is heated up. Thus, the newly heated air is forced to move into the furnace chamber through four different duct-works, placed at different furnace sides and heights.

By adjusting the amount of air plus gas mixture and the flow, it is possible to control the furnace temperature, both manually and automatically. With this devices the gas furnace produces a clean environment in which the main mechanism of heat transfer is radiation from the furnace inner walls at high temperatures and convection from the hot air to the test samples at low temperatures.

The furnace temperature is monitored by thermoplates placed throughout the heating chamber. In this way, the gas furnace can reproduce the standard fire curves with a great accuracy.

The gas furnace is also equipped with an internal ventilation system, a fundamental component to control the pressure and remove the excessive smoke and flying particles inside the heating chamber.

The steel temperatures were evaluated using thermocouples, placed at specific locations and fixe according with the scheme which will be described below. As said before the furnace has a front door that can be removed indeed, in this case, the opening was closed with mineral fiber board, on which an hole was created in order to observe the specimen during the tests (Figure 2.4).

All the temperatures estimated by the thermocouples and thermoplates were collected by a data logger, which was linked to a data acquisition system for data collection and elaboration (Figure 2.4).

Figure 2.3 (a) Gas furnace and data acquisition system.

2.4.2 INPUT FIRE CURVES

The common design method for testing fire protection systems applied to structural steel members in buildings[62][63] require to use the ISO 834 curve.

The standard fire test is the main tool to define the fire resistance class of fire insulation materials. The higher resistance class is the R120 and thus the materials are usually exposed to the standard fire for 120 minutes. In this way, according to the design temperature and the section factor, it is possible to define the fire resistance class. Regarding IC, they can achieve 120 minutes fire resistance for only few cases.

Most commercial IC can traditionally provide up to 60 minutes fire resistance and nowadays, after many improvements, they are increasingly competitive in the 90 minutes market as well [8].

In this particular experimental set-up the fire test were stopped when 700°C were reached in the protected steel, temperature at which the steel begins to lose its resistance characteristics [9].

The cellulosic standard fire curve reaches about 950°C in 60 minutes and about 1050°C in 120 minutes. The fire protection capabilities of intumescent products, the ratings of which were determined using tests based on the

standard temperature-time curve, may be substantially reduced during a slow growing. In particular, the dissolution of the IC, resulting in a reduction of performance, can occur for heating curves with thermal gradients lower than Standard fire curve ISO 834 ([64], [65]) close to the IC initiation temperature. For this reason, in [63] also a slow heating curve (smouldering curve) is defined. In particular the smouldering curve has a slower growth gradient of the ISO834 for the first 21 minutes and after it starts to grow with the same speed of ISO834 [64][65]. So, in this tests two fire curves were considered: the ISO834 and the Smouldering curves (Figure 2.4).

Figure 2.4 shows that there is a very good agreement between the experimental temperatures of the furnace and the theoretical one for each tests for the ISO834 tests; for the tests with the smouldering curve the good agreement mainly concerns the second part of the curve.

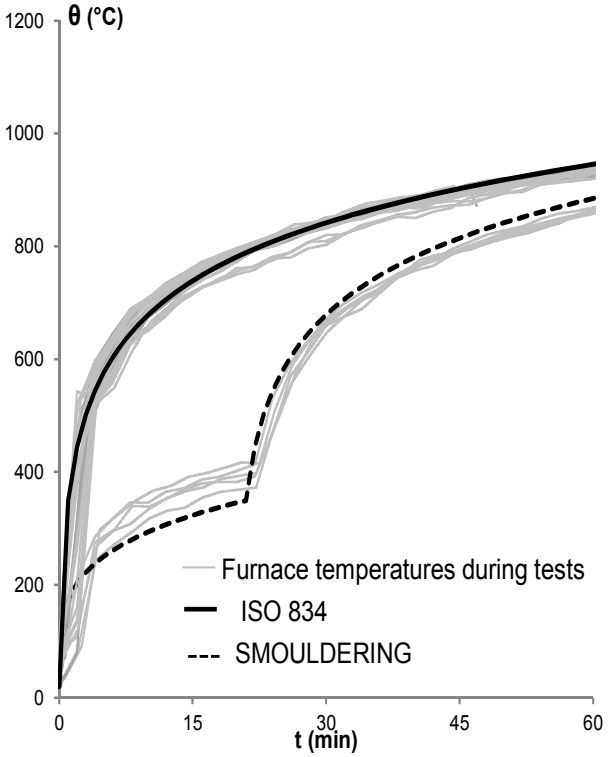

Figure 2.4 input fire curves.

2.4.3 TEST SAMPLES AND EXPERIMENTAL SETUP

The specimens tested in the sets of furnace experiments were 36 carbon steel plates 300×300 mm with different thicknesses, in order to obtain different section factors. Moreover, 12 steel plates (60×60×5, 75×75×10, 135×135×20) were used under different exposure condition to have different dimension with the same section factor (see Table 2-1). In particular, samples from no.1 to no.24 were protected on the lateral thickness by ceramic board strips to expose the top surface of the plate only (Figure 2.5a). The samples from no.25 to no.36 were laterally exposed to heating (see Figure 2.5b). Finally, the samples from n.36 to n.48 are equal to the first 24 samples, but tested under smouldering curve (Table 2-1). Also bare steel plates were tested for each section factor also for monitoring always the test setup, as described in detailed in the following (Appendix B).

A goal of this specific experimental set-up was to understand the influence of the coating thickness and of the section factor on the behaviour of this passive fire protection material, so the exposed surfaces of the samples were protected with different thicknesses d_{IC} (500μm, 1000μm, 1500μm, 2000μm) of water-based commercial IC.

Analysing the literature to date, the majority of previous research studies about the behaviour of IC have been experimental based and mainly focused on understanding the effects of different formulations to help manufacturers develop products to pass the standard fire resistance rating test. Very few studies have been conducted to investigate the performance of intumescent coatings under different fire conditions, with very limited success in modelling.

So another goal of this experimental tests is introducing a different fire curve (Slow heating one) in order to investigate the behaviour of IC (see samples from n° 37 to n°48).

In the case of furnace tests, the IC were applied by professional painters and in order to understand the quality of the execute work and the uniformity of the paint on the samples, the dry film thicknesses were measured by using a non-destructive coating thickness gauge. All the measurements on the test samples with the correspondent statistical values are listed in Appendix A.

Table 2-1 Test matrix_furnace.

Samples	n°	ID	Dimension (mm)	A/V (m^{-1})	IC (µm)	Input Curve
8 plates 300x300x4	1	S_300x300x4-250_500_ISO_1	300x300x4	250	500	ISO834
	2	S_300x300x4-250_500_ISO_2			500	
	3	S_300x300x4-20_1000_ISO_1			1000	
	4	S_300x300x4-250_1000_ISO_2			1000	
	5	S_300x300x4-250_1500_ISO_1			1500	
	6	S_300x300x4-250_1500_ISO_2			1500	
	7	S_300x300x4-250_2000_ISO_1			2000	
	8	S_300x300x4-250_2000_ISO_2			2000	
8 plates 300x300x8	9	S_300x300x8-125_500_ISO_1	300x300x8	125	500	ISO834
	10	S_300x300x8-125_500_ISO_2			500	
	11	S_300x300x8-125_1000_ISO_1			1000	
	12	S_300x300x8-125_1000_ISO_2			1000	
	13	S_300x300x8-125_1500_ISO_1			1500	
	14	S_300x300x8-125_1500_ISO_2			1500	
	15	S_300x300x8-125_2000_ISO_1			2000	
	16	S_300x300x8-125_2000_ISO_2			2000	
8 plates 300x300x15	17	S_300x300x15-67_500_ISO_1	300x300x15	67	500	ISO834
	18	S_300x300x15-67_500_ISO_2			500	
	19	S_300x300x15-67_1000_ISO_1			1000	
	20	S_300x300x15-67_1000_ISO_2			1000	
	21	S_300x300x15-67_1500_ISO_1			1500	
	22	S_300x300x15-67_1500_ISO_2			1500	
	23	S_300x300x15-67_2000_ISO_1			2000	
	24	S_300x300x15-67_2000_ISO_2			2000	
4 plates 60x60x5	25	S_60x60x5-250_500_ ISO _1	60x60x5	250	500	ISO834
	26	S_60x60x5-250_500_ ISO _2			500	
	27	S_60x60x5-250_1500_ ISO _1			1500	
	28	S_60x60x5-250_1500_ ISO _2			1500	
4 plates 75x75x10	29	S_75x75x10-125_500_ ISO _1	75x75x10	125	500	ISO834
	30	S_75x75x10-125_500_ ISO _2			500	
	31	S_75x75x10-125_1500_ ISO _1			1500	
	32	S_75x75x10-125_1500_ ISO _2			1500	
4plates 135x135x20	33	S_135x135x20-67_500_ ISO _1	135x135x20	67	500	ISO834
	34	S_135x135x20-67_500_ ISO _1			500	
	35	S_135x135x20-67_1500_ ISO _1			1500	
	36	S_135x135x20-67_1500_ ISO _1			1500	
4 plates 300x300x4	37	S_300x300x4-250_500_SM_1	300x300x4	250	500	SMOULDERING
	38	S_300x300x4-250_1000_SM_1			1000	
	39	S_300x300x4-250_1500_SM_1			1500	
	40	S_300x300x4-250_2000_SM_1			2000	
4 plates 300x300x8	41	S_300x300x8-125_500_SM_1	300x300x8	125	500	SMOULDERING
	42	S_300x300x8-125_1000_SM_1			1000	
	43	S_300x300x8-125_1500_SM_1			1500	
	44	S_300x300x8-125_2000_SM_1			2000	
4 plates 300x300x15	45	S_300x300x15-67_500_ SM _1	300x300x15	67	500	SMOULDERING
	46	S_300x300x15-67_1000_ SM _1			1000	
	47	S_300x300x15-67_1500_ SM _1			1500	
	48	S_300x300x15-67_2000_ SM _1			2000	

The plates were placed on an insulating support, in ceramic fibre mat 25,4 mm thick. Both the ceramic fibre mat and the ceramic board strips are inserted

to minimize ambient influences on samples and to realize approximately adiabatic conditions [50].

The plate and the insulating system are finally placed on cellular concrete bricks (Figure 2.5).

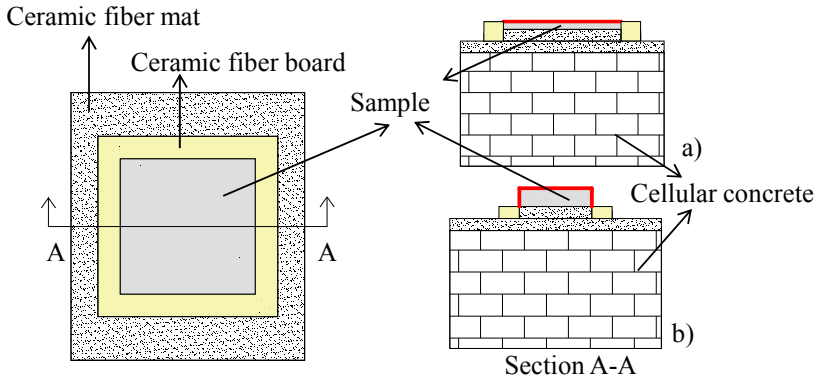

Figure 2.5 Test setup: (a) section A-A for "big" sample and (b) section A-A for "small" sample.

2.4.4 THICKNESS MEASUREMENT

The test setup involves the insertion of a camera in front of the opening of the furnace in order to take a series of pictures of the specimen during the test Figure 2.6.

Figure 2.6 Camera insertion.

The pictures were shot with five-second time interval during all tests and then they were used to obtain the variation of IC thickness by means of the Digital Image Correlation technique (DIC).

Digital image correlation is an optical method that employs tracking and image registration techniques for accurate 2D and 3D measurements of changes in images.

This method is often used to measure full-field displacement and strains, and it is widely applied in many areas of science and engineering, with new applications being found all the time.

DIC techniques have been increasing in popularity, especially in micro- and nano-scale mechanical testing applications due to its relative ease of implementation and use. Advances in computer technology and digital cameras have been the enabling technologies for this method and while white-light optics has been the predominant approach, DIC can be and has been extended to almost any imaging technology.

Commonly, DIC relies on finding the maximum of the correlation array between pixel intensity array subsets on two or more corresponding images, which gives the integer translational shift between them. It is also possible to estimate shifts to a finer resolution than the resolution of the original images, which is often called "subpixel" registration because the measured shift is smaller than an integer pixel unit.

For subpixel interpolation of the shift, there are other methods that do not simply maximize the correlation coefficient. An iterative approach can also be used to maximize the interpolated correlation coefficient by using nonlinear optimization techniques.

The nonlinear optimization approach tends to be conceptually simpler, but as with most nonlinear optimization techniques, it is quite slow, and the problem can sometimes be reduced to a much faster and more stable linear optimization in phase space.

DIC has proven to be very effective at mapping deformation in macroscopic mechanical testing, where the application of specular markers (e.g. paint, toner powder) or surface finishes from machining and polishing provide the needed contrast to correlate images well.

Very recently, advances in pattern application and deposition at reduced length scales have exploited small-scale synthesis methods including nano-scale chemical surface restructuring and photolithography of computer-generated random specular patterns to produce suitable surface contrast for DIC.

In this project an automatic procedure can not be used because the surface of the intumescent coating is not regular during the swelling. So three points on the surface have been fixed and monitored one by one and then an average value of these points was made to evaluate the swelling of the IC during the thermal transient.

Before each test, it was checked that the support on which the plate was positioned and the plate itself were in a horizontal position to minimize or/and avoid optical distortions; also a picture of the meter stick resting on the samples was made in order to have a precise indication of the thickness during calibration with DIC (Figure 2.7).

Figure 2.7 Meter stick for DIC calibration.

2.4.5 EXPERIMENTAL SET-UP VALIDATION

The experimental set-up presented in this section was validated respect to the heat transfer model of well-known unprotected steel[9].

The temperature-time curves of the unprotected steel provided by the tests in the gas furnace were compared to the analytical model implemented in the FE code SAFIR16[75].

As it is possible to state from Figure 2.8 and from Appendix B, the numerical and the experimental curves were very similar to each other.

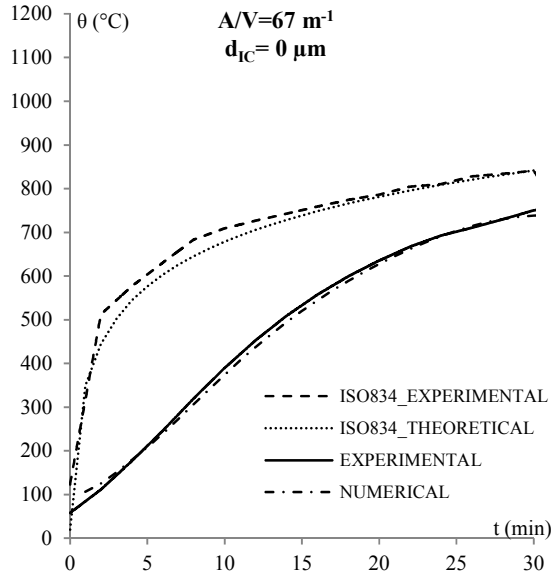

Figure 2.8 comparison between unprotected samples (experimental and numerical).

Based on these considerations, the experimental set-up was considered suitable for the development of these tests, according to the adopted analytical model.

2.4.6 TEMPERATURE ACQUISITION

The control and the measurements of the temperature of the different examined components had a key importance in these sets of experiments.

An easy and not expensive way of measuring temperature is using thermocouples, devices which consist on two different conductors that contact each other at one or more spots, where a temperature differential is experienced by the different conductors. It also produces a voltage when the temperature of

one of the contact points differs from the reference temperature of the other, in a process known as the thermoelectric effect. The different conductivity of the two conductors induces a current in this circuit and a special device is able to evaluate the temperature starting from a potential difference.

The main limitation with thermocouples is the accuracy: system errors of less than one degree Celsius (°C) can be difficult to register, but they are really useful for big temperature gradient, for instance in a fire scenario, like in the case of this project.

In these sets of experiments, temperature measurements were executed by using type K thermocouples (chromel–alumel) which is the most common general-purpose thermocouple with a sensitivity of approximately 41 μV/°C, composed of conductor wires of nickel and chromel (diameter 0.5 mm) with a combined outer diameter of 1.4 mm and a theoretical maximum service temperature of 1350 °C.

The two conductors (Ni and Cr) were coated by an insulation material which prevents short circuits in the thermocouple and so systematic errors.

The temperature was evaluated by connecting the thermocouples to a data logger, able to translate the potential difference of the two conductors into a temperature gradient.

In particular four K-type thermocouples were placed on each plate, according to the scheme of Figure 2.9.

In particular, four holes were created in the ceramic fiber mat under the plate in order to introduce four metallic platelet (0.6 mm) to which the thermocouples are welded. The platelet were used to ensure the contact between the thermocouple and the specimen.

Figure 2.9 Position of the thermocouples .

2.4.7 CRITICAL POINTS

As shown in section 1.3.3, the four phases are identified according to some critical points that can be recognized on the thermal conductivity development curve throughout the temperature.

The first one is the "activation point". It is identified as the maximum value of the thermal conductivity before the intumescent process of the IC. This point refers to when the intumescent chemical process begins and dry film thickness starts swelling and creating the char structure, which oppose a thermal resistance to the heat penetration.

The so-called "end of reaction" point refers to the end of the procedure when the paint absorbs heat for the intumescent chemical reaction. The exhaustion of this endothermic reaction is the only reason for such a distinct change in the thermal conductivity.

Therefore, the minimum value of thermal conductivity indicates the point where the chemical reaction stops and the end of the intumescence of the char.

The "steady point" represents the instant when the gradual increase of the thermal conductivity during the transient phase reaches a steady value, which will be approximately kept constant during the steady phase. Mathematically, it was identified as the maximum curvature point (third derivative equal to zero) of the hypothetical trend curve of the thermal resistance during the decreasing branch of the transient phase and the steady phase.

Finally, the "austenitization point" refers to a particular temperature phenomenon which takes place in the steel at 735°C. At this temperature, a molecular transformation of steel occurs and, in particular, its structures changes from ferrite to the face-centred cubic configuration of iron, also known as austenite. This point is also well-known as eutectoid temperature and usually it is about 730-735°C [63]. This endothermic transformation is taken into account by adopting the expression of the thermal capacity of the steel suggested by the Eurocode. Since at the austenitization point the thermal capacity of the steel is almost 10 times respect to its common value, there is a drop in the derivation of the thermal resistance: the main reason is the fact that

the majority of the heat absorption, and so the thermal insulating properties, are addressed to the really high thermal capacity of the steel.

Unfortunately this point can not be identified in the Figure 1.7, because all the tests stop when 700°C have been achieved in steel samples.

2.5 RESULTS AND DISCUSSION FOR FURNACE TESTS

IC are materials characterized by a swelling behavior when exposed to high temperatures, due to the generation of gaseous compounds during thermal decomposition of the organic matrix[30].

The charred layer latter perfectly insulates the substrate against an excessive increase of temperature and oxygen access, thanks to its low thermal conductivity. The thickness variation Δd_{IC} was firstly made and after calculating also the equivalent conductivity λ_{IC} , a comparison between the several test results was carried out, both in the case of ISO834 and Smouldering curves.

In the following, the Mean Thickness is indicated with "M.T.", the Mean Conductivity with "M.C" and the Mean Temperature with "M.θ." [71].

2.5.1 DATA PROCESSING AND COMPARISONS (ISO834 CURVE)

An elaboration of the temperatures during the test was performed and the Figure 2.10 shows, for example, the temperature trends for samples with A/V=67 m^{-1}. All the other temperatures, for each sample, are contained in Appendix C. The temperatures recorded on the unprotected specimens are very close to each other; the same is for specimen with 2000 μm, while a variability is observed for the sample protected with 500 μm.

Observing all the pictures shot during the tests, this difference could be related to the IC swelling, which, in the case of protection 2000 μm is more regular than the one observed for the 500 μm, as the Figure 2.10 shows.

The same trend was observing for almost the samples, underlining an instable behavior of the samples protected with 500 μm of IC.

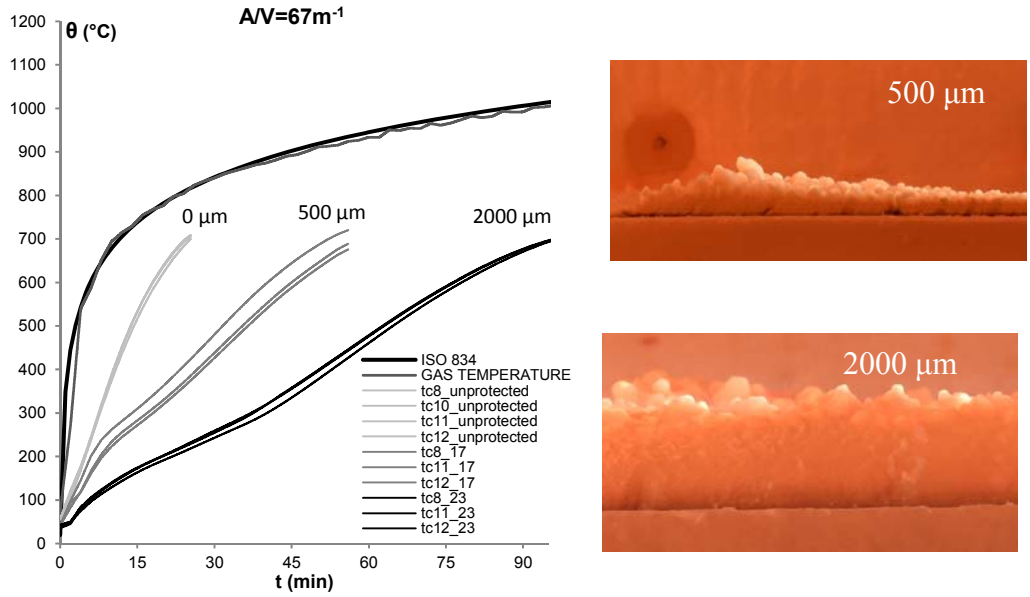

Figure 2.10. temperatures and IC swelling for samples with A/V=67 m-1.

The increase of IC thickness was obtained, in this project, thanks DIC tecnique, elaborating the pictures taken with five-second interval during all test, as described befores. An average thickness was obtained for each samples, fixing three different points on the IC surface and monitoring them during the thermal transitory.

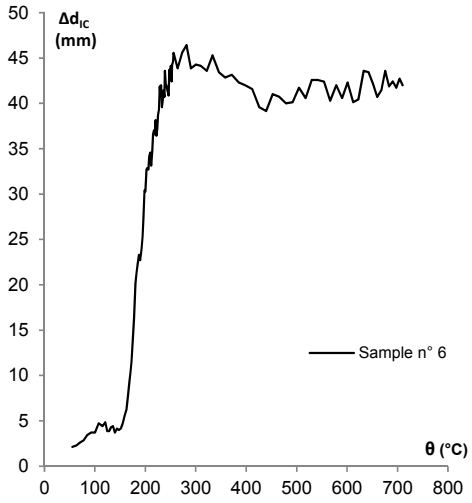

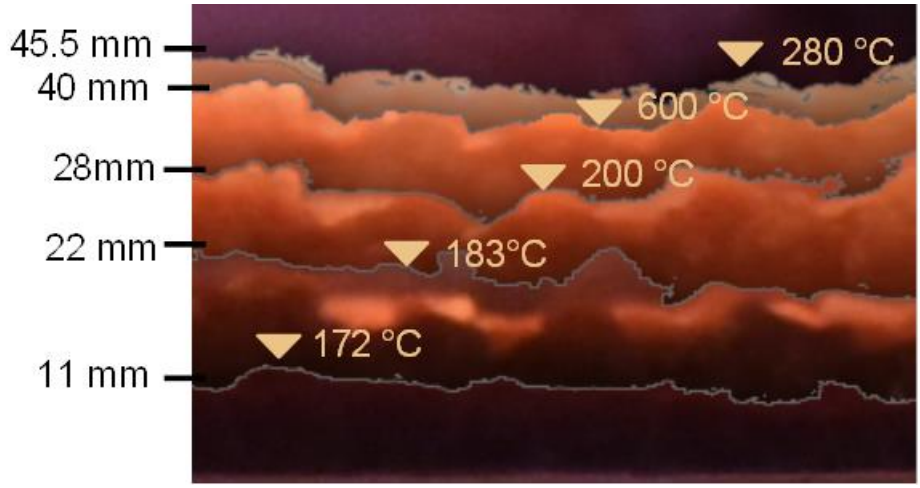

Figure 2.11. thickness increase during tests 6.

The Figure 2.11 shows , for example, the variation of thickness of one test; a fast increase of thickness is observed between 150°C and 300°C, then it becomes stable until the end of the test. This trend was observed for all the tests with 1000 μm, 1500 μm and 2000 μm. While in the case of 500 μm, a more irregular swelling of the IC was observed, with localized concentrations of higher thickness on the surface of the specimen.

All the other IC swelling are represented in the following.

The equivalent thermal conductivity of reactive coatings was assessed by using the "Variable λ Method", as described in previous paragraph.

In the following figures, for each couple of equal samples, the value of Mean Thickness (M.T.S._n°), Mean Conductivity (M.C.S._n°) and Mean Temperature (M.θ.S._n°) are shown.

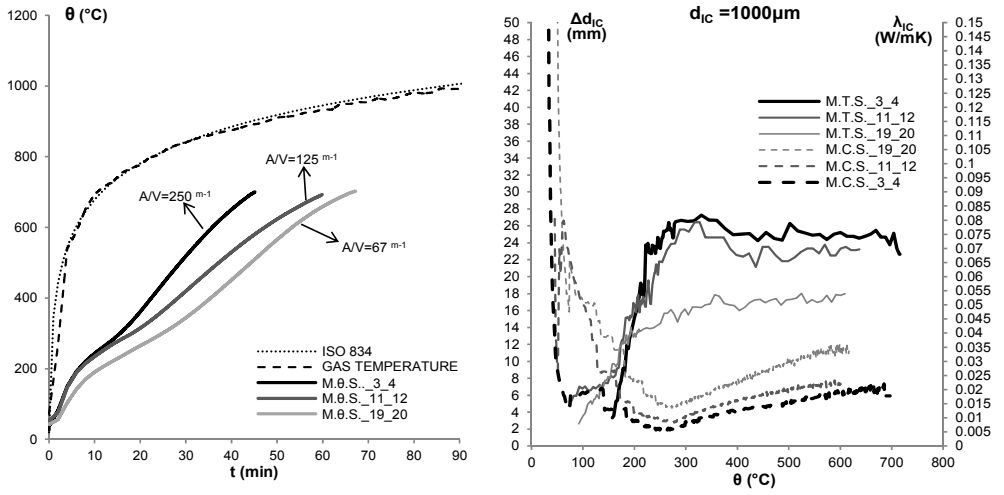

(a) (b)

Figure 2.12. Results for samples with 1000 μm of IC- (a) temperatures, (b) thickness and conductivity.

The Figure 2.12 shows a comparison in terms of temperatures, conductivity and swelling between samples with different section factors but protected with the same IC thickness (1000μm).

The samples with the highest section factor have the highest temperature, but they have also the biggest swelling; correspondingly, the conductivity is the lowest.

The considerations are the same observing Figure 2.13, which refers to specimens having the IC thickness 1500 μm, but of different section factors.

These results show that both the swelling and the IC conductivity depend on the section factor.

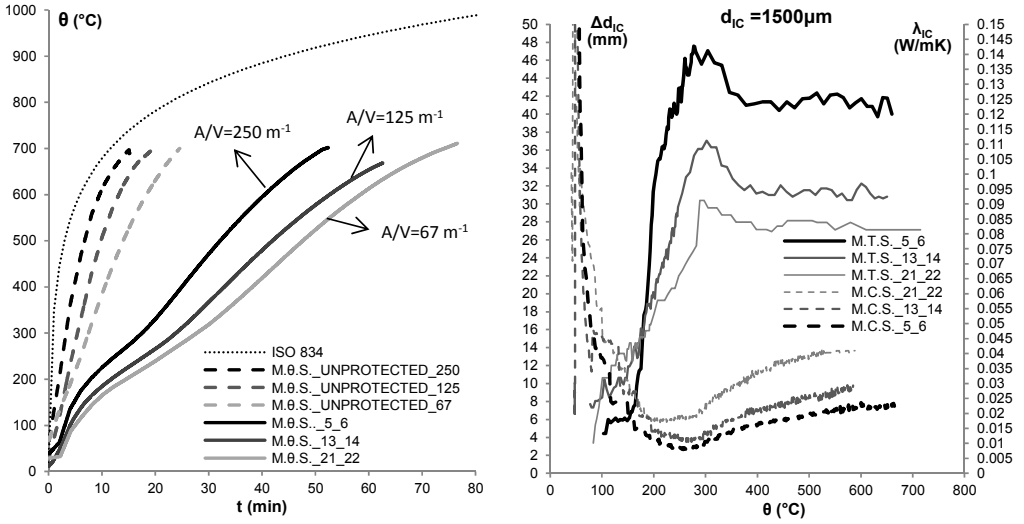

Figure 2.13. Results for samples with 1500 μm of IC- (a) temperatures, (b) thickness and conductivity

The following figures show the trends of the thickness and the conductivity as a function of temperature for samples having equal section factor, but different thicknesses of IC.

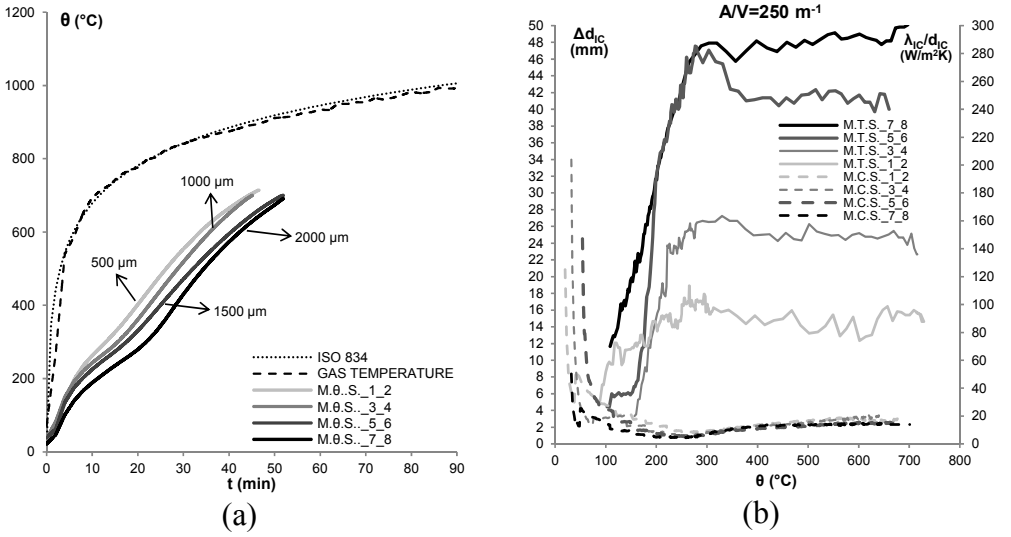

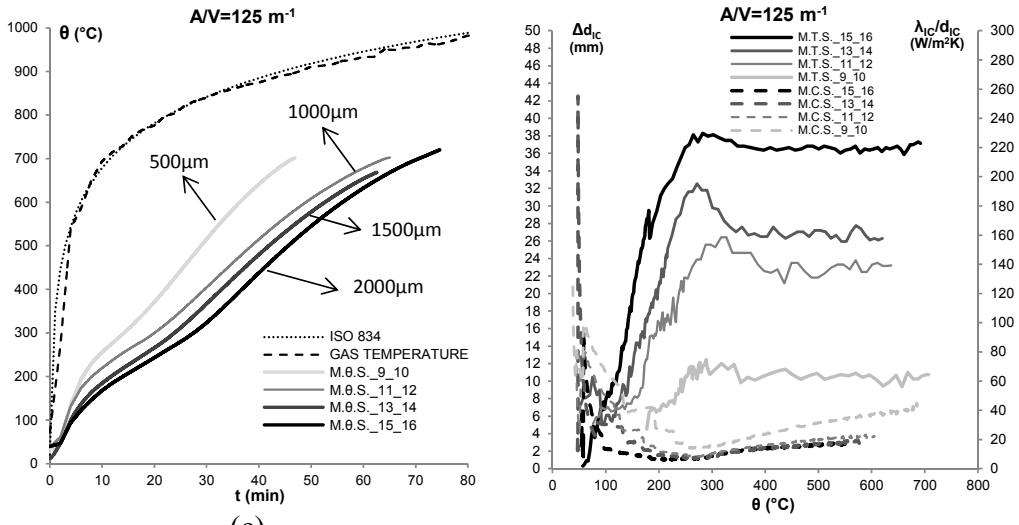

Figure 2.14. Results for samples with A/V= 250 m-1 and A/V= 125m-1 -(a) and (c) temperatures, (b) and (d) thickness and conductivity

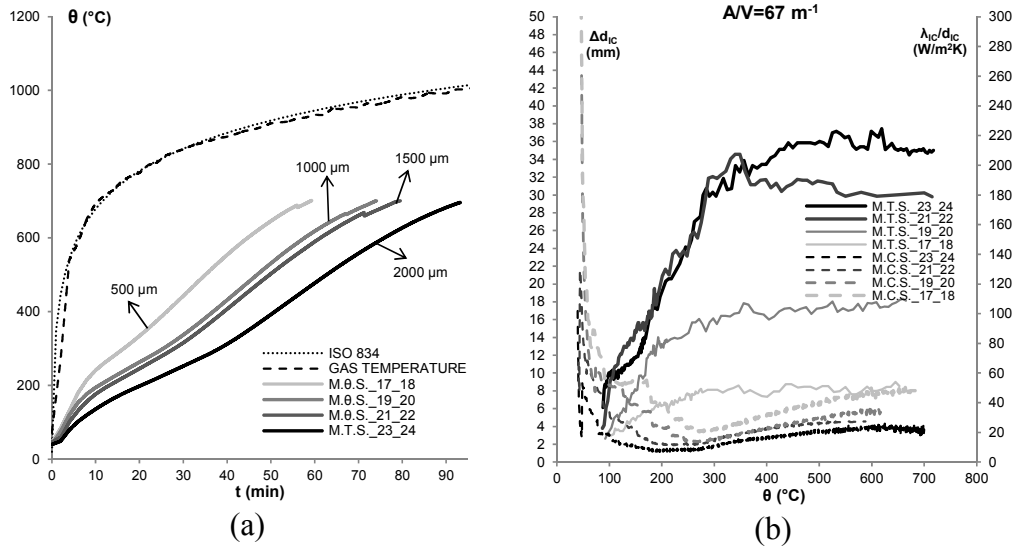

Figure 2.15. Results for samples with A/V=67 m-1 -(a) temperatures, (b) thickness and conductivity

Figure 2.14 shows that, for A/V=250 m^{-1} there isn't a significant dependence between conductivity and swelled thickness, obtaining an unique trend of conductivity with temperature; this result is fully confirmed in the case

of A/V=125 m^{-1} , partially in the case of A/V=67 m^{-1}. Nervertheless, the IC with d_{IC}=500μm can behave differently from the others (Figure 2.15), confirming the unstable behavior.

In both cases (Figure 2.14 and Figure 2.15), the results show that although the thickness after about 300°C stabilizes, the conductivity is not constant with the increase of temperature.

As shown in the previous graphs, during furnace test, the equivalent thermal conductivity of IC reaches a minimum value (λ_{IC_min}) at a certain temperature $\theta_{\lambda,min}$, and after it starts to grow until 700 °C.

The Figure 2.16a shows that, the temperature θ_{λ_min} at which the minimum value of equivalent thermal conductivity is reached is almost the same for all the samples (about 250 °C).

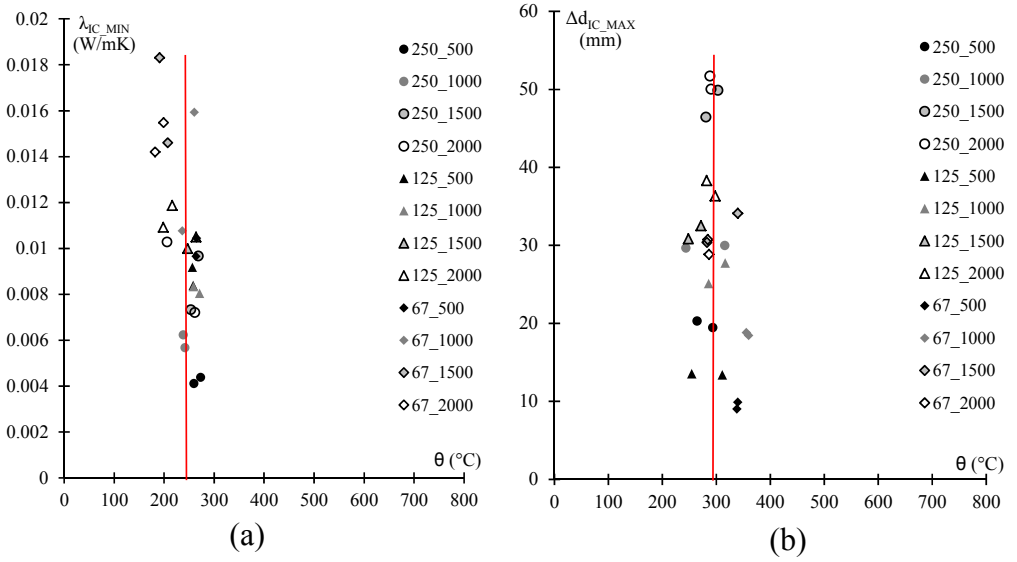

Figure 2.16. (a) Minimum values of IC conductivity (λ_{IC_min}) and (b) maximum value of IC swelled thickness (Δd_{IC_MAX})

Figure 2.16b shows that the maximum swelling is observed for many samples at about 300°C.

As also said before IC react to heat by swelling in a controlled manner to many times their original thickness to produce a carbonaceous char which acts as an insulating layer to protect the steel section to which it is applied.

Intumescence is a complex process in which chemical reactions take place to convert the coating to a viscous liquid. At the same time, gases are produced and trapped within the liquid. This causes the swelling and formation of the insulating char. The intumescent mechanism and subsequent char formation absorbs heat from the fire helping to keep the temperature of the steel below its limiting temperature and to provide the required period of structural fire-resistance. So, the difference between the temperature at which the thermal conductivity is minimum, θ_{λ_min}, and the maximum swelling occurs, θ_{d_max}, is due to the fact that the intumescence reaction is endothermic.

Figure 2.17 shows that both the specific thermal conductivity at θ_{λ_min} and θ_{d_max} depend on the section factor: bigger is the section factor, smaller is the specific thermal conductivity.

The behavior of the samples with 500 μm IC is not stable, as already shown in Figure 2.10.

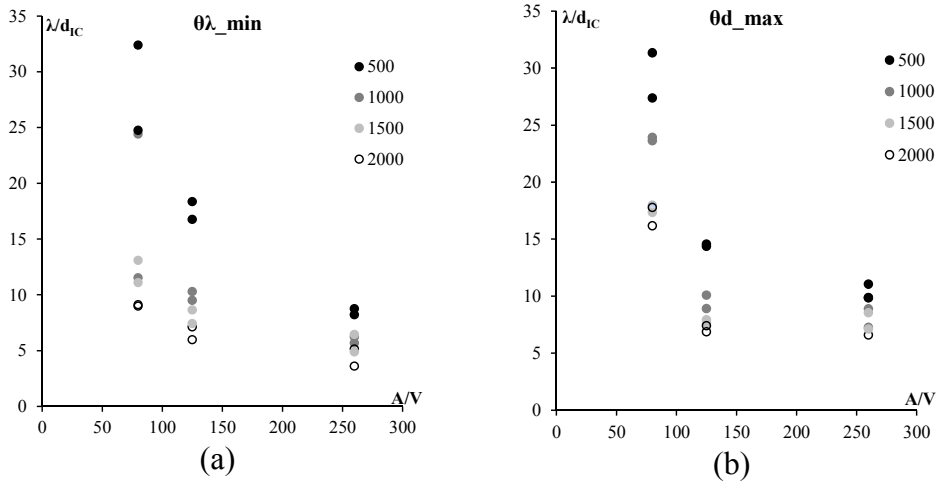

Figure 2.17. (a) Variation of specific thermal conductivity at θ_{λ_min} and (b) at θ_{d_max}

Another relevant point for the IC behavior, as described in paragraph 2.5.1, is the activation point, identified also in Figure 1.7. Also in this case the

activation temperature is very similar for all the samples (Figure 2.18), so, in the following the mean temperature $\theta_{activation}$= 120 °C will be considered.

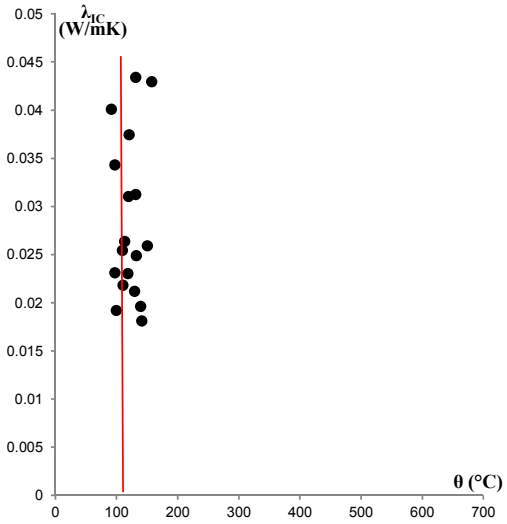

Figure 2.18. Activation temperature for ISO samples.

2.5.2 COMPARISON BETWEEN "SMALL" AND "BIG" SAMPLES

Figure 2.19 shows a comparison between the "big" samples (from no.1 to no.24) and "small" samples (from no.25 to no.36) with the same section factors. Even if between samples 13_14 and 31_32, 5_6 and 27_28 the section factors and the IC thickness are the same, the behavior is different. The temperature are different due to the absence of reaction of IC on the exposed lateral surfaces of the "small" samples (see Figure 2.19a). This is also confirmed by comparing the "small" and "big" samples temperatures without any protection (see Figure 2.19b) which are practically the same, so there is no effect of the shape of the sample, fixing the section factor in the case of unprotected samples. Since the thermal conductivity can be calibrated according to Eurocode for "big" samples only (see par.2.1.2), in the theoretical model the thermal conductivity calibrated for the "big" samples is used for the model of the "small" one as well. While for the "big" sample the 2D analysis was performed, for the "small" one a 3D analysis was necessary because the lateral thickness of the samples were also exposed. Since the IC on the lateral sides of "small" samples did not react

during the test, in FE model the lateral surface is assumed not protected by IC and it was directly exposed to fire. The results are in a good agreement in both cases (see Figure 2.20*).*

(a)

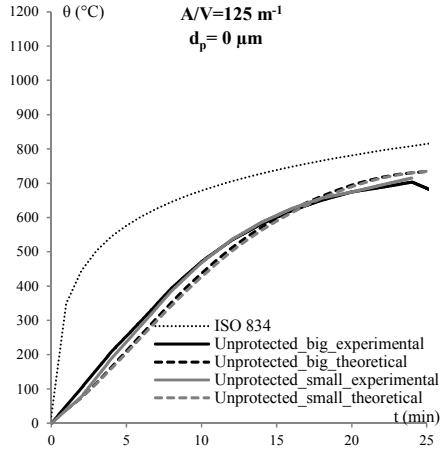

(b)

Figure 2.19. Small samples in the furnace (a), comparison between "small" and "big" samples without protection.

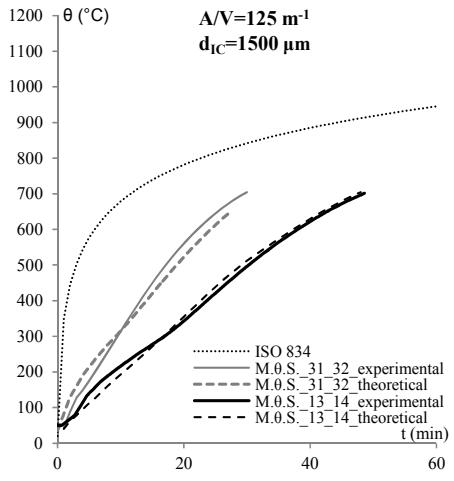

(a)

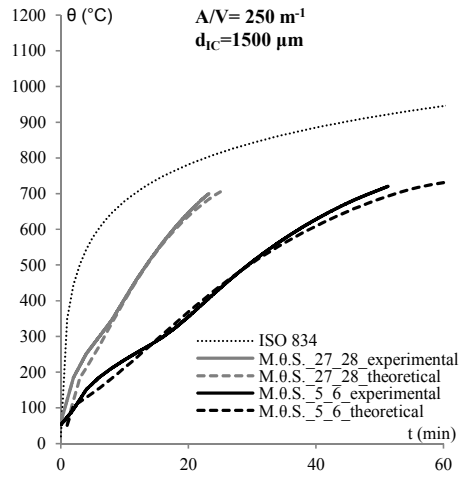

(b)

Figure 2.20. Temp. of "big" and "small" samples_ d_{IC} 1500 µm (a) A/V 125 m-1,(b)250m^{-1}

2.5.3 DATA PROCESSING AND COMPARISONS (SMOULDERING CURVE)

Many results presented for the samples with ISO834 curve, are confirmed for the ones with Smouldering curve, as shown in the following figures (Figure 2.21, Figure 2.22, Figure 2.23).

The Figure 2.21, Figure 2.22 show that the behavior of the IC depends on the section factor both in terms of swelling and in terms of conductivity.

In particular, as before, bigger is the section factor, bigger are both the temperature and the swelling; while lower is the thermal conductivity.

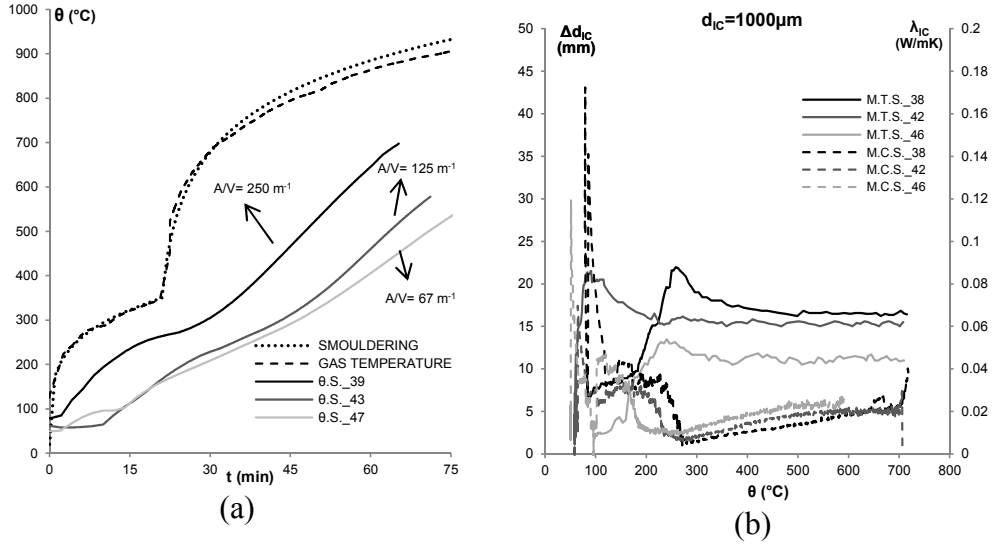

Figure 2.21. Samples results with 1000 μm of IC - (a) temperatures, (b) thickness and conductivity.

Figure 2.22 shows the behavior in terms of swelled thickness and "specific equivalent conductivity" (λ_{IC}/d_{IC}) versus the temperature, of samples with same section factors but with different thickness of IC.

In particular, observing the Figure 2.22, a dependency of the "specific equivalent conductivity" on the thickness of IC appears, but this is not confirmed by the Figure 2.23, where all the samples having A/V= 67 are represented. In addition, from Figure 2.22a, a strange behavior of the specimen S_37 appears: at about 250 °C there is a sudden increase of the temperature

with a consequent increase of the conductivity of IC (Figure 2.22b); once again, unstable behavior of protected specimens with 500 is confirmed, with irregular swelling of IC (Figure 2.22c).

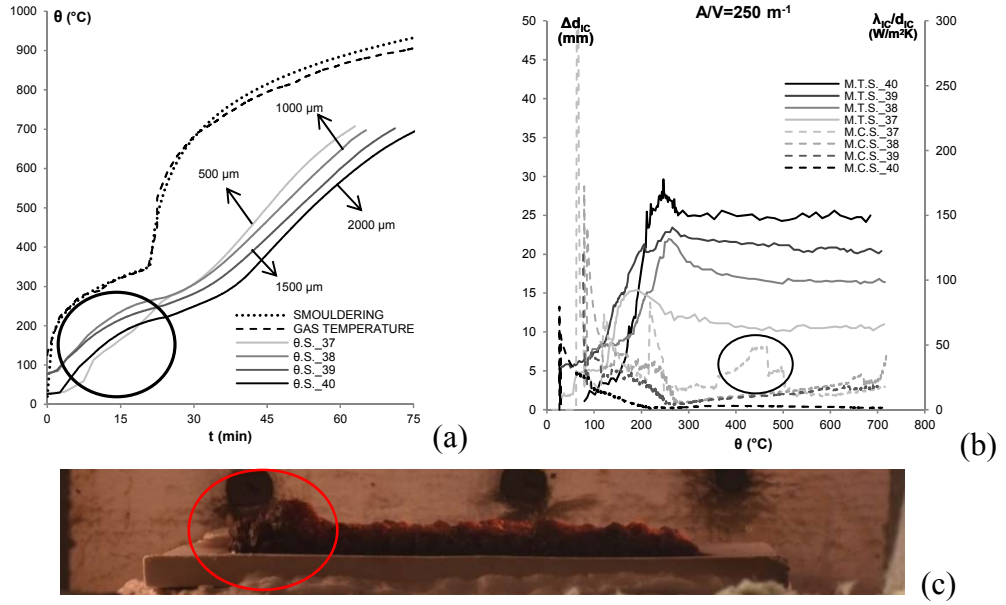

Figure 2.22. A/V= 250 m-1 -(a) temperatures, (b) thickness variation ΔdIC and specific conductivity λIC/dIC; (c) picture of sample n°37.

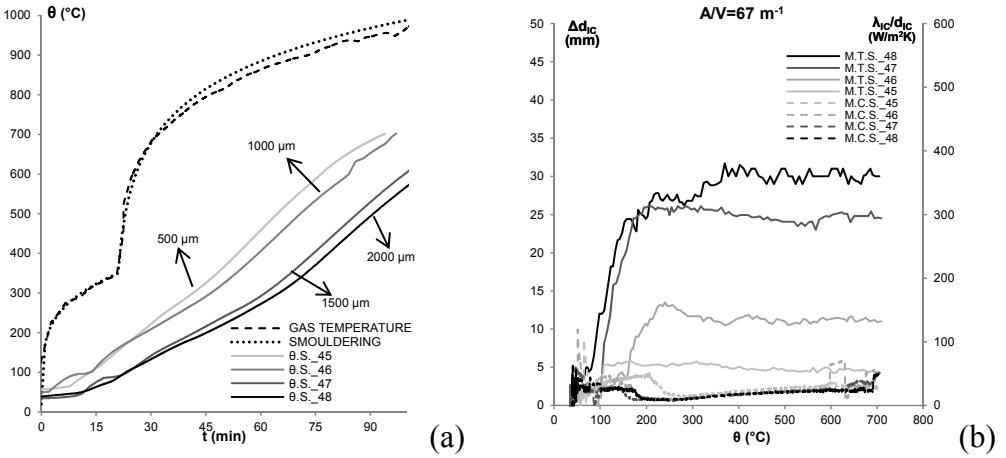

Figure 2.23. A/V= 67 m^{-1} -(a) temperatures, (b) thickness variation Δd_{IC} and specific conductivity λ_{IC}/d_{IC}.

As shown in the previous graphs, during furnace test, the equivalent thermal conductivity of IC reaches a minimum value (λ_{IC_min}) at a certain temperature $\theta_{\lambda,min}$, and after it starts to grow until 700 °C: this behavior is confirmed also in the case of smouldering test results.

The Figure 2.24a shows that, the temperature $\theta_{activation}$ is very similar for all the samples and the mean value is again approximately 120°C, while θ_{λ_min} at which the minimum value of equivalent thermal conductivity is reached is almost the same for all the samples, again about 250 °C.

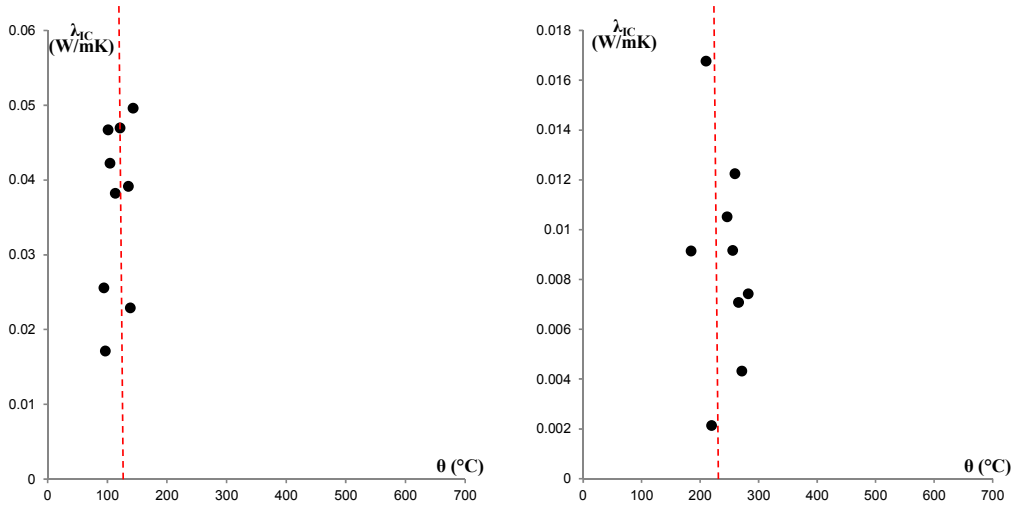

Figure 2.24. (a) . Results with smouldering curve: Value if IC conductivity at activation temperature, (b). Minimum values of IC conductivity.

2.5.4 COMPARISON BETWEEN THE RESULTS WITH ISO834 AND SMOULDERING CURVES

To date, the majority of previous research studies into the behavior of IC have been experimental based and mainly focused on understanding the effects of different formulations to help manufacturers develop products to pass the standard fire resistance rating test [53][54][47].

Very few studies have been conducted to investigate the performance of intumescent coatings under different fire conditions, with very limited success in modelling.

But anyway, as stated above, the regulations[63] require tests in furnace under the slow heating curve as well, in order to check that the performances of the IC are not affected by fire curves with low thermal gradients.

In the Figure 2.25. A/V= 250 m-1 and 1500 μm -(a) temperatures, (b) thickness variation ΔdIC and specific conductivity λIC/dIC.a,b the samples with same section factor and with same thickness of IC, but with different fire curves, are compared.

The temperature reached in the samples under the ISO834 fire curve are greater than those achieved under the Smouldering curve (Figure 2.25a); also the swelling of IC for the samples under ISO834 curve is bigger, but the specific equivalent conductivity is practically the same in the both fire curves.

In both fire curves the specific equivalent conductivity of IC reached a minimum value around 250°C-300°C and after it seems to be stabilized. At about the same temperature (250°C-300°C) the thickness of IC has a pick and then it becomes almost constant, as shown also in the previous figures.

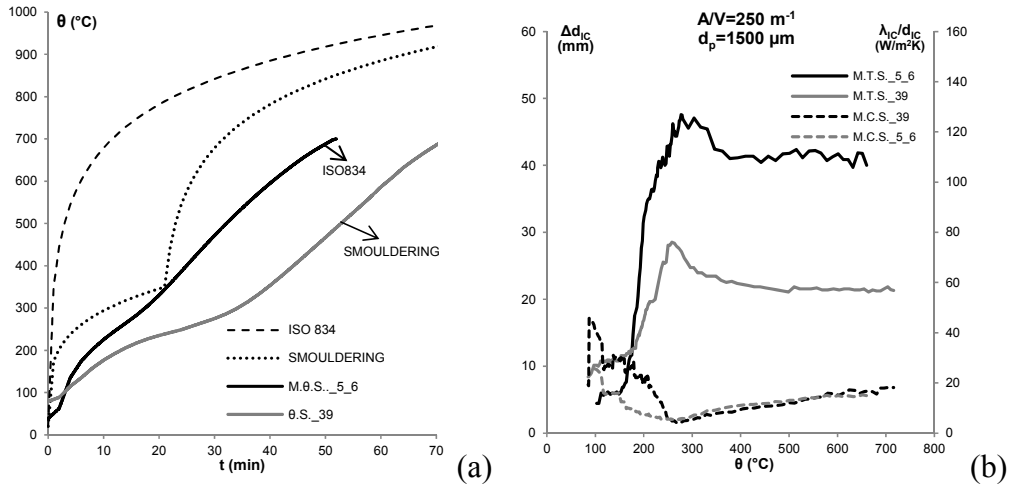

Figure 2.25. A/V= 250 m-1 and 1500 μm -(a) temperatures, (b) thickness variation Δd_{IC} and specific conductivity λ_{IC}/d_{IC}.

Probably this behavior is related to the different swelling mechanism of the IC in the case of the two fire scenarios (ISO and Smouldering): the maximum temperature, the heating rate and the test duration have influenced the intumescent process and the char structure formation. This leads in many different char structures with various characteristics, such as the size and shape of the bubbles [76]. Indeed, the Figure 2.26a,b show the microscopic pictures of the foam in the both cases of ISO and Smouldering curves.

The bubbles of the IC under ISO 834 curve, appear more round, regular and close to each other, while those of the Smouldering appear more irregular and larger. This different swelling does not seem to affect the efficiency of IC, in terms of thermal conductivity Figure 2.25a,b)[76].

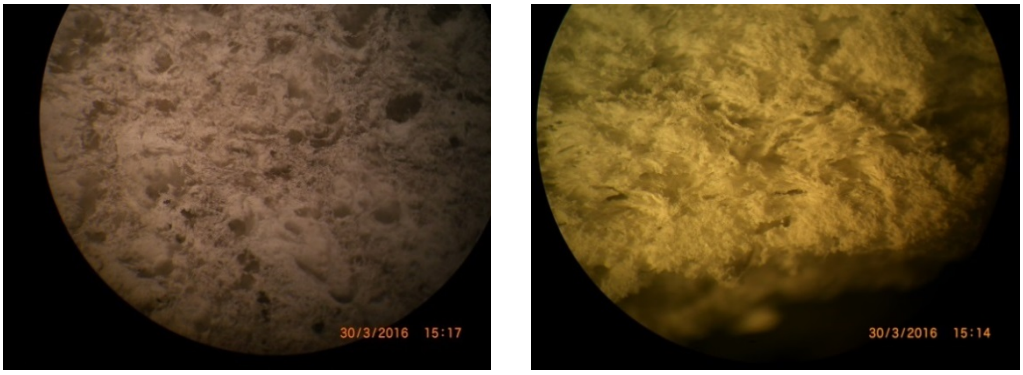

(a) (b)

Figure 2.26. Microscopic pictures of foam for- (a) ISO834 curve and (b) Smouldering curve.

As described in the previous paragraphs, $\theta_{activation}$ in the case of ISO834 and smouldering curves are approximately 120°C, while the temperature θ_{λ_min} is about 240 °C for both the series of tests (Figure 1.7, Figure 2.18, Figure 2.24).

In particular, even if the activation temperature is very similar for ISO and Smouldering samples, the values of the thermal conductivity of the smouldering samples are, on average higher than the ISO ones (Figure 2.27a), while, for $\theta_{\lambda\_min,}$ both the temperatures and the thermal conductivity values are very close to each other (Figure 2.27b).

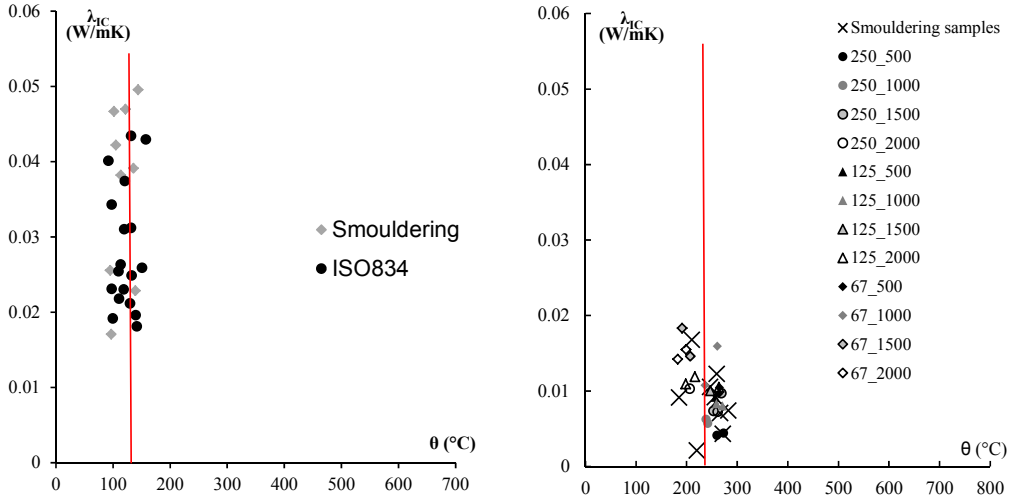

Figure 2.27. (a)Value of IC conductivity at activation temperature for all the samples, (b) Minimum values of IC conductivity for all the samples.

2.6 EXPERIMENTS IN THE CONE CALORIMETER

The cone calorimeter is a performance-based bench scale fire testing apparatus[77][78]. Sample plates 100x100x6 mm in size are investigated under forced-flaming conditions[79]. The sample size is of the smallest order of magnitude discussed in fire engineering and of the largest used in polymer analysis. Hence, the cone calorimeter constitutes an important link between fire engineering and polymer science, which is crucial in the interdisciplinary area of fire science. Furthermore, it provides comprehensive insight into not only fire risks such as heat release rate, total heat release, and time to ignition, but also fire hazards such as smoke release and CO production.

The cone calorimeter setup [80] was developed thoroughly to target the properties of materials rather than to correspond to a special full-scale scenario of a real fire. Cone calorimeter investigations can be used as a universal approach to ranking and comparing the fire behavior of materials. Therefore, it is not surprising that the cone calorimeter is finding increasing implementation as a characterization tool in the research and development of fire retarded polymeric materials. However, each experimental setup defines a specific fire

scenario. As is typical for all fire tests, samples' performance in the cone calorimeter depends on the specific characteristics of the test, including ignition source, ventilation, irradiance (external heat flux), temperature, and the geometry of the specimen. Strictly speaking, the cone calorimeter test characterizes the performance resulting from an interaction of material properties, specimen, and the defined fire scenario.

The meaning of the results may have little relevance for other fire scenarios or fire tests that differ in their essential setup. Some of the crucial setup characteristics are obvious, such as horizontal sample positioning, melt dripping prevention, and well-ventilated combustion, and the effects of these characteristics on the results are well known. However, some cone calorimeter characteristics are less obvious and are sometimes neglected detrimentally in performing cone calorimeter tests or discussing their results. Since the cone calorimeter constitutes an important link between fire engineering and polymer science, the second set of experiments in this project consists of several tests in cone calorimeter. The experimental tests were performed at the Fire Safety Engineering Research and Technology Centre (FireSERT) laboratory in a cone heater where the steel plates samples were exposed to a controlled radiation.

Also in this case, the main aim was to better understand the behavior of three different commercial intumescent coatings subjected to different fire scenarios, in particular different heat fluxes on a flat horizontal surface.

2.6.1 TEST INSTRUMENTATION: CONE CALORIMETER

The mass loss cone heater is an established device for measuring the heat release rate of combustible materials in respect to different fire impacts.

In particular, it has the ability to create a heat flux on a small area (about 100 cm^2) at a particular distance from the heat generation device. The radiation is provided by a steel spiral located in the cone above the sample. Samples can be exposed to different heat fluxes: by adjusting the temperature of the spiral, a desired level of radiation is provided to the specimens at a defined distance.

All the dimension of the mass loss cone heater are the ones according to the standard ISO 5660-1 [80]. This regulation explains the method for performing

the cone calorimeter test in terms of heat release rate and smoke production rate of specimens exposed to irradiance under control levels from external igniter.

The cone heater generates radiant heat fluxes up to 100 kW/m^2 at 25 mm distance corresponding to a post-flashover room fire at a very high level. The cone heater was used to simulate radiant heat fluxes typical for room fires Figure 2.28.

In particular, test apparatus, shown in Figure 2.28, consists of an exhaust hood, conical heater, sample holder, load call and various other parts.

As the intumescent materials expand during exposure to heat, hence, the specimen holder was placed such that there was a distance of 60mm between the top surface of the specimen bottom of cone heater to avoid any contact with the source as recommended by the guidelines [80].

Figure 2.28. Cone calorimeter.

2.6.2 INPUT HEAT FLUX

Also in the cone calorimeter, the steel plates were exposed to non-standard fire curves, in order to understand the relationship between the intumescent coating characteristics and heating fluxes.

According to the suggestion given in a previous study by Zhang et al. [76], different heat fluxes were implemented for the experiments conducted in the cone heater in order to investigate the influence of two heat fluxes on the

behavior of intumescent coatings. The desired heat fluxes were achieved by adjusting the temperature of the cone heater spiral to some defined values, obtained by a calibration procedure. The spiral temperatures were strictly related to the specimen distance, set to 60 mm according to the corresponding standard [80], but sometimes this distance was increased in order to make the IC visible during the test and to measure the thickness increase. In particular, all the unprotected and protected steel specimens (with different IC applied in two different d_p) were exposed to thermal radiation from the cone heater with heat fluxes of 30 and 50 kW/m^2.

The test durations were decided based on the time necessary for the intumescent coating and the steel sample to reach a steady condition: all the experiments lasted for 30 minutes. Moreover, this tests focus on the first phase of IC activation, which is most critical for this material and it especially depends on several conditions like the input fire curve.

2.6.3 TEST SAMPLES AND EXPERIMENTAL SETUP IN CONE CALORIMETER

The experimental set-up is well defined in the corresponding IS0 5660-1 international standard [80]. In particular test specimens consisted of square steel plates with an area 100 cm^2 having a thickness of 6 mm each, so the section factor is approximately 166 m^{-1} [80]. Specimen holder used during the test has a square shape with 151.29 cm^2 area and a depth of 26 mm as shown in Figure 2.29. The lower 13 mm part of the specimen holder was made from the wool board while the upper 13mm part was made from stainless steel having a thickness of 2.5mm.

Figure 2.29. Sample holder.

The platform, on which the specimen holder was to be mounted, was built using stainless steel and placed under the conical heater exactly in the middle. On the inner sides of the specimen holder, 3mm thick mineral wool (which is a material that stands very high temperatures and has a low thermal conductivity) was laid in two layers in order to minimize the heat loss to the surrounding environment and to provide adiabatic boundary conditions to the specimen leaving an area of approximately 112.36 cm^2 to place the specimen.

However, it is important to underline that the standard ISO 5660-1 assesses that the distance between the bottom surface of the cone heater and the upper surface of the specimen shall be adjusted to 60±1 mm for dimensionally unstable materials, so the vertical distance between the top surface of the specimen and the bottom surface of the cone calorimeter was kept 25mm or 60mm as recommended by ISO-5660 [80] for different tests depending upon the IC expansion during the tests.

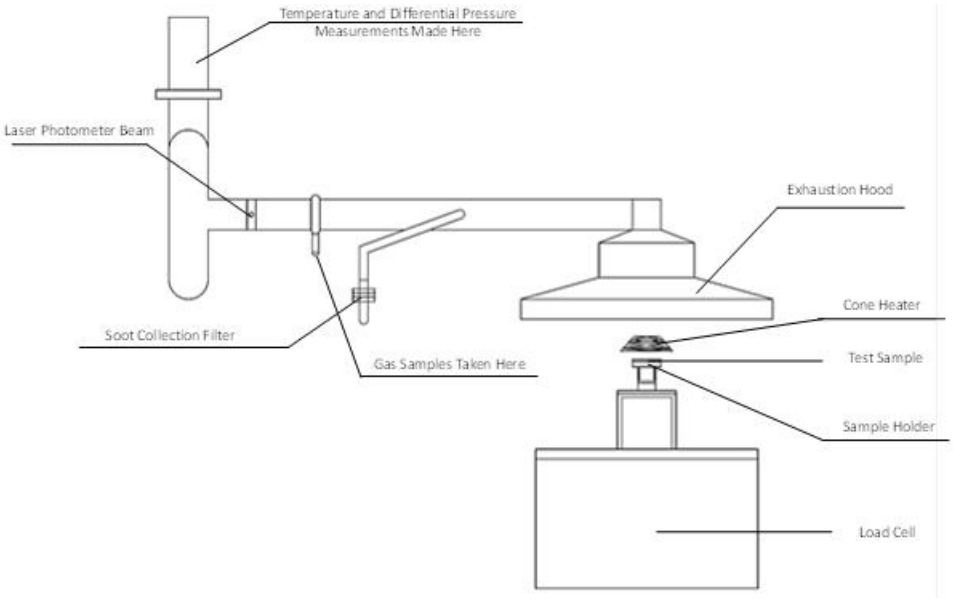

Figure 2.30. illustrative diagram of experimental set-up in the cone calorimeter

As also described before three different water based intumescent coating materials, IC_A, IC_B and IC_C, were used during the tests.

A total of 18 painted specimens, 6 from each intumescent type were prepared. Three specimens had a thickness of 1000 μm while the other three had a thickness of 1500 μm (Table 2-2).

To achieve the required thickness of the intumescent coating material, bare steel plates with holes drilled for thermocouples were weighed and painted with a layer of material (Figure 2.31).

Figure 2.31. samples preparation.

First group of tests were performed to study the behavior of different available materials at elevated temperatures while the later was performed to assess the efficiency of mode of application, sprayed application and painted application.

Approximate thickness of the material was found by weighing the painted steel plates and comparing the weight of the bare steel before application. During this calculation, the density of the intumescent material was used as given by the manufacturer for each type.

Thickness of the layer and the time between multiple layers was used as specified by the manufacturer.

Finally, after application of multiple layers, the required thicknesses of the intumescent coating material were obtained. One of the type of intumescent coating material, in this case IC_C, was randomly selected and used to prepared 6 additional painted specimens with a thickness of 1000 μm.

These specimens were prepared by apply the IC on the steel plate by professional painters with airless, while in the previous cases it was applied

through painting. Once again, material was applied in layers as recommended by the manufacturer.

The purpose of preparing samples with a different mode of application was to assess the efficiency of application technique.

All the finished specimens were kept in the conditioning room for a period of four weeks before test, as recommended by manufacturer. Further, the specimens were also kept in the conditioning room between the application of layers to ensure uniformity in drying of the applied coating.

Table 2-2 Test matrix_cone calorimeter.

ID	IC Type	d_p (µm)	Heat Flux (kW/m^2)
A1_1000_50	IC_A	1000	50
A2_1000_50		1000	50
A3_1000_30		1000	30
A4_1500_30		1500	30
A5_1500_50		1500	50
A6_1500_50		1500	50
B1_1000_30	IC_B	1000	30
B2_1000_50		1000	50
B3_1000_50		1000	50
B4_1500_30		1500	30
B5_1500_50		1500	50
B6_1500_50		1500	50
C1_1000_30	IC_C_painted	1000	30
C2_1000_50		1000	50
C3_1000_50		1000	50
C4_1500_30		1500	30
C5_1500_50		1500	50
C6_1500_50		1500	50
C*2_1000_30	IC_C_spryed	1000	30
C*4_1000_30		1000	30
C*9_1000_50		1000	50
C*10_1000_30		1000	30
C*11_1000_50		1000	50
C*12_1000_50		1000	50

Data logging system was used to measure the temperature development and thermal radiations emitted lateral to the surface of the test specimen.

Two camcorders were used, one positioned in front of the apparatus and other at the left-hand side to record the behavior of intumescent coating material during the test (Figure 2.32).

Figure 2.32. experimental set-up in the cone calorimeter.

2.6.4 EXPERIMENTAL SETUP VALIDATION

Also the cone calorimeter experimental set-up was validated respect to the heat transfer model of unprotected steel subjected to pure radiation.

During the test, experimental setup was calibrated with reference to the guidelines [80] and initially four tests on bare steel plates were performed.

Two of these tests were conducted on exposure of 30kW/m^2 heat flux while the other two were exposed to 50kW/m^2. Temperature developments on the bare steel plates will provide a direct comparison to check the effect of the intumescent coating material on temperature development and its efficiency and after the temperature-time curves of the unprotected steel provided by the tests in the mass loss cone heater were compared to the analytical model implemented in the FE code SAFIR16.

As it is possible to state from Appendix B, the analytical and the experimental curves were really similar.

2.6.5 TEMPERATURE ACQUISITION

Also in this experimental set-up, the temperatures were monitored by installing thermocouples on the specimens. Once again, the thermocouples were placed in the steel substrate of major interest in order to reproduce accurate distributions of the average temperature.

Two thermocouples 1.0 mm diameter were placed centrally the steel plate specimens and 3 centimeters distant from each other on the back the steel sample. Two holes, one in the center and one at a distance of 20 mm (Figure 2.33) from the center were drilled in the specimen holder insert the thermocouples through in the later stages. In addition to the holes, groves were formed to enable easy passing of thermocouples wires connecting to the data logging system. In particular two NiCre-Ni thermocouples of type K, 1.0 mm diameter thermocouples were mounted on the steel plate to measure the temperature during the tests. Thus, the thermocouples tips were placed inside the drilled holes and a small amount of aluminum tape was used to fix the thermocouple wire to the surface of the steel.

Also in this particular experimental set-up, the thermocouples attachment method has a crucial importance in the data collection, in particular to reduce the possibility of technical and systematic errors. Once again, the method adopted represents the best solution that was reached for this case after many preliminary tests, regarding practical simplicity and ease of execution.

Unfortunately, it was not possible to directly evaluate the surface temperature of the IC, since the coating expanded during the test and more sophisticated techniques were necessary for this purpose, for example thermographic phosphor technique [44], which is, however, not entirely reliable.

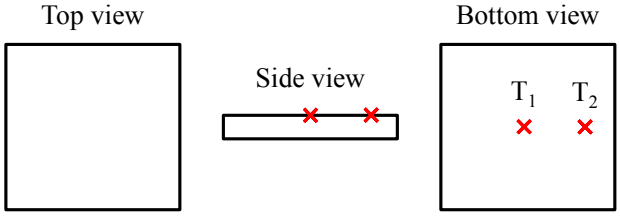

Figure 2.33. thermocouples positions in the cone heater experimental set-up

2.6.6 THICKNESS MEASUREMENT

A CCD camera was used to observe the varying thickness of the IC also in this case. In this case a direct reading of IC expansion was possible because one meter stick was placed behind the sample during the test Figure 2.34.

Figure 2.34. sample during cone calorimeter test.

Compared to the DIC technique, the reading with meter stick are more convenient and faster, but, in the first swelling zone it is less precise because only when it reaches the millimeter scale it starts to be measurable

2.7 RESULTS AND DISCUSSION FOR CONE TESTS

As described before, the performance of three different water based intumescent materials on the protected steel was investigated under a cone colorimeter for different radiative heat fluxes; also the thickness of IC were different in 1000 μm or 1500 μm.

2.7.1 DATA PROCESSING : TEMPERATURES

The first analysis of the results was done in terms of the temperatures reached in the different samples. Figure 2.35 shows the average temperature of the backside of the bare steel plate plotted against time with the 30 kW/m^2 and 50 kW/m^2 heat fluxes and a comparison with the same plate exposed to ISO834 and smouldering curve: the greater thermal increasing is observed for 50 kW/m^2 of heat flux.

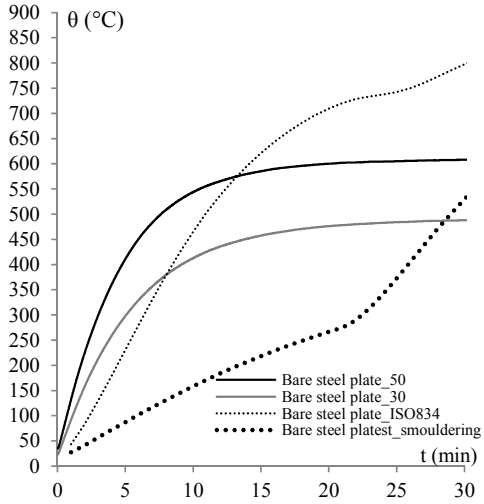

Figure 2.35. Temperature of the bare steel plate under 30 and 50 kW/m^2 , under the ISO and the smouldering curves..

The temperature measurements show the temperature of the covered steel reached steady state conditions after 10 minutes both with 30 kW/m^2 and 50 kW/m^2 heat fluxes. In the following graphs the red lines (at about 500 °C and at about 500°C) represent the ambient temperature, equivalent to the imposed heat flux (30 kW/m^2 and 50 kW/m^2) calculated with Eq. 2-10.

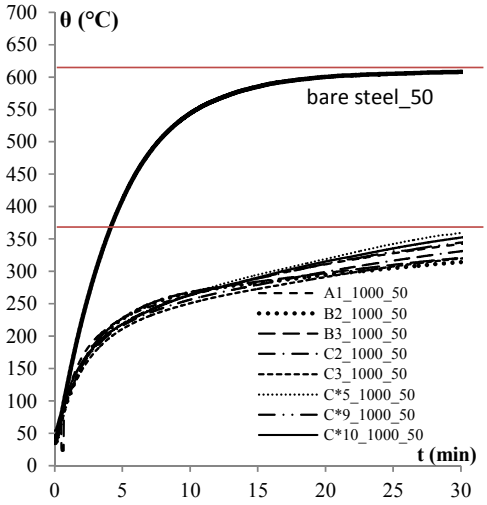

(a)

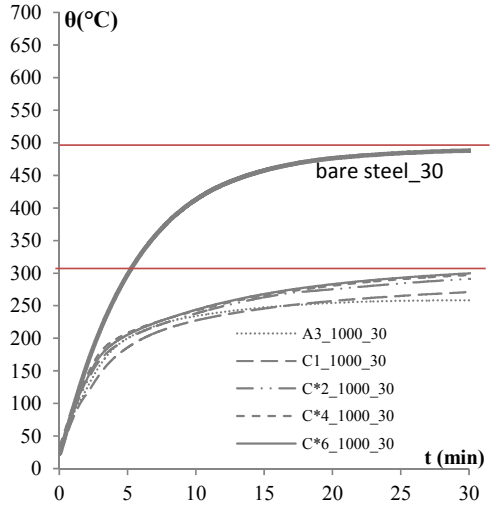

(b)

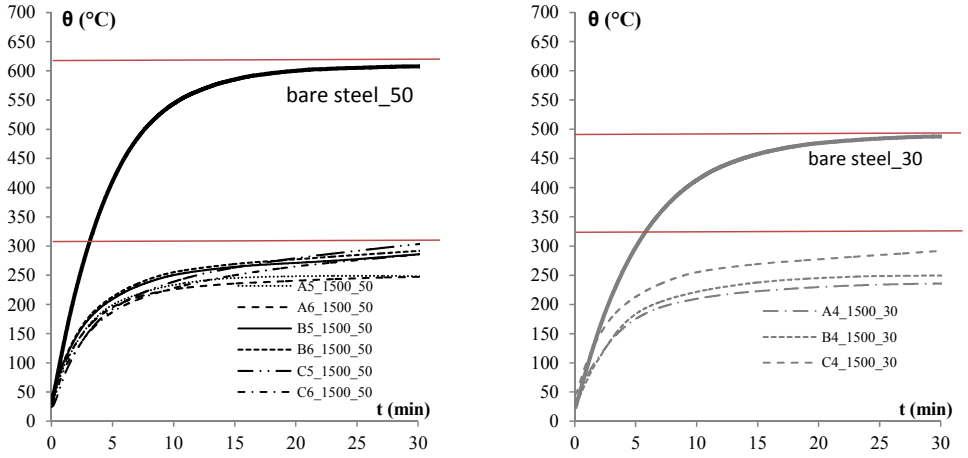

(c) (d)

Figure 2.36. Average temperature of the painted steel plate (a) 1000 μm and 50 kW/m^2, (b) 1000 μm and 30 kW/m^2, (c) 1500 μm and 50 kW/m^2 , (d) 1500 μm and 30 kW/m^2.

The Figure 2.36 shows a comparison in terms of temperatures between the painted samples, fixing the thickness and the heat flux; a small difference of the temperature between the different types of IC appear for both 30 kW/m2 and 50 kW/m2 heat fluxes and for both thickness of IC, while a decrease in temperature is evident, ranging from 1000 μm to 1500 μm of IC applied.

The solid back and grey curves represent the behavior of the bare steel plates; the temperature reduction with respect to the bare steel is remarkable for all cases.

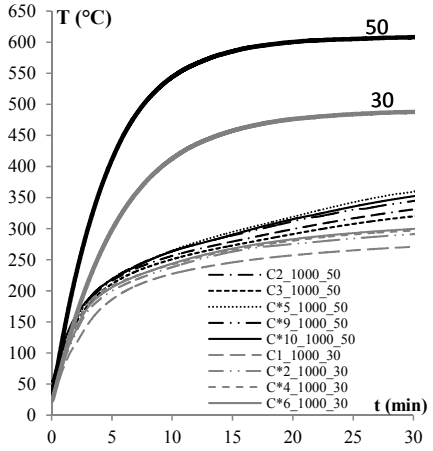

Figure 2.37. Comparison between sprayed and painted plates.

Observing the Figure 2.37, a small influence of the way of IC application appears because the temperatures in the painted specimens are slightly lower than those of the sprayed specimens, both in the case of 30 kW/m^2 and 50 kW/m^2 heat fluxes. Again the solid back and grey curves represent the behavior of the bare steel plates.

2.7.2 DATA PROCESSING : EQUIVALENT THERMAL CONDUCTIVITY

As previous mentioned, the equivalent thermal conductivity is obtained by Eq. 2-9, setting the coating thickness to the initial value d_{IC}.

Since the intumescent coating surface temperature θ_{IC} is really difficult to evaluate and it can be estimated by adopting sophisticated equipment, for instance a thermographic phosphor technique, in this case, in a simplified way the temperature of the IC surface was calculated from Eq. 2-10, fixing Q_e equal to 50 kW/m^2 and 30 kW/m^2 respectively, ε_{IC} =0.95, θ_a is the temperature measured inside the steel plates and σ in the Stefen Boltzman costant. So, in the case of 50 kW/m^2, θ_{IC}=620 °C, while for 30 kW/m^2 θ_{IC}=470°C.

Figure 2.38a,b,c,d compare the equivalent thermal conductivity-temperature relationships with different steel plate thicknesses and different heat fluxes, while in Figure 2.38e there is a comparison between sprayed and painted steel plates.

The intumescent coating temperature is taken as the average value of the steel plate temperature (θ_s) recorded by the two thermocouples.

It can be seen that the equivalent thermal conductivity starts to drop sharply after the intumescent coating temperature has reached approximately 120°C-300°C, which may be taken as the reaction temperature of this type of IC. Before this reaction, the intumescent coating is hardly effective so that the calculated thermal conductivity is high and subject to wild fluctuations.

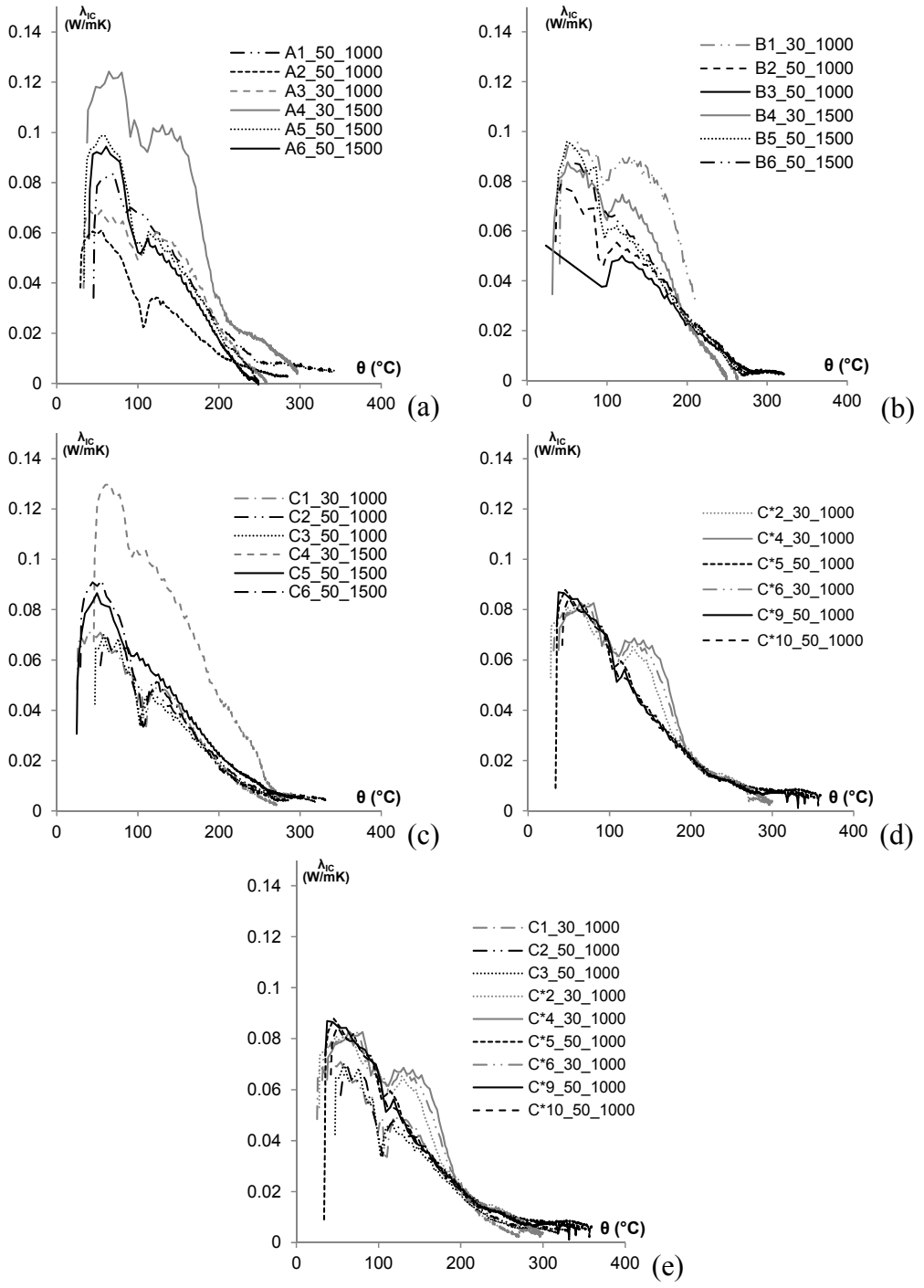

Figure 2.38. Equivalent thermal conductivity.

The calculated equivalent thermal conductivity values seems to become more stable after the IC has reached about 300°C when the IC would have been almost fully effective throughout its thickness.

Therefore, it can be understood that within engineering fire protection it is more convenient to focus on the stable value of IC thermal conductivity because it is during this stage that the IC is the most effective in providing insulation to the protected steel elements, as already observed from the results of furnace tests.

Figure 2.38e shows a comparison between the same samples but sprayed and painted; even if the sprayed sampled with 30 kW/m^2 have a pick around 150 °C, the behavior is very similar, so there is no a significant effect of the way of application.

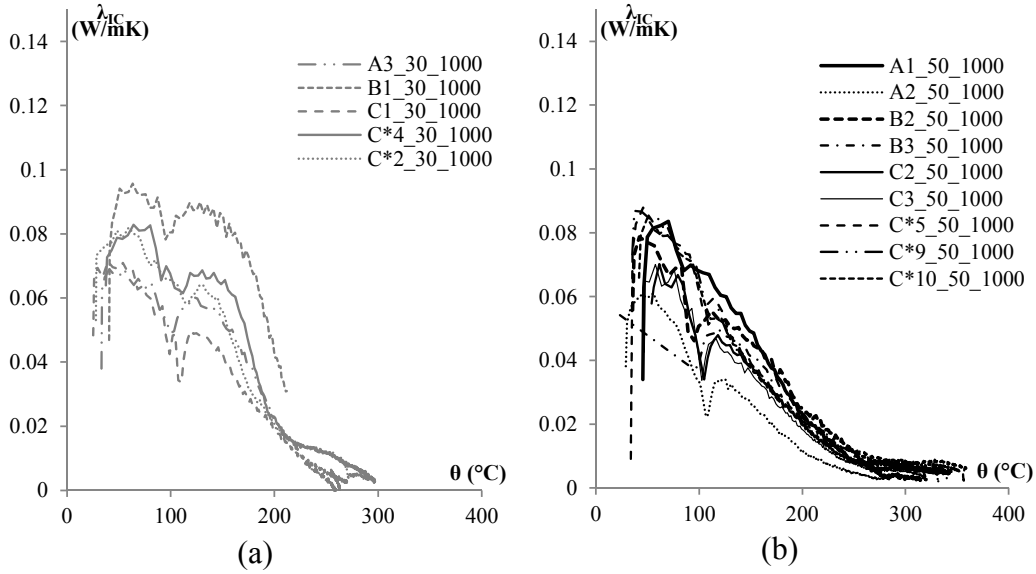

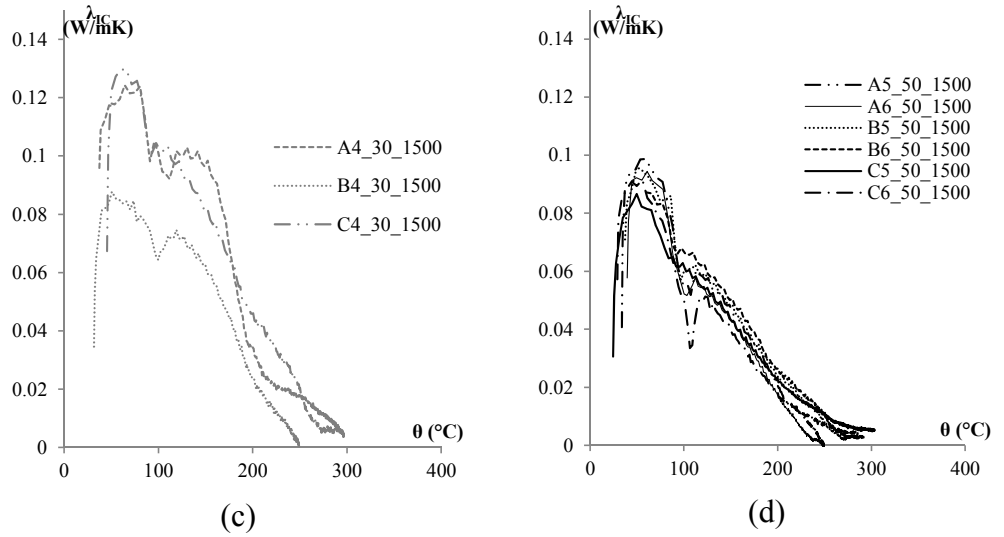

Figure 2.39. Equivalent thermal conductivity: comparison between different IC.

Figure 2.39 compare the behavior of samples with same IC thickness and under the same heat flux, but with different commercial brands: up to 200°C the IC behaviors are different, but after 200°C, it seems to stabilize and the equivalent thermal conductivities become more similar to each other, especially in the case of 50 kW/m^2 (Figure 2.39b,c).

2.7.3 DATA PROCESSING : THERMAL EXPANSION

Clearly, temperature is not the only factor that can affect the equivalent thermal conductivity of IC, otherwise, the equivalent thermal conductivity – temperature relationships of different tests would be similar. One other possible factor is the swelling.

A relatively simple theory [81] for expansion rate of IC is to relate it to the final expansion rate and its density by a power function. However, this model is still not practical to use as it would be necessary to evaluate a number of empirical constants under different conditions.

Bearing in mind the difficulty of obtaining accurate information on thermal conductivity of even conventional fire protection materials, it appears that the scatter using equivalent thermal conductivity of intumescent coating is

practically acceptable. On this assumption, it is now necessary to obtain the expansion rate of IC.

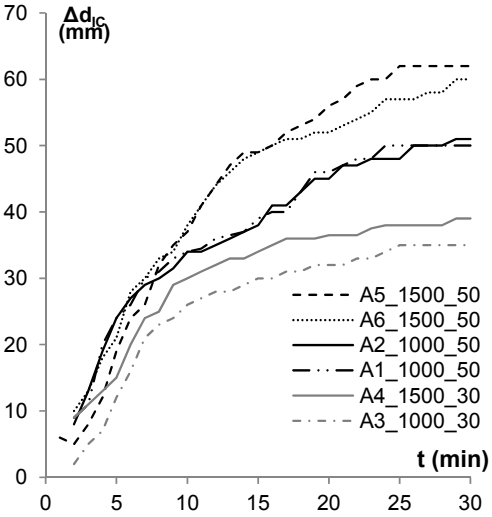

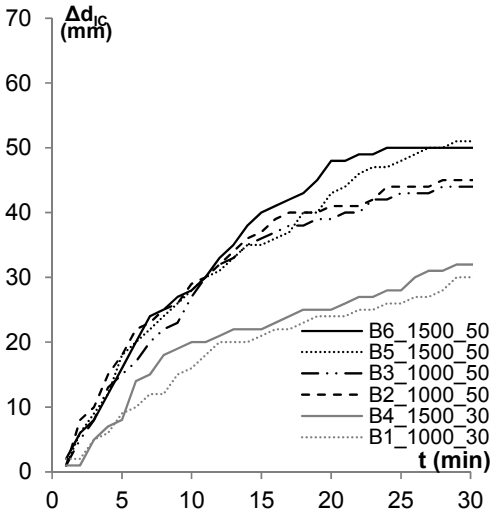

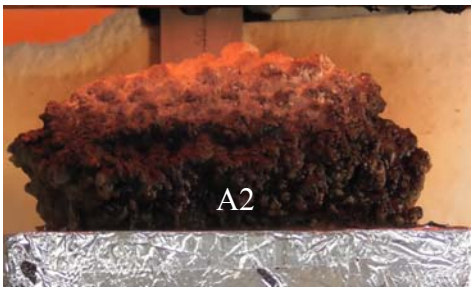

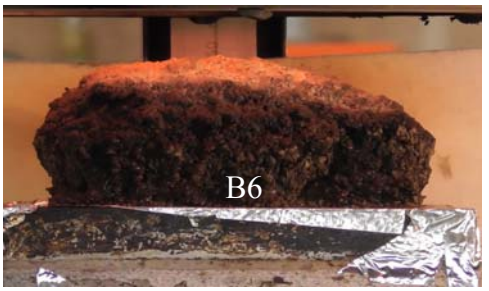

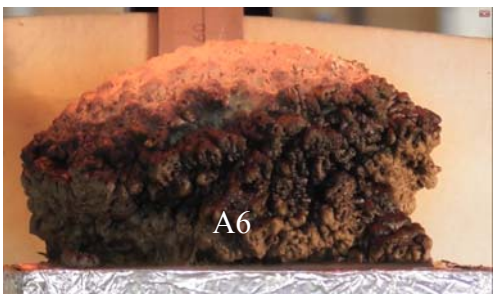

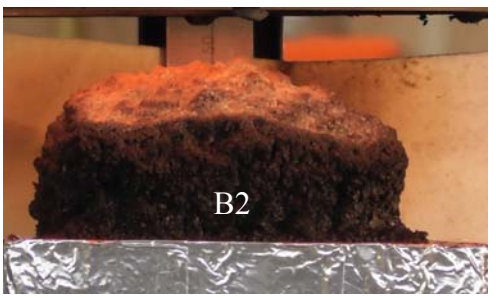

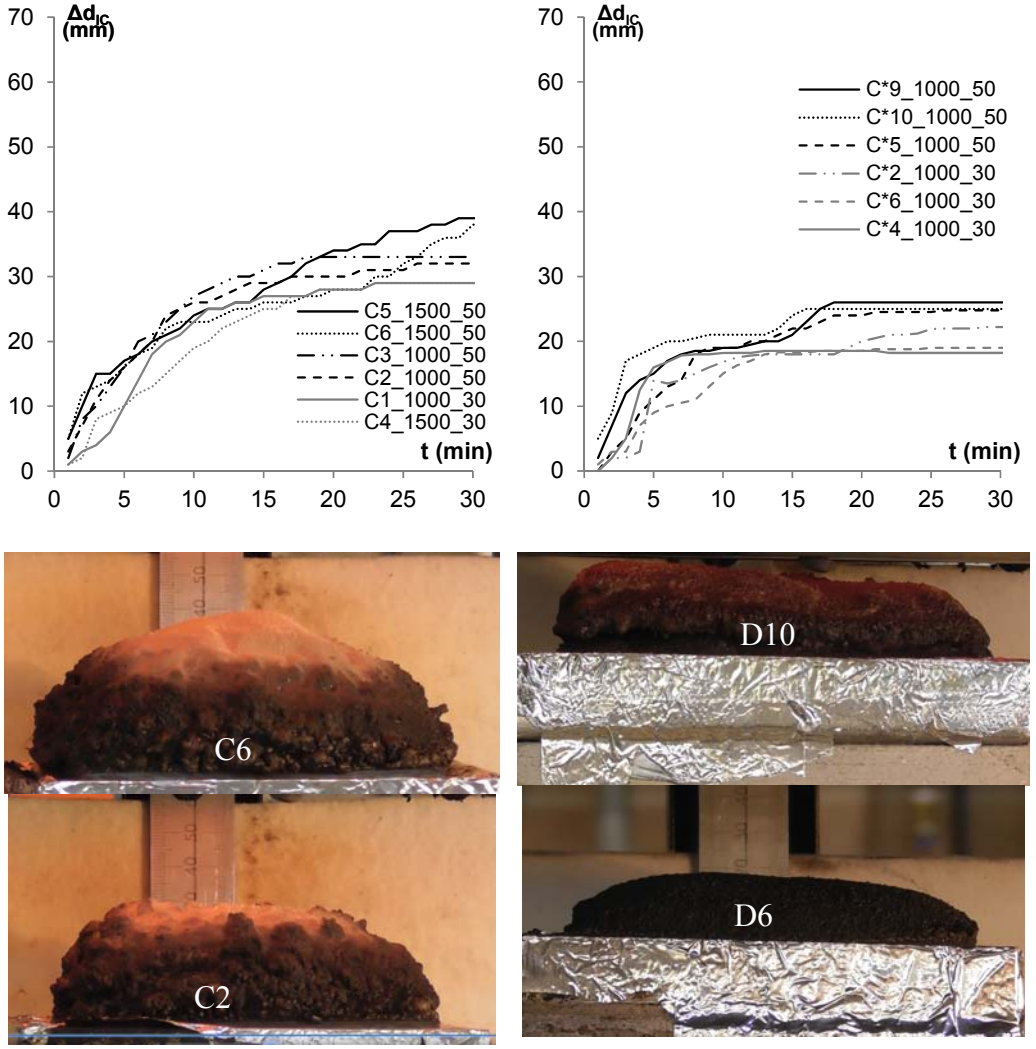

Figure 2.40. Thermal expansion: comparison between different IC.

Since the objective of this research is to find a relatively simple way of estimating the thermal conductivity of intumescent coating, the expansion of IC can only be useful to better understand IC behavior in different conditions and how it could influence the thermal conductivity of IC.

Figure 2.40 shows the different expansion of IC during the thermal transitory (30 kW/m^2 or 50 kW/m^2 of heat fluxes) for all the samples; the IC thickness start to increase with the temperature increasing and after 20 minutes it seems to stabilize.

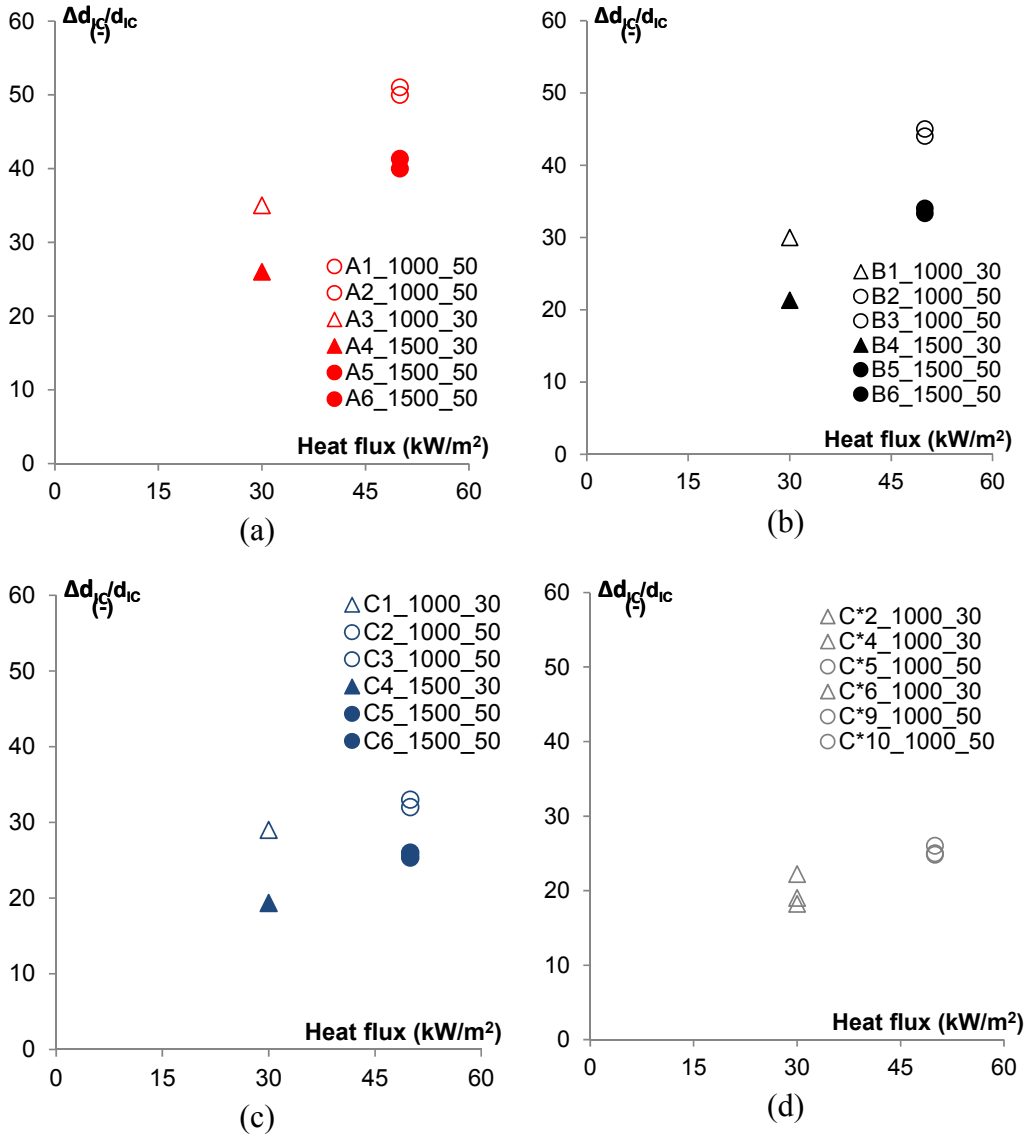

Figure 2.41. Expansion factor $\Delta d_{IC}/d_{IC}$ with varying heat flux and dry film thickness for different IC.

As expected, higher expansion factors were recorded for higher heat fluxes, thus for a higher amount of energy received (see Figure 2.41) .

Furthermore, the highest expansion factors per each heat flux were obtained for the samples protected by the thinnest d_{IC} 1000 µm. This aspect underlined

the ability of IC to expand and develop their char structures in a better way when the paint layer is thin and the heat can penetrate through all its thickness; this is confirmed in all the cases.

Furthermore, the final maximum expansion Δd_{IC} of the char structure was divided by the initial dry film thickness d_{IC} in order to estimate the expansion factor. The values resulted to be included between 20 and 60 times the initial dry film thickness. Figure 2.41a shows that the IC_A has the greater expansion factor between all the three IC. In addition, the painted IC_C registered slightly higher expansions (Figure 2.41c) the same sprayed IC.

2.8 COMPARISON BETWEEN FURNACE AND CONE CALORIMETER TESTS RESULTS

As previously mentioned, IC_B has been tested both in the furnace and under cone heater, so to compare the behavior in the two different cases of fire exposure is interesting: this paragraph describes this comparison.

The comparison is possible fixing the thickness at 1000 μm and 1500 μm and the section factor at 125 m^{-1} and 166 m^{-1} respectively.

2.8.1 MACROSCOPIC COMPARISON BETWEEN DIFFERENT SAMPLES: CHAR STRUCTURES

This section treats the IC_B physical characteristics, which were highlighted by a visual inspection during the experiments in furnace and under the cone calorimeter.

The tests have produced different intumescent coating char structures at the end of the heat exposures. This aspect is related to the two different input fire conditions, which have influenced the intumescent process and the char structure formation.

Regarding the gas furnace experimental set-ups, a huge amount of energy was provided to the steel samples during the tests. Peculiarities of these experiments are long exposures and high temperatures and as a result, the IC

completely expanded. At the end of the intumescent chemical reaction, the gradual combustion of the carbon binder took place.

This component has a dark color and it is the main responsible for the cohesion of the char (see paragraph 2.1.2). Consequently, the char structures produced by the gas furnace tests looked like a white brittle dusty foam.

On the other hand, the cone heater submitted the protected steel samples to high heat fluxes for a short period. During the tests, the two paints had the chance to develop their expanded char structures. However, during this short duration, the carbon binder did not have the possibility to burn out. As a result, the resulting char structures were characterized by a black/grey color and a better cohesion (Figure 2.42).

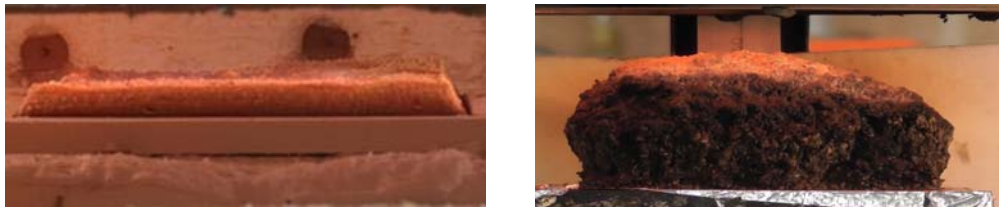

(a) (b)

Figure 2.42. Comparison between same samples (a) under furnace conditions and (b) in cone heater.

2.8.2 MACROSCOPIC COMPARISON BETWEEN DIFFERENT SAMPLES: EXPANSION FACTOR

Also the expansion of the IC seems to depend on the experimental set-up and to exposing fire scenario. Both in the gas furnace and in the cone heater the Digital Image Correlation technique was used for measuring the IC expansion. In the gas furnace tests, it was more arduous because the char structure was not compact dusty: the different expansion at different locations and the loss of material from the specimens were the main challenges faced to measure the IC expanded thickness.

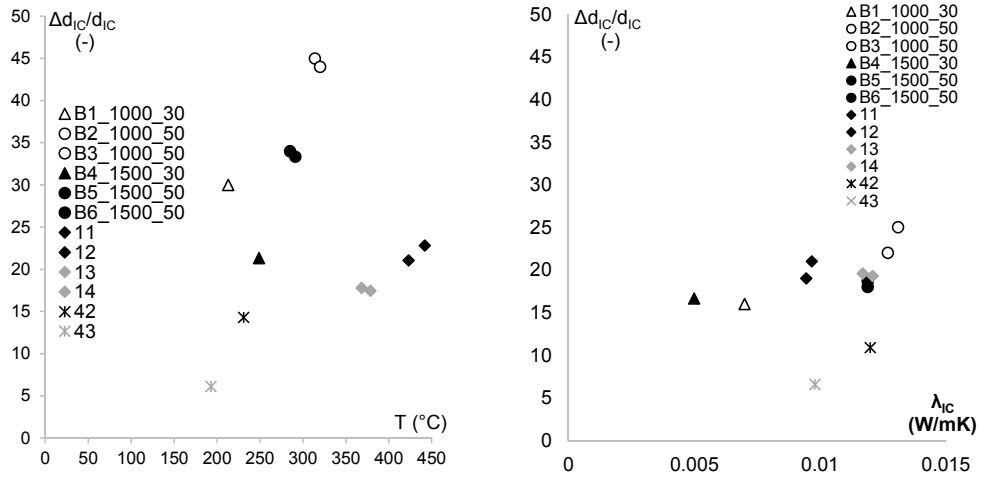

Figure 2.43. Expansion factor $\Delta d_{IC}/d_{IC}$: comparison between different samples (a) after 30 minutes of fire exposure and (b) at 240 °C.

The Figure 2.43a shows the values of the expansion factors after 30 minutes under fire exposure: the maximum expansion is recorded for samples protected with 1000 μm of IC and under 50 kW/m^2 of heat flux; the explanation factor under the smouldering curve is the smallest one.

In addition, The Figure 2.43b shows the explanation factor at 240°C, which, as described before, is the temperature at which the maximum swelling in almost furnace samples is recorded.

The time at which this temperature is reached varies between 10 and 20 minutes for almost samples, while about 35 minutes are necessary for reaching 240°C in the smouldering samples. Also the explanation factor is not very different for each samples at 240°C, it varies between 15 and 20, except for samples with smouldering curve, in which the value decreases at about 10.

However, the highest maximum expansion thickness was always reached by the specimens protected by d_{IC} of 1000 μm: this IC layer is composed of the right amount of material in order to be penetrated by the heat and to generate a complete expansion.

2.8.3 COMPARISON OF THERMAL CONDUCTIVITY

From a practical and engineering point of view, the value of thermal conductivity is one of the most important thermal property of the IC, since it is essential to implement calculation models.

So, understanding which is the effect of changing the fire input on IC thermal conductivity is very important.

As the following Figure 2.44 shows, the value of the equivalent thermal conductivity is very different under several fire condition input: indeed it is higher for the heat flux conditions up to about 240 °C, after that, for the same fire conditions, it become much smaller than both ISO834 and smouldering curves.

However, in all curves, the activation point of the intumescent paint under examination is approximately 120 ° C.

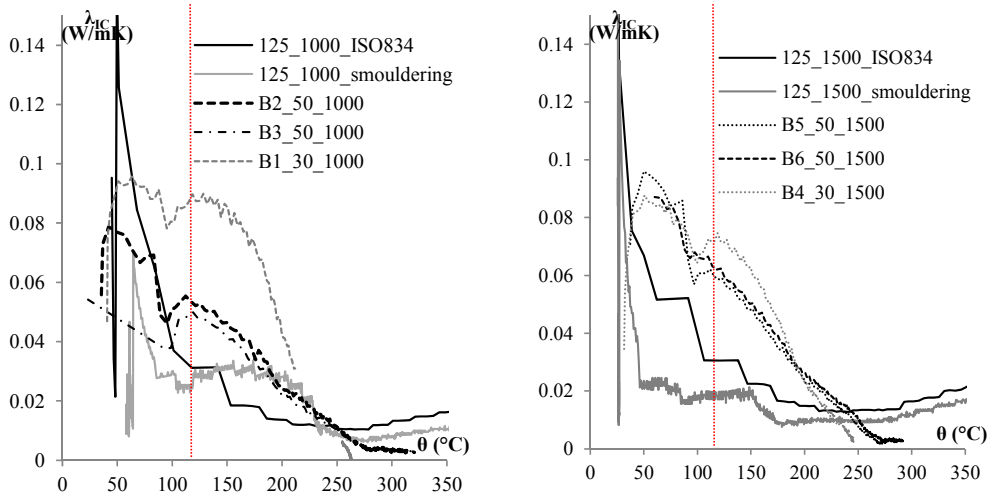

Figure 2.44. Comparison between equivalent thermal conductivity of similar samples under different fire conditions.

From the above discussions, it becomes clear that there is a large amount of scatter in the predicted equivalent thermal conductivity–temperature relationships under different conditions. This makes it impossible to use only one equivalent thermal conductivity– temperature relationship to represent all

cases. Also it is worthwhile to point out that because the behavior of intumescent coating in fire is complex, it is extremely difficult to accurately estimate its behavior. This suggests that the behavior of intumescent coating in fire is affected by many yet to be understood factors. Nevertheless, because of the need to predict thermal performance of intumescent coating protected steel structures under natural fire conditions and the impossibility of conducting testing to cover all natural fire conditions, a practical means has to be made available to obtain the thermal conductivity of intumescent coating. One of the goals of this study can only be about finding a simple means to predict the thermal conductivity of IC as accurately as can be practically accepted.

Chapter 3

ANALYTICAL AND NUMERICAL MODELLING

An important challenge in intumescent coatings development is the requirements for expensive and time consuming approval tests, which must take place prior to a new coating being marketed. To improve fire safety, mapping the influence of furnace process parameters, and optimize coatings for approval tests, a fundamental understanding of the underlying intumescent process mechanisms is of great interest.

To provide such understanding, mathematical models are useful and many modeling activities have taken place as described in[71][72][73][74].

In short, the mathematical models developed are typically validated against experimental data obtained in well-controlled, small-scale laboratory equipment (e.g. cone calorimeters) and they are often of a very high complexity (partial differential equations), requiring a large number of input and adjustable parameters, e.g. melt viscosities of the binder phase and a set of rate constants, which may be tedious and/or time consuming to measure or validate for new coating systems or process conditions. While the advanced models can certainly help to map the phenomena involved, their practical use may be somewhat limited.

The aim of the present work was to obtain several experimental data series for an intumescent coating exposed to different fires. Three experimental series, with an IC inside gas furnace, heating up according to so-called cellulosic fire conditions (ISO834) and according to the Smouldering curve, were conducted and a very good repeatability was evident; the third set of tests in the cone calorimeter on several IC brands.

Measurements include transient temperature developments inside the steel substrate and the variation of the thickness, as described in detailed in the previous sections.

As described in previous paragraphs, the equivalent conductivity development is very similar for all the tests, so it makes sense to identify some salient points for modeling purposes; for examples:

1- 20°C, ambient temperature;
2- Activation point;
3- Point at 241°C, which is the temperature at which the minimum value of thermal equivalent conductivity is reached;
4- Point at 700°C, temperature at which the tests stopped.

Figure 3.1 shows the typical trend of the IC specific thermal conductivity.

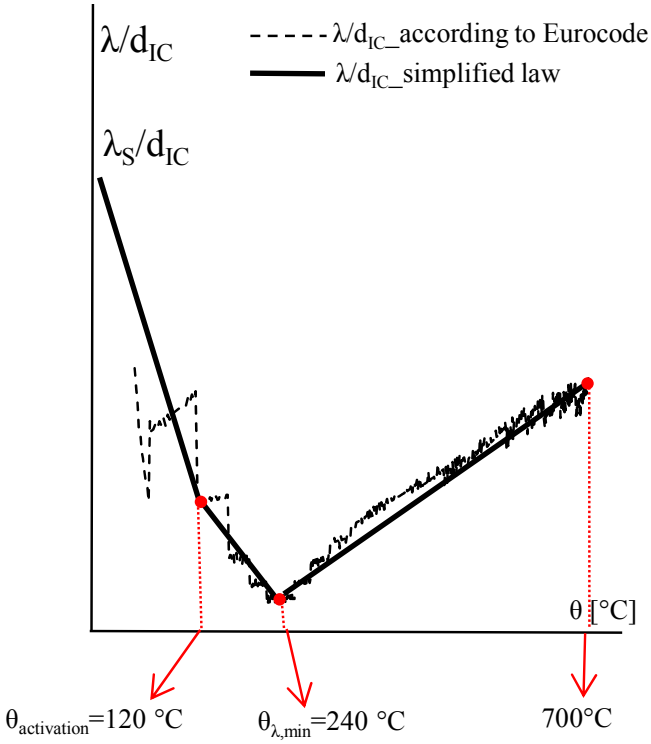

Figure 3.1. Simplified trilinear laws for λ/d_{IC}

Starting from these considerations and from all the results in furnace, a standard segmented multivariate linear regression analysis [99] is applied, in order to obtain a general expression (which is valid for the tested IC) for calculating the thermal equivalent conductivity of IC, useful for performing analytical and numerical modelling.

A mathematical model, describing the intumescent coating behavior and temperatures in the furnace using a single overall reaction was developed and validated against experimental data: a good qualitative agreement was obtained. The model was also validated, modelling tests in real scale on steel element of different shape, protected with the same water based IC, tested in small scale.

The analytical method is also applied, in order to try to use a very simple method for calculating the temperature in a steel element protected with IC, taking into account the variation of the thermal properties of the two material, with the temperature.

After further validation against experiments with other coating formulations, it has potential to become a practical engineering tool.

3.1 THERMAL CONDUCTIVITY FUNCTION

In the previous sections it is shown that the heating rate, fixing the section factor and dry film thickness of the IC, do not drastically affect the development of equivalent thermal conductivity, leading to a proposal for a simplified method for specifying coating requirements and/or performing heat transfer design calculations when designing to different heating regimes as well as the smouldering curve or similar ones.

Indeed, one of the main aims of this research is to develop a general procedure for calculating the thermal conductivity of the IC after identifying, at the previous stage, all the factors that most affect the thermal behavior of the IC.

So, in the next phase of this research, the standard segmented multivariate linear regression analysis [99] is applied to the data gathered in the previous phase for ISO834 curves. For each individual temperature j, identified in the

following, obtaining $N_{samples}$ data points $(d_{IC}^{i}, \frac{A_m^i}{V}, \lambda_{IC}^{i})(i = 1,..., N_{samples})$ where the dry film thickness d_{IC} (in m) and the section factor of the protected element $\frac{A_m}{V}$ (in m^{-1}) are independent variables while λ_{ICj} is the corresponding dependent variable, the next task is to find the equation of a surface:

$$\lambda_{IC,j}(d_{IC}, \frac{A_m}{V},) = a_0^j + a_1^j \, d_{IC} \cdot 10^3 + a_2^j \frac{V}{A_m} \qquad \text{Eq. 3-1}$$

The mathematical relation of Eq. 3-1 should be such that it would provide the best possible fit for the data points available. This should be achieved while minimizing the sum of squares of the differences between observed and calculated values of the dependent variable (i.e. the least-squares approach).

As also said before, since a typical trend of IC thermal conductivity was observed for all tests, the temperatures at which the regression in Eq. 3-1 was applied were fixed.

In particular the following table (Table 3-1) two groups of temperatures were considered.

These two groups of temperatures were chosen for considering, in the numerical models, both the thermal conductivity with reference to the steel temperature and to the IC temperature.

This distinction could be relevant because, on the one hand the Eurocode formula, with which the equivalent thermal conductivity, was calculated refers to the steel temperature, on the other hand, in the calculation program, the variation of the thermal conductivity of the fire protection is indicated by the temperature of the protective itself; so it was interesting to identify the diffrences.

Table 3-1 relevant points of temperature for regressions.

Steel temperature		IC temperature
120 °C as the activation point, which represents also the mean temperature where the first expansions of the coatings were observed in the furnace ($\theta_{activation}$);		
241 °C, mean temperature in the steel at which the minimum value of thermal equivalent conductivity is reached ($\theta_{\lambda,min,s}$);		**486 °C**, mean temperature in IC when 241 °C were reached inside the steel ($\theta_{\lambda,min,IC}$);
680 °C mean steel temperature when 800°C were calculated inside the IC ($\theta_{max,S}$).		**800 °C** mean of maximum value of temperature calculated inside the IC, for all the samples ($\theta_{max,IC}$);

In a simplified way the temperature inside the IC were approximately considered as the average value of the heating source and steel temperature [101]. Also a full regression, starting from ($\theta_{activation}$);, containing all the data point of all the samples was considered. The fitting of each regression was checked through the R-squared function.

In particular the linear regression calculates an equation that minimizes the distance between the fitted line and all of the data points. Technically, ordinary least squares (OLS) regression minimizes the sum of the squared residuals.

In general, a model fits the data well if the differences between the observed values and the model's predicted values are small and unbiased.

Before looking at the statistical measures for goodness-of-fit, the residual plots should be checked . Residual plots can reveal unwanted residual patterns that indicate biased results more effectively than numbers. When residual plots pass muster, numerical results can be trusted and the goodness-of-fit statistics can be checked.

Table 3-2 Regression analysis coefficients of the thermal conductivity function for the analyzed intumescent coating (referring to steel temperature θ_s and to IC temperature θ_{IC}).

	θS (°C)			θIC (°C)		
	120	240	680	120	486	800
a0	0.0187	-0.0033	-0.0004	0.0187	-0.0031	-0.0063
a1	-0.0009	0.0062	0.0125	-0.0009	0.0062	0.0145
a2	1.3866	0.8496	1.3994	1.3866	0.8046	2.0246

Table 3-3 Regression analysis coefficients of the thermal conductivity function for the analyzed intumescent coating (referring to all data points)

All the data	
a0	-0.0056
a1	0.0118
a2	1.4019

The numbers in Table 3-2 and in Table 3-3 are valid within the limits of the tested samples (A/V between 250 m^{-1} and 67 m^{-1}) protected by 1000 μm, 1500 μm or 2000 μm the selected intumescent coating and exposed to standard fire regime. Table 3-2 and Table 3-3 gather results for the regression analysis coefficients a_0. a_1, a_2 of the intumescent coating analyzed in this research for the selected temperatures. The selected details of these samples and their number are considered suitable enough for the purposes of the present research. However, by including higher numbers and broader variety of samples and other heating regimes, the applicability of the model could be propagated and its reliability strengthened.

The regressions (and the function R-squared) were implemented in the software Matlab [103] with the mathematical function “regress”; all the matlab files are contained in [103].

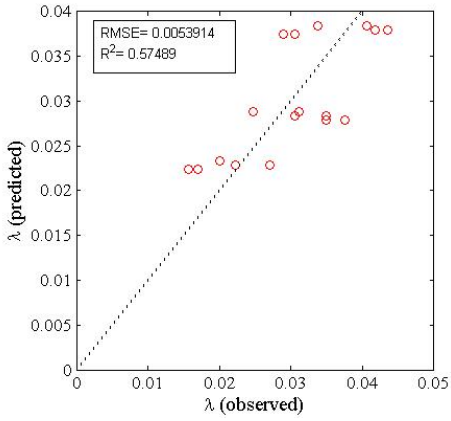

$\theta_s=\theta_{IC}=120°C$

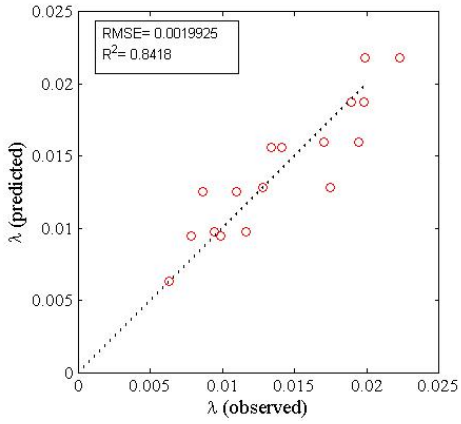

$\theta_s= 240°C$

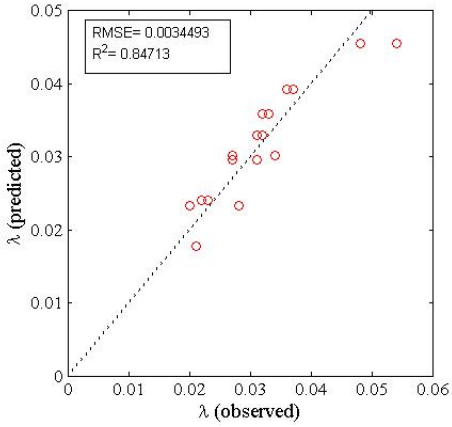

$\theta_s= 680°C$

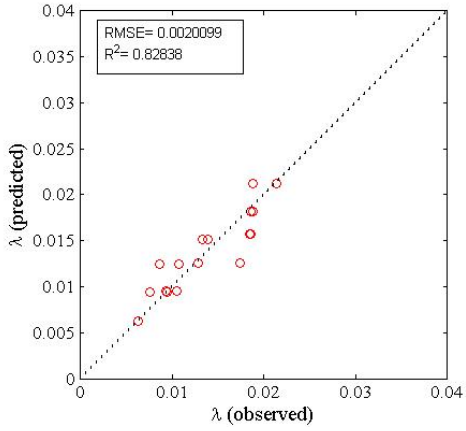

$\theta_{IC}= 486°C$

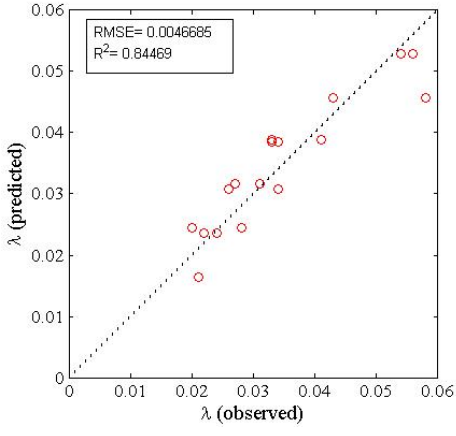

$\theta_{IC}= 800°C$

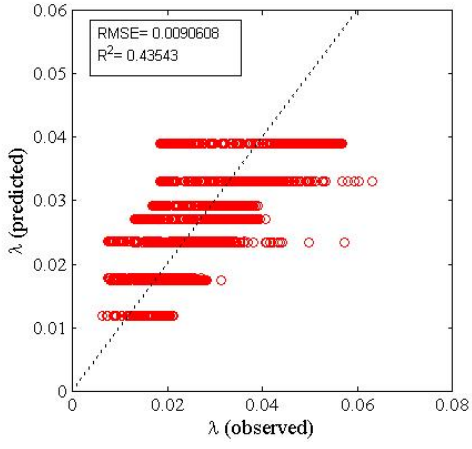

Mean regression: all the data

Figure 3.2. Plots of observed Responses Versus fitted responses for all regressions.

As Figure 3.2 shows, the value of R-squared is very close to one for most cases, only the regression al $\theta_{activation}$=120°C is less precise because in the transient phase the IC behavior is not very stable; obliviously also the regression of all the data point is affected by greater uncertainty. Thanks to the regression formula of Eq. 3-1 a simple law of thermal conductivity can be obtained, varying both the dry film thickness and the section factor of the element (Figure 3.3).

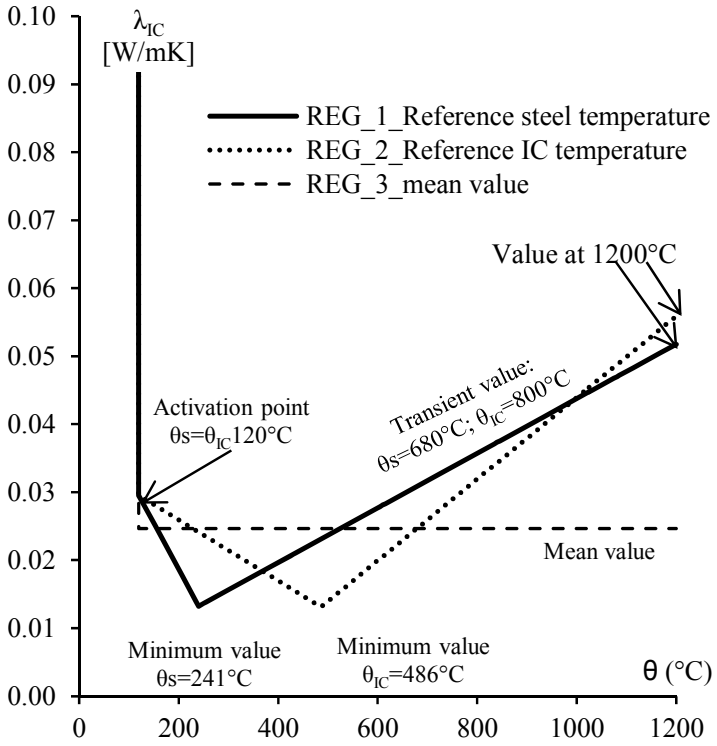

Figure 3.3. Typical trend of IC thermal conductivity calibrated with regression law.

The behavior of the IC depends, as shown above, both on the thickness of the IC and on the section factor; Figure 3.4 shows the conductivity calibrated with the REG_3 law and in particular greater is the section factor, lower Eq. 3-1 is the conductivity and greater is the IC the thickness, greater is the conductivity. This graph (Figure 3.4) confirms the experimental results represented also in Figure 2.17 and in Figure 2.27.

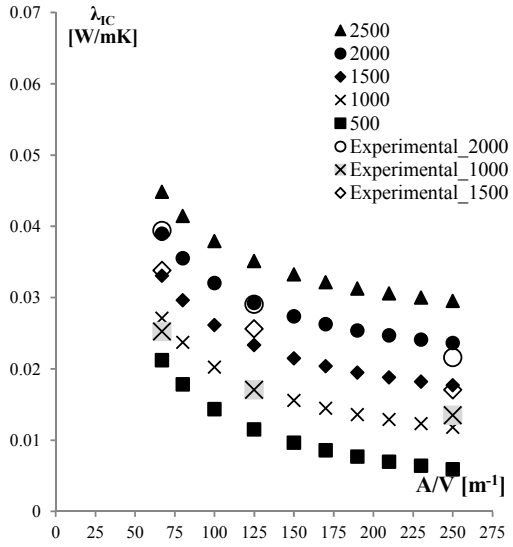

Figure 3.4. IC λ_{IC} trend calibrated with REG_3 law, varying A/V and $d_{IC.}$

As also described in the section 2.6.3, the values of the thermal conductivity of ISO834 and Smouldering samples are very close to each other in the case of $\theta_{\lambda,min,s}$ =241 °C, while they are more different for the $\theta_{activation}$ =120°C. For this reason another regression of the smouldering values at $\theta_{activation}$ =120°C is necessary; the shape of the regression is the same of Eq. 3-1, but obviously the constant coefficient and the estimated error are different.

Smouldering_120°C	
a0	0.0326
a1	-0.0028
a2	0.8936

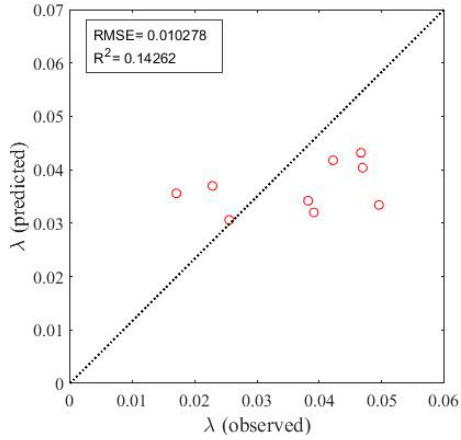

Figure 3.5. Plots of observed Responses-fitted responses for Smouldering regressions

The Figure 3.5 shows that the error on the regression is bigger than the one on other regressions: this is justified by a more instable swelling phenomena for lower thermal gradient such as the smouldering curve.

In the following:

- Regression 1 (REG_1) is considering the steel temperatures;
- Regression 2 (REG_2) is considering the IC temperatures;
- Regression 3 (REG_3) is a mean regression, considering all the values (mean value).

3.2 ANALYTICAL AND FEM THERMAL RESPONSE ANALYSIS

The fitness of the proposed function of the thermal conductivity of the analyzed IC defined by Eq. 3-1 ,Table 3-2 and Table 3-6 is demonstrated by applying this function to the problem of temperature rise in the 24 tested steel plates specimens (from n°1 to n°24) (Section 2.4.3).

The problem of temperature in the protected steel elements was solved both by solving the Eq. 2-3, also according to Eurocode [38], which allows to calculate the steel temperature in the protected elements, knowing the thermal conductivity and the thickness of the protection and by creating a FE model (advanced calculation method): both the models are described in the following.

Both in numerical and analytical modeling the experimental input fire curves have been used. In particular, using the Eq. 2-3, the steel temperature of the protected steel element can be calculated, summing the $\Delta\theta_s$ at each step of the iterative procedure. For applying the Eq. 2-3, the necessary information are:

- $\frac{A_p}{V}$ = section factor of the protected steel plate;
- ρ_s = steel density [kg/m^3], which changes with the temperature according to Eurocode [38];
- c_s = steel specific heat [J/kgK)], which changes with the temperature according to Eurocode[38];

- θ_g = experimental input fire curve [°C];
- λ_{IC} = thermal conductivity[W/mK], calibrated with regressions;
- d_{IC} = dry film IC thickness [m].

This analytical method is very useful for simple calculation, both for manufactures and for designers.

On the other hand, for creating a FEM model for advanced calculation, for the first, i.e. thermal, step of the proposed fire analysis the dedicated thermomechanical software SAFIR11[102] is again adopted.

The model engages 4-node linear heat transfer finite elements for discretization of all of tested steel plates protected with IC and as boundary conditions the ISO834 fire curve is assigned on the exposed surfaces (Figure 3.6). The model considered in SAFIR is that in which heat is distributed in the structure essentially by conduction because most of construction elements are made of solid. Radiation and convection are the heat transfer modes in internal cavities such as those present, for example, in hollow core slabs.

Convection and radiation are the heat transfer mode at the boundaries between the object analyzed and the environment, i.e. the fire.

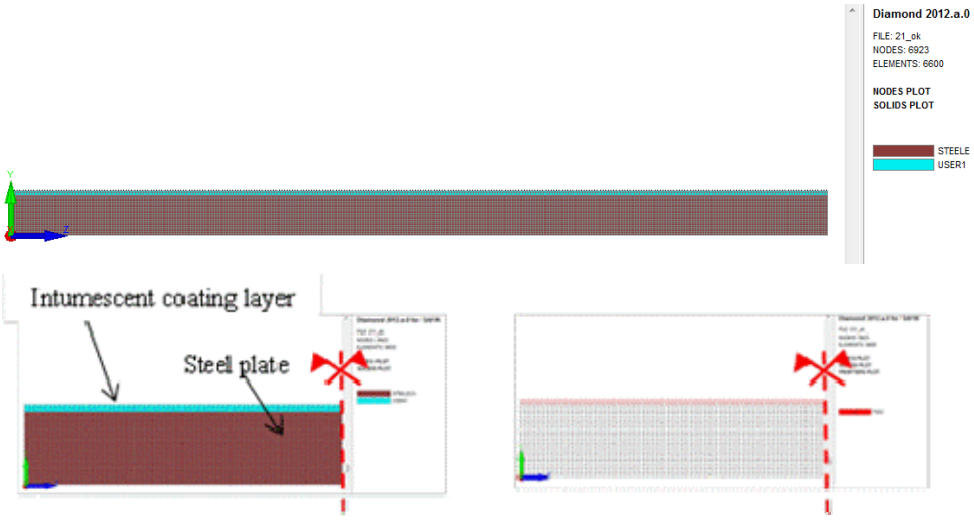

Figure 3.6. FEM analysis for one test simulation with SAFIR.

The thermal properties of the steel are assigned directly by SAFIR, according to Eurocode[38], while the thermal properties of IC are again[100]:

- Thermal conductivity [W/mK], according with the regression laws (section 3.1);
- Specific heat [J/kgK)], equal to 1200;
- Density [kg/m^3], equal to 200;
- Water content [kg/m^3], equal to 0;
- Convection coefficient on hot surfaces, equal to 20;
- Convection coefficient on cold surfaces, equal to 0;
- Relative emissivity, equal to 0,95.

The thermal properties of the IC are directly assigned to the IC layer in the software, so they change in accordance with the temperature inside the protection; this is the reason because also REG_2 is necessary, even if, as said before, there is not a direct measure of the IC temperature, but it was assumed as an average value between the experimental temperature inside the furnace (θ_g) and the experimental temperature inside the protected steel element (θ_s).

Since the ISO834 temperature range is from 20°C to about 1200°C, it is necessary to assign in SAFIR a series of conductivity values that cover the same temperature range.

At 20°C the properties of IC are the same of the steel because there is no activation of the protection; so from 20°C to 120°C there is a linear variation of the IC thermal conductivity from the steel value to the value at 120°C (which change according to regressions).

So, not having a direct calibration of thermal conductivity between 700°C and 1200°C (because 700°C is the threshold value of temperature reached in steel plates for each test), the value assigned at 1200°C is the one reached by the regression line, with the same slope, at 1200 °C (Figure 3.3)

The IC layer was modelled considering the dry film thickness (d_{IC}) therefore the thickness IC variation has been neglected; however, this is consistent with calibrating thermal conductivity.

The Figure 3.7 shows the typical temperature trend inside the IC layer.

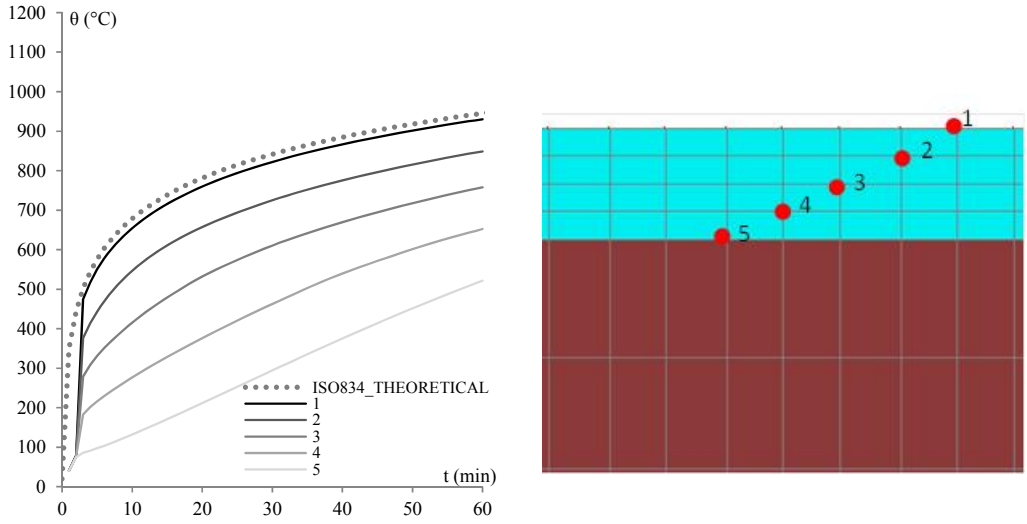

Figure 3.7. Typical thermal temperature trend inside IC.

The Figure 3.8 shows the comparisons between theoretical and experimental temperatures for specimens with the same IC thickness (1500 μm) and for the three tested section factors; all the other simulated tests are in Appendix C.

In particular, the Figure 3.8 shows a good agreement between the experimental curve and the numerical simulation with REG_1; a slight underestimation of the temperature is observed, considering REG_2 and REG_3 in the second phase of the test. This underestimation, in the case of REG_2 is because in the temperature test interval, the temperature inside the IC is a little bit grater then the mean value (see Figure 3.7), while in the analysis, in a simplified way, the mean value is considered, so the thermal conductivity values are smaller.

A good agreement is also obtained between the experimental and analytical method curves, so this method, which is easy to apply, can be used also during the fire designing of the protection.

Table 3-4 thermal conductivity for tests with A/V=250 m^{-1} and d_{IC}=1500 μm (ISO834).

A/V=250 m^{-1}, d_{IC}=1500 μm			
λ(θs (°C))			
120	240	680	1200
0.0244	0.0098	0.0253	0.0437

A/V=250 m^{-1}, d_{IC}=1500 μm			
λ(θIC(°C))			
120	486	800	1200
0.0244	0.0099	0.0248	0.0439

A/V=250 m^{-1}, d_{IC}=1500 μm
λ_REG_3
0.0190

A/V=125m^{-1}, d_{IC}=1500 µm			
λ(θs(°C))			
120	240	680	1200
0.0295	0.0132	0.0309	0.0518

A/V=125 m^{-1}, d_{IC}=1500 µm			
λ(θIC(°C))			
120	486	800	1200
0.0295	0.0131	0.0319	0.0559

A/V=125 m^{-1}, d_{IC}=1500 µm
λ_REG_3
0.0247

A/V=67 m^{-1}, d_{IC}=1500 µm			
λ(θs(°C))			
120	240	680	1200
0.0383	0.0192	0.0405	0.0658

A/V=67 m^{-1}, d_{IC}=1500 µm			
λ(θIC(°C))			
120	486	800	1200
0.0383	0.0187	0.0442	0.0767

A/V=67 m^{-1}, d_{IC}=1500 µm
λ_REG_3
0.0344

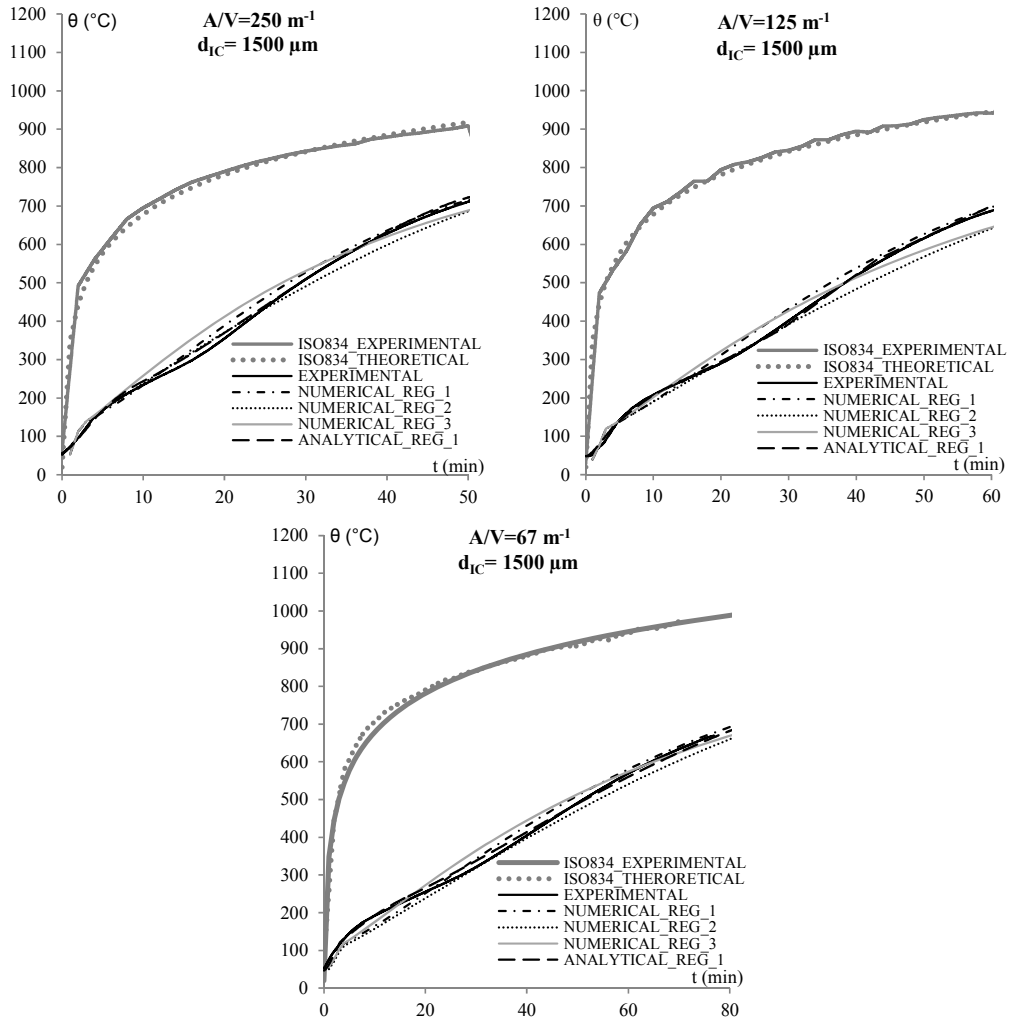

Figure 3.8. Comparison between experimental and simulated results for ISO834 curve.

As also said before, also the tests with the Smouldering curve were modeled; in particular, starting from very similar equivalent thermal

conductivities between ISO834 and Smouldering samples from 240°C, the same regression formula (calibrated on ISO samples) was used to calibrate conductivity from 240 ° C of smouldering samples. While a new regression of thermal conductivity was required at 120 °C, because greater conductivity values in the case of smoldering curve were observed at the activation temperature (120 °C) (Figure 3.5). So, the value are the same of Table 3-4, but at 120°C, the values changes according to Table 3-5 (Figure 3.9).

Table 3-5 thermal conductivity at 120°C for several tests (smouldering).

$A/V=250\ m^{-1}$, $d_{IC}=1500\ \mu m$
λ(θ(°C))
120
0.0316

$A/V=125m^{-1}$, $d_{IC}=1500\ \mu m$
λ(θ(°C))
120
0.0351

$A/V=67m^{-1}$, $d_{IC}=1500\ \mu m$
λ(θ(°C))
120
0.0413

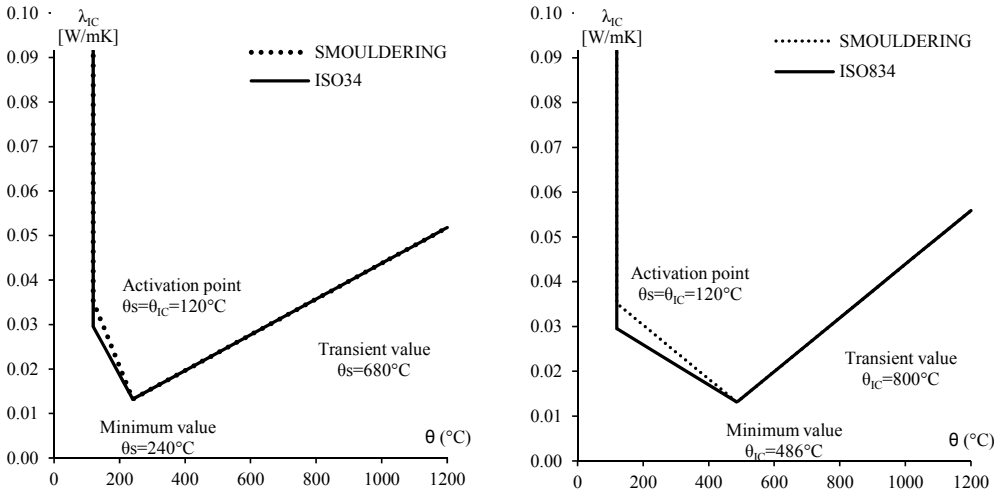

Figure 3.9. Comparison between ISO834 and SMOULDERING thermal conductivity simplified regression laws for a typical case.

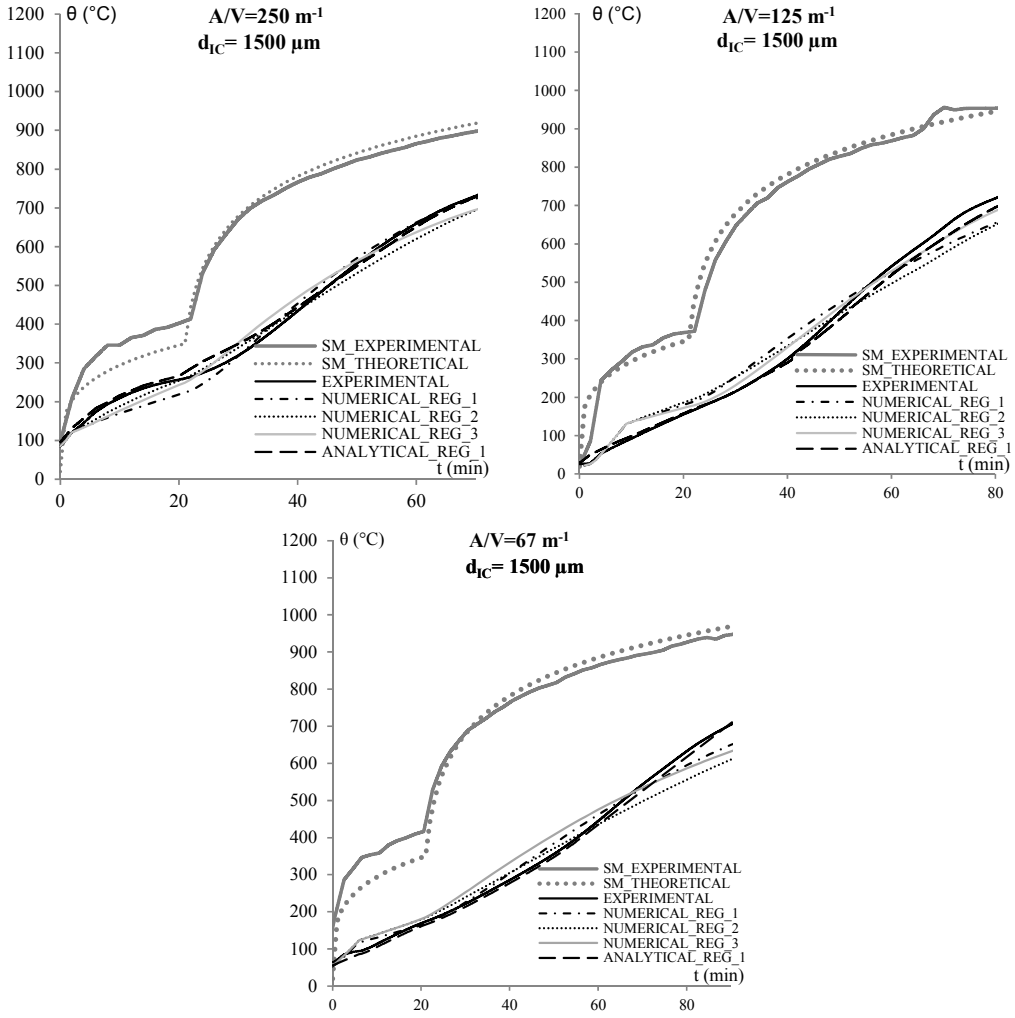

Figure 3.10. Comparison between experimental and simulated results for smouldering curve.

Also in the case of smouldering samples there is a good agreement between the experimental and the simulated temperatures both with numerical and analytical method. In this case the REG_2 and REG_3 a slight underestimation of the temperature is observed as well.

Finally, the analytical method was also used to simulate the tests in cone calorimeter. As shown in the section 2.8.2, the behavior (and the conductivity value) in this case is very different from that of furnace tests, so a thermal

conductivity value directly calibrated with the Eq. 2-9 was used in the analytical method. The Figure 3.11 shows that also in the case of cone calorimeter tests the results of the analytical method are very close to the experimental ones; this is also obvious because the two formulas are directly linked to each other.

The Figure 3.11 shows also that using the thermal conductivity calculated with the Eq- 3-1, using the regression 1, underestimates the temperatures at the beginning and it overestimates the temperatures in the second part. This happens because the thermal conductivity, in the case of cone calorimeter tests, has a very different trend than the furnace ones (see Figure 2.44), so, for a better result, a thermal conductivity calibrated for cone heater tests should be used in the modelling. This is just a confirmation that there is a dependency of the behavior of IC on the fire exposure.

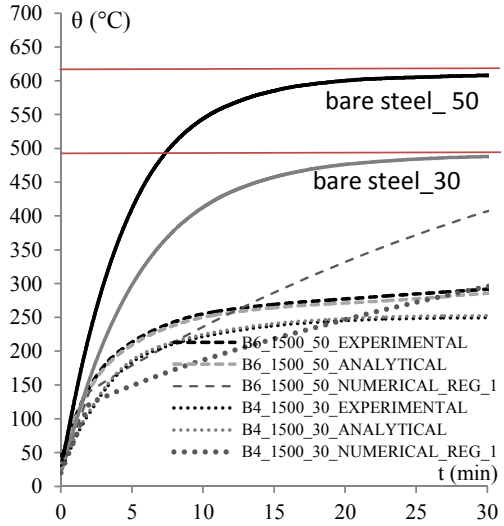

Figure 3.11. Comparison between experimental and simulated results cone calorimeter.

One general common conclusion is that the analytical model with the regression 1 is always the best for fitting experimental values because it is the more consistent with the formula for calibrating the equivalent thermal conductivity (Eq. 2.5), indeed both refer to the steel temperature.

This level of the agreement between results of all the cases is accepted as reasonable enough for the purposes of the present investigation and further analyses.

3.3 VALIDATION OF THE MODEL ON REAL SCALE ELEMENT

According to [63], for examples, to get the certification and in order to sell the IC on the market, a series of tests must be conducted on several steel element protected with different thickness of IC.

In particular H and I shape, hollow circular and hollow square section elements must be tested in different configurations (tall and short columns and beams).

So, an experimental results report, carried out in accordance with the [63], was considered and the behavior of this real-scale samples was simulated, adopting the regression of the thermal conductivity law (section 3.2), calibrated on the same IC protecting steel plate samples. In particular 3 different shape were considered:

-hollow circular section;

-H shape sections;

-I shape section;

all of them are short column; they are pointed out in Figure 3.12.

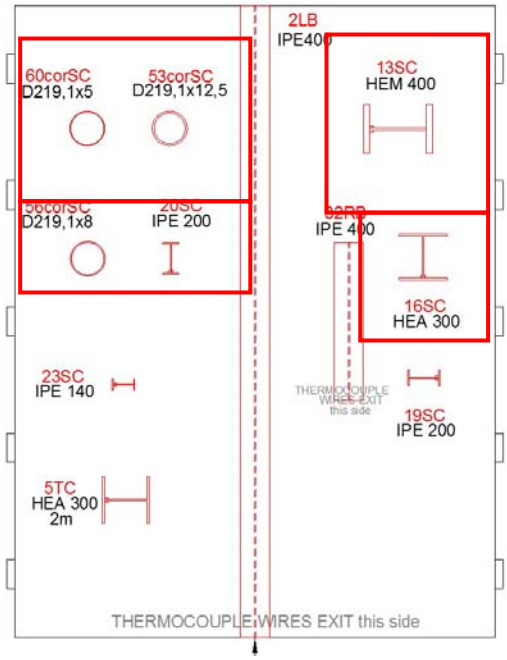

Figure 3.12. Real scale tests: distribution in the furnace.

The tests were performed with the standard fire curve ISO834.

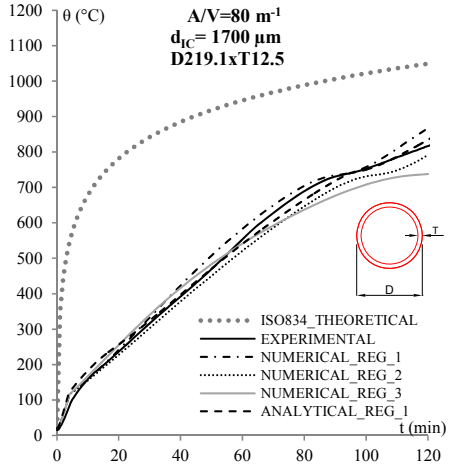

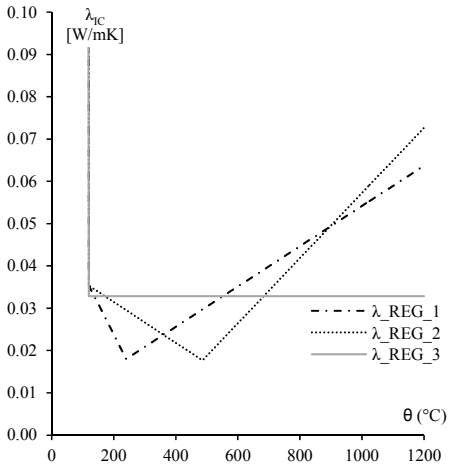

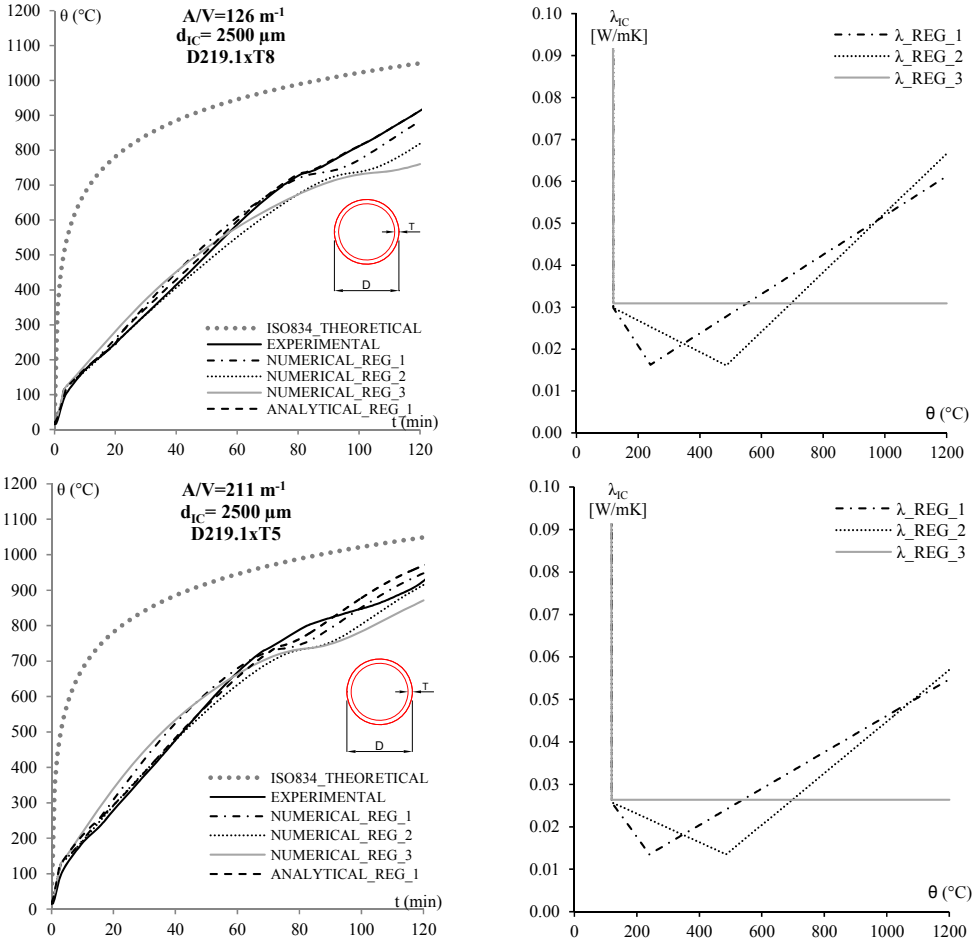

Figure 3.13. Comparison between experimental and simulated results for real scale hollow circular section .

As the Figure 3.13 shows, there is a very good agreement between the experimental and numerical/analytical results; in particular, the best fitting is reached with the analytical and numerical model, calibrating the thermal conductivity with the regression 1 (ANALYTICAL_REG_1 and NUMERICAL_REG_1) for all the samples, while NUMERICAL_REG_2 and NUMERICAL_REG_3 underestimates al little bit the temperature in the second phase of the test: this is especially true for specimens 80_1700 and 126_2500.

Also samples with different shapes were simulated; the results are in Figure 3.14. In all the cases there is an overestimation of the temperature with both the

analytical and numerical models, using REG_1 for calibrating the thermal conductivity; while the fitting is better in the case of regression 2.

So, an effect of the type (shape) of section seems to be in this case, probably due to the different swelling of the IC on the web and on the flanges, or/and due to the different IC thickness on the section, because the application of IC in this case could be more irregular; another factor that could affect the different behavior is the shadow effect: all this factors are not taken into account in the models and especially in the Eq. 3-1.

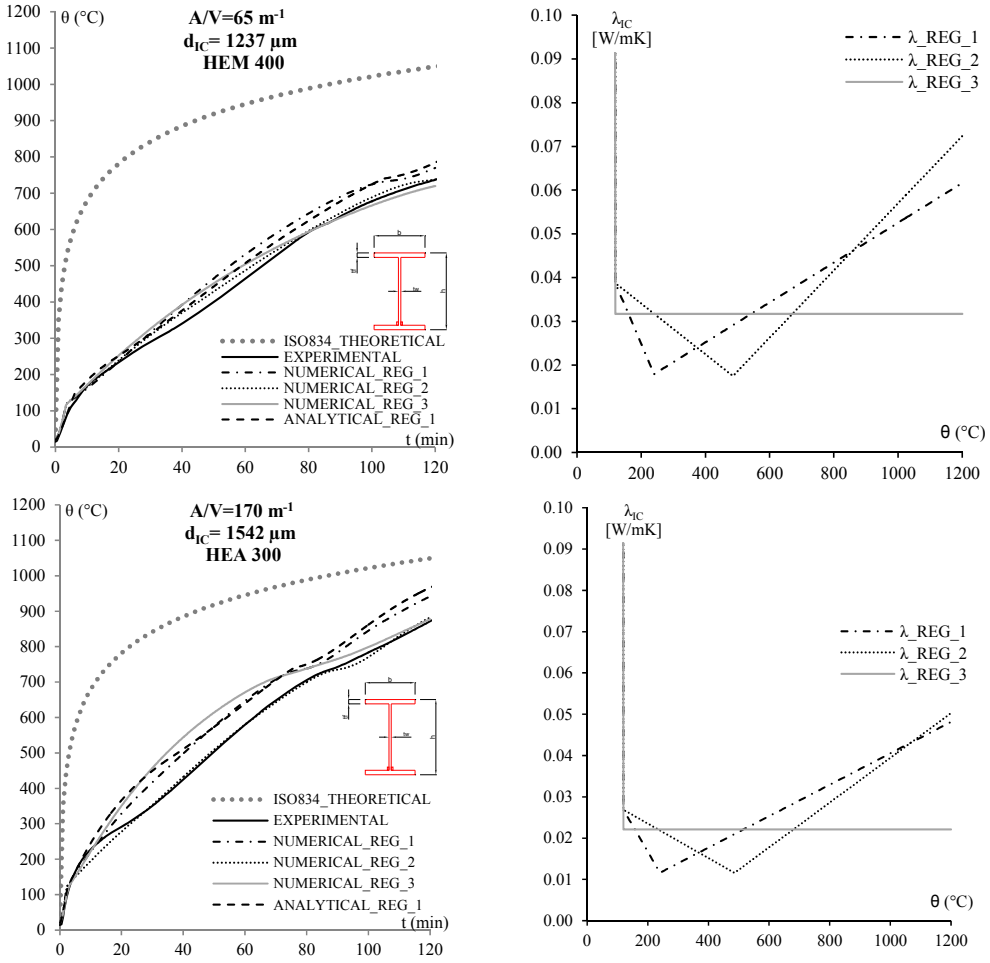

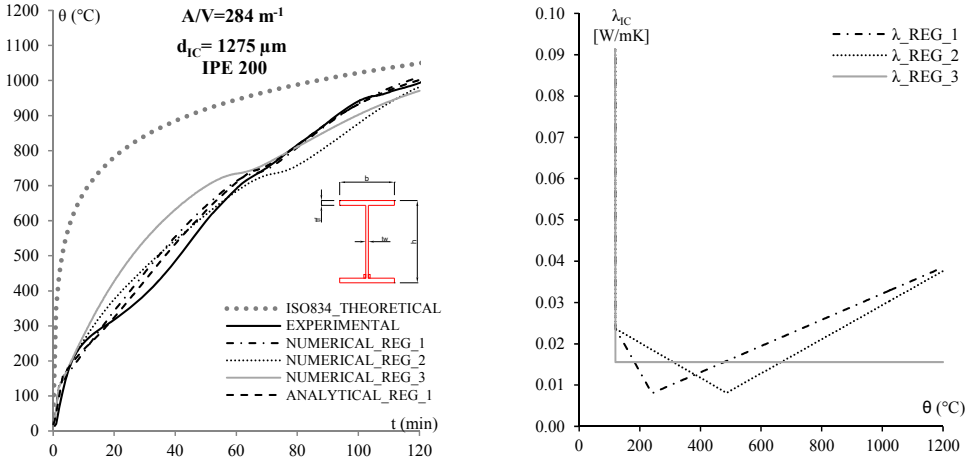

Figure 3.14. Comparison between experimental and simulated results for real scale H and I shape section .

The fundamental advantage of the composed procedure is that it is based on experimental data, that sometimes are easily accessible by the current state-of-the-art testing procedures. Another important advantage of the model is that it enables calculations of fire response of intumescent painted structures of different cross-sectional details and the coating thickness.

Indeed, the numerical and the analytical models with regression 1 can be useful for designing the fire resistance of real structure on the side of safety, slightly overestimating the temperatures.

Having the possibility of designing the IC in an advanced calculation method (e.g. FEM), knowing its thermal properties, allows one side to optimize the IC thickness to be applied for reaching a certain safety level, on the other hand, to take into account, through advanced modeling of the whole structure, the actions that may arise in the event of a fire (e.g. redundancy actions), which cannot be taken into account with simplified methods (e.g. analytical method for single elements).

Chapter 4

GENERAL CONCLUSION

Intumescent fire protective coatings are an efficient way to protect steel structures from high temperatures and subsequent collapse in the event of a fire. The coating expands according to a complex mechanism of temperature triggered reactions and accompanying physical phenomena.

This Ph-D work is based on the study and explanations of the behavior of water-based thick film intumescent coating, applied on steel element, under different heating regimes and varying several parameter. In particular, the different aspects that can affect the performance of intumescent coatings and their behavior in different fire scenarios are investigated.

4.1 EXPERIMENTAL PROGRAMME

The current study investigated two different experimental set-ups representing different types of heating exposures: gas furnace and cone calorimeter.

In particular 48 tests in furnace were conducted on steel plates protected with one commercial water based intumescent coating, varying the applied IC thickness (500 μm, 1000 μm, 1500 μm and 2000 μm), the section factors (250 m^{-1}, 125 m^{-1} and 67 m^{-1}) of the steel plates, the shape of the samples (fixing the section factors) and the fire curve (ISO834 and Smouldering curves).

Also 24 tests under the cone calorimeter were conducted, with 30 and 50 kW/m^2 of heat fluxes, on steel plates (with section factor 167 m^{-1}) protected with 3 different commercial water based intumescent coatings and with 2

different IC thickness (1000 μm, 1500 μm) were tested; for the IC_C also the influence of the way of application is evaluated .

In both experimental set-ups the temperature inside the steel plates (by thermocouples) and the thickness variation (through the Digital Image Correlation (DIC) technique) were measured.

4.2 EXPERIMENTAL OUTCOMES

Regarding the gas furnace set-ups, the insulating performance of intumescent coatings was investigated by considering the temperature reached inside each samples, by the equivalent thermal conductivity and by the measures of the IC swelling. According with the Eurocode, the trend of the equivalent thermal conductivity was obtained for all the tests.

For every section factor the smallest thickness of IC (500 μm) does not react homogeneously, indeed numerous irregularities in the swelling, as well as in the temperatures were observed.

The equivalent thermal conductivity, calibrated for each sample, starting from the temperatures recorder during the test, depends on both the initial thickness and the section factor, but the equivalent thermal conductivity does not depend significantly (in the second part of the thermal transient) on input fire curve in the case of ISO834 and smouldering curve and on the shape of the sample, being equal section factor and IC thickness.

In particular, in the initial phase of the tests (up to about 240°C) the thermal conductivity of the smouldering samples is higher than the one of the ISO834 samples, but the temperatures at which the minimum values of IC thermal conductivity is observed, are very similar for almost the samples, regardless of thermal input.

Although some outcomes could depend on the simplified formula used for the calculation of equivalent conductivity, the direct reading of the thicknesses during the tests allows to verify the real dependency of the swelling phenomenon of IC on the section factors and on the input fire curves.

Furthermore, in the first phase of fire exposure the equivalent thermal conductivity of smouldering samples in higher than the ISO ones, while in the

second phase there is no significant variation of the thermal conductivity under the two fire curves; however a greater swelling of the IC is observed for faster heating of the steel specimen; indeed higher foams are measured in both cases of bigger section factors section and with the ISO834 curve.

The microscopic pictures of specimens with ISO and Smouldering curves show a different foam's bubbles shape and therefore there is a dependency of the swelling mechanism on the input curve.

The trend of the thermal equivalent conductivity was divided into four general phases, defined according to four critical points. By defining the activation point, it was found that the activation temperature of the intumescent coating was constant in the two different fire curves. In particular, about 120 °C is the activation point for this IC. Also the temperature at which the minimum value of thermal conductivity was observed, is the same for both the fire curves (240°C).

While the maximum expansion of the IC was observed for almost the samples at about 300°C; this shift in temperature between 240°C and 300°C is probably due to the endothermic intumescence reaction.

Moreover, in some cases, the performance in terms of specific equivalent thermal conductivity (λ_{IC}/d_{IC}) of the steel samples protected by 1000 μm, 1500 μm and 2000 μm of dry IC layer, were very similar, while the performance of the thinner layer, 500 μm was lower than the other. This aspect highlighted that the intumescent coatings are not very sensitive to their applied thicknesses.

Regarding the cone heater set-up, the insulating performance of intumescent coatings was investigated again by considering the equivalent thermal conductivity and the expansion factor, which is defined as the ratio between the final swelled IC thickness and the initial one. As expected, it was found that the intumescent coating expansion factor increased with increasing heat fluxes for all the three tested intumescent coatings.

The highest expansion factors were obtained for the thinnest dry paint layer (1000 μm). This confirmed the ability of intumescent coatings to expand and develop their char structures in a better way when the paint layer is thin and the heat can penetrate through all its thickness.

Even if the expansion of the three IC is different (the paint A swelled much than the others) there is no significant difference in terms of equivalent thermal conductivity between all the IC.

The cone calorimeter results were important to check the dependence of the IC behavior on the thermal fire input in the first exposure phase.

Observing the trend of the thermal conductivity of IC under cone calorimeter, again the activation point can be identified at about 120° for IC_B (which is the same tested in the furnace as well). From the above discussions, it becomes clear that there is a large amount of scatter in the predicted equivalent thermal conductivity–temperature relationships under different conditions. This makes it impossible to use only one equivalent thermal conductivity–temperature relationship to represent all cases.

Furthermore a small influence of the way of IC application appears because the temperatures in the painted specimens are slightly lower than those of the sprayed specimens, both in the case of 30 kW/m^2 and 50 kW/m^2 heat fluxes.

Also it is worthwhile to point out that because the behavior of IC in fire is complex, it is extremely difficult to accurately estimate its behavior. This suggests that the behavior of IC in fire is affected by many yet to be understood factors.

4.3 ANALYTICAL AND NUMERICAL MODELS

As widely described above, the need to have an advanced method for modeling whole structures protected with intumescent coating is very important, especially in the current regulatory framework (e.g. performance based approach).

So, one of the main goals of this work was to find a thermal conductivity law of the IC, based on a series of experimental data, which can also be applied to cases of real structures, in order to model them.

The proposed procedure is valid only for the IC tested in this experimental phase work, but it can be expanded, integrating experimental tests on other types (e.g. solvent or epoxy – based or different brand) of IC.

In particular, starting from the typical development of the IC equivalent conductivity, calculated according the Eurocode formula, a standard segmented multivariate linear regression analysis was applied to the data gathered in the previous phase at significant temperatures, depending on the two factors that have been seen to have a greater influence on IC behavior: the section factor and initial thickness of IC.

The activation temperature ($\theta_{activation}$ = 120°C), the temperature at which the minimum value of equivalent thermal conductivity was reached ($\theta_{\lambda,min}$) and the maximum value of temperature reached inside the IC ($\theta_{max,IC}$), were chosen as significant temperatures.

From 20°C to $\theta_{activation}$ the thermal conductivity law is linear, starting from the value of steel conductivity; between $\theta_{activation}$ and $\theta_{\lambda,min}$ it was again linear; also the last branch, between $\theta_{\lambda,min}$ and the θ_{max} is linear; two regressions considering $\theta_{\lambda,min,S}$ - $\theta_{max,S}$ and $\theta_{\lambda,min,IC}$ - $\theta_{max,IC}$ were carried out.

Another regression, considering all the value of thermal conductivity selected at temperature with Δt=30 seconds, was considered.

Thermal FE analysis with the thermal conductivity calculated with the three regressions respectively were conducted and also the analytical methods was used with the regression 1, which refers to the steel temperature.

In all the cases the analytical methods fits very good the experimental data, as well as simulation with REG_1 (which refers to the steel temperatures), while REG_2 (which refers to the IC temperatures) and REG_3 (which refers to all temperatures) simulations slightly underestimate the temperatures in the second phase of the test.

In order to validate the calibrated regression laws of the equivalent IC conductivity, several real scale tests were also simulated.

In particular, starting from experimental data (on the same IC tested in small scale), that are easily accessible by the current state-of-the-art testing procedures, several section of different type and protected with different IC thickness were modeled: hollow circular section, H shape sections and I shape section were considered.

As results, in the hollow circular section there is a very good agreement between the experimental and numerical/analytical curves, while for H and I

shapes, there is an overestimation of the temperature with both the analytical and numerical models, using REG_1 for calibrating the thermal conductivity; while the fitting is better in the case of REG_2.

So, an effect of the type (shape) of section seems to be in this case, probably due to the different swelling of the IC on the web and on the flanges, or/and due to the different IC thickness on the section, because the application of IC in this case could be more irregular; another factor that could affect the different behavior is the shadow effect: all this factors are not taken into account in the models and especially in the simplified regression laws.

Anyway the use of the calibrated IC thermal conductivity laws, in particular in the numerical and analytical models with REG_1, can be useful for designing the fire resistance of real structure on the side of safety, slightly overestimating the temperatures.

Indeed modeling the whole structure in advanced calculation method (e.g. FEM), knowing IC thermal properties, allows one side to optimize the IC thickness to be applied for reaching a certain safety level overcoming the usual design approach based on tables; on the other hand, it is possible to take into account the indirect actions that may arise in the event of fire (e.g. redundancy actions due to thermal expansion), that cannot be taken into account applying simplified methods (e.g. analytical method for single members). In other words, we could have the opportunity to design a steel structure protected by intumescent coatings applying a modern fire design according to Fire Safety Engineering approach.

4.4 SHORT CONCLUSION

This work presents an experimental program to characterize the thermal properties of the IC, starting from the temperatures measured during the tests by thermocouples and thermoplates and from the measurement of the IC thickness variation made during the tests through the Digital Image Correlation (DIC) technique.

The results of the furnace experiments show that:

- the thickness expansion has a peak at about 300°C and after it stabilizes;
- small thickness of IC (500 μm) does not react homogeneously for all the section factors;
- both the IC thickness swelling and the IC equivalent thermal conductivity depend on the section factor and initial IC thickness of the protected steel plate;
- there is an influence of the input curve on swelling mechanism: the higher is the increment of temperature, the bigger is the swelled thickness;
- however the equivalent thermal conductivity seems dependent only slightly on the considered input fire curve (standard or smouldering);

The results of the cone calorimeter experiments show that:

- The expansion factor is bigger for the greater heating rate (50 kW / m^2) for each of the three IC tested;
- The biggest expansion factor is the one for 1000 μm of IC;
- Even if the expansion is different for the three tested IC, the thermal conductivity is not particularly different;
- A slight influence of the way of IC application emerges, in fact the temperature in the painted plates is slightly lower.

Comparing the results of the tests in furnace with ones in cone calorimetric a dependency from the way of heating (test mode) emerges both of thermal conductivity and of IC swelling;

Since the factors that most influence the thermal conductivity of IC are the section factor and the initial IC thickness, a formula for the calculation of the conductivity of the IC has been calibrated with a multiple regression referring respectively to the temperature of the steel (REG_1), to the IC temperature (REG_2) and also an "average" regression on all temperature values (REG_3) was considered. The FE modeling and the analytical method showed that:

- REG_1, both with FE analysis and with the analytical method, gives results in good agreement with the experimental ones;
- REG_2 and REG_3 slightly underestimate the temperatures in the second phase of the test;
- the calibrated formula is also able to simulate tests with the smouldering curve;
- the calibrated formula also allows to simulate the behavior of elements protected with VI in real scale, so that this formula can also be used in the design process with both prescriptive and performance approaches.

4.5 FUTURE WORK

The research presented in this thesis represents an attempt at understanding the different aspects influencing intumescent coatings performance under various fire conditions and varying the initial thickness of IC, the section factors and the shape of the steel samples, in order to fix a method for calculating the IC thermal conductivity.

The project focused on many features of intumescent paints and fire exposures, but future research will be necessary to improve understanding as well as to expand the results to all relevant fire scenarios (e.g. natural fire curves).

First of all, the same experiments should be conducted on other intumescent products available in the market with different compositions and produced by different manufacturers. The performances of other water-based IC should be tested, maybe adding also solvent-based IC and compared in order to confirm the theory exposed in the current study.

Further studies are also needed to investigate the behavior of intumescent coatings under different types of heating. In particular, regarding the tests in furnace, the ISO834 curve is much faster and more extreme than the smouldering curve. It is advisable that a future work should expose steel samples to temperature time-curves between the previously described ones or eventually with higher growth rates of ISO834 or slower than the smouldering

as well. In this way, it should be possible to obtain a general understanding of the IC performance for a huge variety of heating rates, from the cellulosic standard fire curve to the much slower ones, in order to check the activation of the IC as well.

In addition, a future work should concentrate on finding a technique aimed to evaluate the intumescent coating surface temperature in the mass loss cone heater set-up, for instance through the use of thermographic phosphor equipment. In this way, interesting conclusions could be drawn from the direct comparison of the thermal conductivity obtained in different experimental set-ups, with a more precise superficial IC temperature.

It is recommended that further research should also focus on the analysis of the chemical composition. In particular, the future work should aim at understanding which components and quantities can influence the intumescent coatings performance under different fire conditions. Future studies on the current topic are also required in order to clarify the characteristics of the "post-austenitization phase", since the intumescent coating behavior at really high temperatures is still not completely understood. In addition, special attention should be paid to the crack development during this phase. Furthermore, future work should concentrate in analyzing the different aspects that could influence the crack development of the intumescent coating char structure, e.g. the steel profile type (open or closed section).

As an influence of the shape of the steel profile on the behavior of IC (in terms of temperatures reached inside the steel) emerges from the comparisons performed in this work, what are the phenomena that come into play and what is their effects, have to be understood in future work. So, full-scale tests should be carried out: large beams, columns or steel frames protected by intumescent coatings should be exposed to several fire scenarios.

These future real-scale experiments should also cover elements protected by intumescent coating, subjected to different load condition. In this way there is the possibility of studying the phenomenon of stickability or the ability of the IC to adhere to the steel without slumping, cracking or falling off under loads in fire conditions.

By deepening all these aspects with further experimental tests, it will be possible to calibrate, based on the approach using these work, an even more general formula that may foresee, during modeling, the behavior of any structure protected with any intumescent coating.

BIBLIOGRAPHY

[1] Fitzgerald P., Mawhinney J. and Slye O., "Water-based fire suppression – History of fire protection engineering", National Fire Protection Association, Quincy, MA, 2003.

[2] Richardson K., "Historical evolution of fire protection engineering - History of fire protection engineering", National Fire Protection Association, Quincy, MA, 2003.

[3] Cote A., "Founding organizations - History of fire protection engineering", National Fire Protection Association, Quincy, MA, 2003.

[4] Nelson H.,"Fire severity and fire resistance - History of fire protection engineering", National Fire Protection Association, Quincy, MA, 2003.

[5] Lund D., "Fire protection engineering professional societies - History of fire protection engineering", National Fire Protection Association, Quincy, MA, 2003.

[6] Skowronski W., "Fire safety of metal structures", Wydawnictwo Naukowe PWN, 2001.

[7] Lataille J.I., "Fire protection engineering in building design", Elsevier Science, 2003.

[8] Buchanan A.H., "Structural design for fire safety", John Wiley & Sons, 2001. Corus Construction and Industrial, "Fire resistance of steel-framed buildings", North Lincolnshire, 2006.

[9] Nigro E., Pustorino S., Cefarelli G:, Princi P.(2009): “Progettazione di strutture in acciaio e composte acciaio-calcestruzzo in caso di incendio”, Hoepli, Novembre 2009. ISBN 978-88-203-4400-9.

[10] Yuan J., "Intumescent coating performance on steel structures under realistic fire conditions", Doctor of Philosophy thesis, School of Mechanical, Aerospace and Civil Engineering, University of Manchester, 2009.

[11] Global Market Insight - Report ID: GMI357

[12] European Committee for Standardization (CEN), "Eurocode 3: Design of steel structures - Part 1-2: General rules - Structural fire design", EN 1993-1-2, April 2005.

[13] Hellomagazine.com, "The Shard: London’s skyscraping innovation and jawdropping city views", ttp://www.hellomagazine.com, January 2013.

[14] A. Lucherini, “Experimental study of the behaviour of steel structures protected by different intumescent coatings and exposed to various fire scenarios”. DTU Master Thesis Project.

[15] Gillet M., Autrique L. and Perez L., "Mathematical model for intumescent coatings growth: application to fire retardant systems

evaluation", Institute of Physics Publishing, Journal of Physics D: Applied Physics 40, pp. 883-899, 2007.
[16] Tramm H. et al., "U.S. Patent 2,106,938", February 1938.
[17] Butler K., "Physical modelling of intumescent fire retardant polymers", Building and Fire Research Laboratory, National Institute of Standards and Technology, Gaithersburg, Maryland, 1997.
[18] Underhill W., "King's Cross Station Western Concourse", http://www.architectmagazine.com, May 2012.
[19] Dowling J., "Fire protection costs for structural steelwork", New Steel Construction, UK, 2003.
[20] CMD (Construction Market Data), "The market for fire protection of steel frames total market (beams and columns) by Types of Fire Protection, Great Britain,years 2001-2014", http://www.cmdgroup.com, February 2015.
[21] Sorathia U., Gracik T., Ness J., Durkin A., Williams F., Hunstad M. and Berry F., "Evaluation of Intumescent Coatings for Shipboard Fire Protection", Journal of Fire Sciences, vol. 21, pp. 423-428, November 2003.
[22] Perez L., Autrique L. and Pechoux F., "Modelling and experimental testing of intumescent coatings under high thermal flux for military applications", Fire Safety Science, 2014.
[23] Michael G. Goode "Fire Protection of Structural Steel in High-Rise Buildings" U.S. Department of Commerce Technology Administration.
[24] H. L. Vandersall: "Intumescent Coating Systems, Their Development and Chemistry," Journal of Fire and Flammability, Vol. 2, p. 97-140 (April 1971).
[25] Roberts T., Shirvill L., Waterton W. and Buckland I., "Fire resistance of passive fire protection coatings after long-term weathering", Process Safety and Environmental Protection, vol. 88, pp. 1-19, 2010.
[26] Kandola B.S., Akonda M.H. and Horrocks A.R., "Use of high-performance fibres and intumescents as char promoters in glass-reinforced polyester composites", Poly. Deg. and Stab., 88, 123, 2005.
[27] Jimenez M., Duquesne S. and Bourbigot S., "Characterization of the performance of an intumescent fire protective coating", Surface and Coating Technology, vol. 201, pp. 979-987, 2006.
[28] Mamleev V.S., Bekturov E.A. and Gibov K.M., "Dynamics of intumescence of fire-retardant polymeric materials", J. Appl. Polym. Sci., vol. 70(8), pp. 1523–1542, 1998.

[29] Bourbigot, S., M.L. Bras, F. Dabrowski, J.W. Gilman and T. Kashiwagi, 2000. PA-6 clay nanocomposite hybrid as char forming agent in intumescent formulations. Fire Mater., 24: 201-208.
[30] Camino G., Costa L. and Trossarelli L., "Study of the mechanism of intumescence in fire retardant polymers: mechanism of action in polypropylene-ammonium polyphosphate-pentaerythritol mixture", Poly. Deg. and Stab., vol. 7, pp. 25, 1984.
[31] Andersen J., "Experimental study of the thermal resistance of intumescent coatings exposed to different heating rates", Master of Science thesis, Civil Engineering Department, Technical University of Denmark, Copenhagen, Denmark, 2015.
[32] Li G.Q., Lou G.B., Zhang C., Wang L. and Wang Y., "Assess the fire resistance of intumescent coatings by equivalent constant thermal resistance", Fire Technology, vol. 48, pp. 529-546, 2012. 88
[33] Wang L., Dong Y., Zhang D., Zhang D. and Zhang C., "Experimental study of heat transfer in intumescent coatings exposed to non-standard furnace curves", Fire Technology, vol. 51, no.1, pp. 627-643, 2015.
[34] Zhang Y., Wang Y., Bailey C.G. and Taylor A.P., "Global modelling of fire protection performances of an intumescent coating under different furnace fire conditions", Journal of Fire Science, vol. 31, no.1, pp. 51-72, 2012.
[35] Horaceck H. and Pieh S., "The importance of intumescent systems for fire protection of plastic materials," Polymer International, vol. 49, pp. 1106-1114, 2000.
[36] Comité Europeeén de Normalization (CEN), "EN 13381-4: Test methods for determining the contribution to the fire resistance of structural members - Part 4: Applied protection to steel members", Bruxelles, Belgium, 2002.
[37] International Organization for Standardization (ISO), "ISO 834-1:1999: Fire resistance test - Elements of building construction - Part 1: General requirements for fire resistance testing", Geneva, Switzerland, 1999.
[38] European Committee for Standardization (CEN), "Eurocode 1: Actions on structures-Part 1-2: General actions – Actions on structures exposed to fire ", EN 1991-1-2, June 2007.
[39] Parkinson D., "Performed-based design of structural steel for fire conditions", Master of Science thesis, Worcester Polytechnic Institute, Massachusetts, July 2002.

[40] Pettersson O., Magnusson S. and Thor J., "Fire engineering design of steel structures", Swedish Institute of Steel Construction (SBI), Stockholm, 1976.
[41] Wang Y., Burgess I., Wald F. and Gillie M., "Performance-based fire engineering of structures", CRC Press, Taylor & Francis Group, 2013.
[42] Hertz K., "Parametric Fires for Structural Design", Fire Technology, vol. 48, pp. 807-823, October 2011.
[43] Lane B., "Performance-based design for fire resistance", Modern Steel Construction, December 2000.
[44] Wang Y., Goransson U., Holmstedt G. and Omrane A., "A model for prediction of temperature in steel structure protected by intumescent coating, based on tests in the cone calorimeter", International Association for Fire Safety Science, Proceedings of the 8th International Symposium on Fire Safety Science, pp. 235-246, Beijing, China, 2005.
[45] Kolsek J. and Cesarek P., "Performance-based fire modelling of intumescent painted steel structures and comparison to EC3", Journal of Constructional Steel Research, vol. 104, pp. 91, October 2014.
[46] Vandersall H.L., "Intumescent coating systems, their development and chemistry", Journal of Fire and Flammability, vol. 2, pp.97-140, April 1971. 89
[47] Camino G. and Costa L., "Performance and mechanism of fire retardants in polymers- A review", Poly. Deg. and Stab., vol. 20, pp. 271, 1988.
[48] Camino G., Costa L. and Martinasso G., "Intumescent fire-retardant systems", Poly. Deg. and Stab., vol. 23, pp. 359, 1989.
[49] Bilotta A., de Silva D., Nigro E.(2016), Tests on intumescent paints for fire protection of existing steel structures, Construction and Building Materials 121 doi:10.1016/j.conbuildmat.2016.05.144,410–422 pp.
[50] Bilotta A., de Silva D., Nigro E.(2016), General approach for the assessment of the fire vulnerability of existing steel and composite steel concrete structures, Journal of Building Engineering, http://dx.doi.org/10.1016/j.jobe.2016.10.011
[51] Le Bras M., Bugajny M., Lefebvre J. and Bourbigot S., "Use of polyurethanes as char-forming agents in polypropylene intumescent formulations", Polym. Int., vol. 49, pp. 1115, 2000.
[52] Le Bras M., Camino G., Bourbigot S. and Delobel R., "Fire retardancy of polymers: the use of intumescence", The Royal Society of Chemistry, Cambridge, UK, 1998.

[53] Di Blasi, C. and Branca, C. (2001). Mathematical Model for the Nonsteady Decomposition of Intumescent Coatings, AIChE Journal, 47(10): 2359-2370

[54] Bourbigot S., Le Bras M., Duquesne S. and Rochery M., "Recent advances for intumescent polymers", Macromol. Mater. Eng., vol. 289, pp. 499, 2004.

[55] P. Schaumann, W. Weisheim. “Effect of heating rates in natural fires on the thermal performance of a solvent-borne intumescent coating”, IFireSS 2017 2nd International Fire Safety Symposium Napoli, Italy June 7-9, 2017

[56] Cagliostro D.E., Riccitello S.R., Clark K.L. and Shimizu A.B., "Intumescent coating modelling", Journal of Fire and Flammability, vol. 6, pp. 205, 1975.

[57] Anderson C.E., Ketchum D.E. and Mountain W.P., "Thermal conductivity of intumescent chars", Journal of Fire Science, vol. 16, pp. 390-410, 1988.

[58] Butler K., Baum H.R. and Kashiwagi T., "Three-dimensional modelling of intumescent behaviour in fires", Fire Safety Science, Proc. 5th Int. Symp. 523, 1997.

[59] Bartholomai M., Schriever R. and Schartel B., "Influence of external heat flux and coating thickness on the thermal insulation properties of two different intumescent coatings using cone calorimeter and numerical analysis", Journal of Fire Materials, vol. 27, pp. 151-162, 2003.

[60] Dai X.H., Wang Y.C. and Bailey C., "A simple method to predict temperatures in steel joints with partial intumescent coating fire protection", Fire Technology, vol. 46, pp. 19-35, 2010.

[61] ISO834-1, Fire resistance tests - Elements of building construction - Part 1: General requirements for fire resistance testing, Geneva, Switzerland, 1999.

[62] EN 13381-4, Test methods for determining the contribution to the fire resistance of structural members - Part 4: Applied protection to steel members, European Committee for Standardization, Brussels, 2002.

[63] EN 13381-8 - Test methods for determining the contribution to the fire resistance of structural members – Part 8: Applied reactive protection to steel members, European Committee for Standardization, Brussels, 2013.

[64] EN 1363-1 - Fire resistance test: General requirements, European Committee for Standardization, Brussels, 2012.

[65] EN 1363-2 - Fire resistance tests. Alternative and additional procedures, European Committee for Standardization, Brussels, 2011.
[66] P. E. Anuta, "Spatial registration of multispectral and multitemporal digital imagery using fast Fourier transform techniques", IEEE Trans. Geosci. Electron., vol. GE-8, p. 353–368, Oct. 1970.
[67] Jump T. J. Keating, P. R. Wolf, and F. L. Scarpace, "An Improved Method of Digital Image Correlation", Photogrammetric Engineering and Remote Sensing 41(8): 993–1002, (1975).
[68] ETAG018, Guideline for European Technical Approval of Fire Protective Products, Part 2: Reactive Coatings for Fire Protection of Steel Elements, European Organization for Technical Approvals, Brussels, 2006.
[69] UNI 10898-1 - Fire proofing systems- Inspection modes for the installation. Part 1: Intumescent coating. 2012.
[70] Y. Sakumoto; J. Nagata; A. Kodaira; and Y. Saito Durability "Evaluation of Intumescent Coating for Steel Frames", Journal of Materials in Civil Engineering 13(4) · August 2001 DOI: 10.1061/(ASCE)0899-1561(2001)13:4(274)
[71] D. de Silva, A. Bilotta, E. Nigro (2016). Experimental tests on intumescent coating for protecting steel structures. "9th International Conference on Structures in Fire SiF'" Princeton-USA; 8-10 June 2016
[72] D. de Silva, A. Bilotta, E. Nigro (2017) Experimental analysis on the effectiveness of intumescent coatings in fire. "IFireSS – International Fire Safety Symposium, Naples, Italy, 7th-9th June 2017"
[73] D. de Silva, A. Bilotta, E. Nigro (2017) "Effect of the thermal input on the behavior of intumescent coatings" ASFE 2017 - Applications of Structural Fire Engineering, 7-8th September 2017, Manchester, UK.
[74] D. de Silva, A. Bilotta, E. Nigro (2017) "Analisi del comportamento di vernici intumescenti per la protezione al fuoco delle strutture in acciaio" accettato per la pubblicazione negli atti della conferenza:- XXVI GIORNATE ITALIANE della COSTRUZIONE IN ACCIAIO 28-30 Settembre 2017".
[75] J.-M. Franssen, SAFIR: A thermal/structural program modelling structures under fire, Eng. J. A.I.S.C. 42 (3) (2005) 143–158.
[76] Zhang Y., Wang Y., Bailey C.G. and Taylor A.P., "Global modelling of fire protection performances of intumescent coatings under different cone calorimeter heating conditions", Fire Safety Journal, vol. 50, pp. 51-62, February 2012. Staticstools, "Cross-Section Properties", http://www.staticstools.eu.

[77] Karlsson B. Performance-based test methods for material flammability. In: Horrocks AR, Price D, editors. Fire retardant materials. Cambridge, UK: Woodhead Publishing Limited; 2001. p. 355e77 [chapter 12].
[78] Babrauskas V. The cone calorimeter. In: Babrauskas V, Grayson SJ, editors. Heat release in fires. Barking, UK: Elsevier Science Publishers Ltd; 1992. p. 61e91 [chapter 4].
[79] Lyon RE. Plastics and rubber. In: Harper CA, editor. Handbook of materials in fire protection engineering C. New York, US: McGraw-Hill Handbooks; 2004. p. 3.1e3.51 [chapter 3].
[80] ISO 5660-1:2002: Reaction-To-Fire Tests – Heat Release, Smoke Production and Mass Loss Rate. Part 1: Heat Release Rate (cone calorimeter method), International Organization for Standardization, 2002.
[81] Henderson, J.B., Wiebelt, J.A., and Tant, M.R., "A Model for the Thermal Response of Polymer Composite Materials with Experimental Verification," Journal of Polymer Materials, 19, 1985, pp. 579-595.
[82] Fire Protection for Structural Steel in Buildings, 4th Edition (Revised 17thDecember 2007). Association for Specialist Fire Protection (ASFP), The Steel Construction Institute (SCI) and The Fire Test Study Group (FTSG), 2007
[83] BS EN ISO 12944-1 to 6: 1998 Paints and Varnishes – Corrosion protection of steel structures by protective paint systems. British Standards Institution. 8.
[84] BS EN ISO 8501-1:2001. Preparation of steel substrates before application of paints and related products. British Standards Institution.
[85] ASFP Technical Guidance Note 010:2008. Guidance note for the refurbishment and upgrading of fire protection of structural steelwork. Available at: www.asfp.org.uk.
[86] ASFP Technical Guidance Note 008:2008. Guidance on the junction between different fire protection systems when applied to load bearing structural steel elements. Available at: www.asfp.org.uk
[87] BS 8202-2:1992 Coatings for fire protection of building elements. Code of practice for the use of intumescent coating systems to metallic substrates for providing fire resistance.
[88] Council Directive 1999/13/EC on the limitation of emissions of volatile organic compounds due to the use of organic solvents in certain activities and installations. Official Journal L85, 29.3.1999.
[89] Pollution Prevention and Control (England and Wales) Regulations 2000. SI 2000 No 1973

[90] Directive 2004/42/CE of the European Parliament and of the Council on the limitation of emissions of volatile organic compounds due to the use of organic solvents in certain paints and varnishes and vehicle refinishing products and amending Directive 1999/13/EC. Official Journal of the EU L 143/87. 30.4.2004.
[91] VOCs in Paints, Varnishes and Vehicle Refinishing Products Regulations 2005, SI 2005/2773.
[92] BS EN ISO 9000:2000. Quality management systems – Requirements. British Standards Institution.
[93] Kay T.R., Kirby B.R. and Preston R.R., "Calculation of the heating rate of an unprotected steel member in a standard fire resistance test", Fire Safety Journal, vol. 26. pp. 327-350, 1996.
[94] Mooney J., "Surface radiant-energy balance for structural thermal analysis", Fire and Materials 1992;16:61-6, 1992.
[95] European Committee for Standardization (CEN), "Eurocode 1: Actions on structures Part 1-1: General actions - Densities, self-weight, imposed loads for buildings", EN 1991-1-1, April 2002.
[96] Han Z., Fina A., Malucelli G. and Camino G., "Testing fire protective properties of intumescent coatings by in-line temperature measurements on a cone calorimeter", Progress in Organic Coatings 69, pp. 475-480, 2010. 90
[97] Omrane A., Wang Y.C., Goransson U., Holmstedt G. and Alden M., "Intumescent coating surface temperature measurement in a cone calorimeter using laser-induced phosphorescence", Fire Safety Journal, vol. 42, pp. 68-74, October 2006.
[98] Babrauskas V., "The cone calorimeter", Heat release in fires, Grayson SJ (eds), Elsevier Applied Science, London, New York, 1992.
[99] Hastie T, Tibshirani R, Friedman J. The elements of statistical learning, data mining, inference and prediction. Springer; 2009.
[100] Wald F., Strejček M., Tichá A.: “On Bolted Connection with Intumescent Coatings”. 4th International Workshop "Structures in Fire - SiF'06", University of Aveiro (2006), 371-378
[101] Wickström, U.; Temperature analysis of heavily-insulated steel structures exposed to fire; Fire of Safety Journal, 9, pp281-285, 1985.
[102] Franssen J.-M.: SAFIR. A Thermal/Structural Program Modelling Structures under Fire. Engineering Journal, A.I.S.C., (2005)Vol 42, No. 3, 143-158.
[103] MathWorks, (2016). Bioinformatics Toolbox:User's Guide (R2016a)from:www.mathworks.com/help/pdf_doc/nnet/nnet_ug.pdfww.mathworks.com/help/pdf_doc/bioinfo/bioinfo_ug.pdf

A. Appendix A

Measured dry film thickness (d_{IC})

This appendix inspects all the dry film thicknesses measured on the test samples with a coating thickness gauge.

Measured d_{IC} on steel plate samples for furnace tests

The theoretical dry film thickness (d_{IC}) of the samples tested in furnace were:

-500 μm;

-1000 μm;

-1500 μm;

-2000 μm.

The IC was directly applied on the plates with airless pump in the Amonn Laboratoty, so the process was automatically controlled.

In order to understand the quality of the executed work and the uniformity of the IC on the samples, the dry film thicknesses were measured by using coating thickness gauge (Fig. A.1). Before performing the measurements, the instrument calibration was performed as described in the instrument instruction booklet. Each measurement was performed by firmly pressing the head of the device down on the coated surface.

Fig. A.1- coating thickness gauge.

The coating thickness gauge evaluates the d_{IC} thanks to a magnet and it collects all the measurements inside its own memory.

In order to ensure the repeatability and compatibility between the different measurements, the dry film thickness was evaluated at specific locations on the samples: Fig. A.2 represents a schematic illustration of the measurement points.

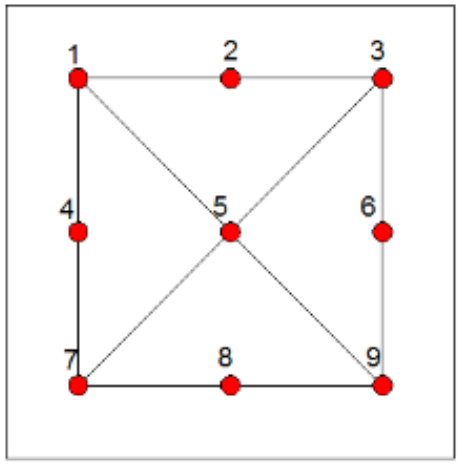

Fig. A.1- Measurements point.

All the dry film thicknesses measured on the test samples with the correspondent statistical values are listed in table A.1 and expressed in microns.

Table. A.1- d_{IC} Measurements_furnace tests.

Samples	1	2	3	4	5	6	7	8	9	Mean value	DevST.	CoV
S_300x300x4-250_500_ISO_1	485.00	490.00	500.00	510.00	490.00	486.00	485.00	500.00	510.00	495.11	10.19	2%
S_300x300x4-250_500_ISO_2	500.00	510.00	515.00	560.00	515.00	520.00	512.00	480.00	500.00	512.44	21.51	4%
S_300x300x4-20_1000_ISO_1	980.00	999.00	1000.00	985.00	1012.00	1100.00	1000.00	988.00	1000.00	1007.11	36.16	4%
S_300x300x4-250_1000_ISO_2	1010.00	1000.00	998.00	985.00	1000.00	1000.00	1012.00	1000.00	998.00	1000.33	7.71	1%
S_300x300x4-250_1500_ISO_1	1512.00	1500.00	1600.00	1450.00	1500.00	1520.00	1500.00	1529.00	1500.00	1512.33	39.55	3%
S_300x300x4-250_1500_ISO_2	1500.00	1500.00	1512.00	1560.00	1486.00	1500.00	1500.00	1524.00	1560.00	1515.78	27.10	2%
S_300x300x4-250_2000_ISO_1	2000.00	2000.00	2005.00	2012.00	2000.00	2000.00	1955.00	1900.00	1986.00	1984.22	35.62	2%
S_300x300x4-250_2000_ISO_2	2012.00	2000.00	2025.00	2000.00	1999.00	1980.00	2000.00	2000.00	2000.00	2001.78	11.95	1%
S_300x300x8-125_500_ISO_1	500.00	512.00	525.00	500.00	500.00	512.00	526.00	500.00	500.00	508.33	10.98	2%
S_300x300x8-125_500_ISO_2	513.00	500.00	500.00	510.00	500.00	516.00	500.00	510.00	500.00	505.44	6.69	1%
S_300x300x8-125_1000_ISO_1	978.00	991.00	999.00	1000.00	1000.00	1100.00	1050.00	1000.00	1000.00	1013.11	37.95	4%
S_300x300x8-125_1000_ISO_2	1000.00	1000.00	1000.00	999.00	1000.00	1025.00	1020.00	1000.00	1050.00	1010.44	17.83	2%
S_300x300x8-125_1500_ISO_1	1500.00	1486.00	1489.00	1500.00	1512.00	1486.00	1520.00	1489.00	1500.00	1498.00	11.95	1%
S_300x300x8-125_1500_ISO_2	1500.00	1500.00	1500.00	1548.00	1490.00	1500.00	1490.00	1500.00	1500.00	1503.11	17.38	1%
S_300x300x8-125_2000_ISO_1	1985.00	2000.00	2000.00	2015.00	2000.00	2016.00	2000.00	2000.00	1995.00	2001.22	9.47	0%
S_300x300x8-125_2000_ISO_2	2000.00	1985.00	2000.00	1985.00	1999.00	2000.00	1985.00	1999.00	2000.00	1994.78	7.34	0%
S_300x300x15-67_500_ISO_1	500.00	512.00	525.00	500.00	500.00	512.00	526.00	500.00	500.00	508.33	10.98	2%
S_300x300x15-67_500_ISO_2	500.00	500.00	520.00	488.00	500.00	520.00	526.00	530.00	530.00	512.67	15.72	3%
S_300x300x15-67_1000_ISO_1	1000.00	1000.00	998.00	1100.00	1012.00	1000.00	1156.00	900.00	985.00	1016.78	72.61	7%
S_300x300x15-67_1000_ISO_2	998.00	1012.00	1000.00	988.00	1000.00	999.00	998.00	1000.00	1000.00	999.44	6.06	1%
S_300x300x15-67_1500_ISO_1	1500.00	1500.00	1589.00	1463.00	1495.00	1498.00	1500.00	1500.00	1500.00	1505.00	33.72	2%
S_300x300x15-67_1500_ISO_2	1495.00	1500.00	1500.00	1498.00	1500.00	1500.00	1498.00	1500.00	1560.00	1505.67	20.45	1%
S_300x300x15-67_2000_ISO_1	2000.00	2000.00	2000.00	2000.00	2000.00	2000.00	1985.00	2000.00	2015.00	2000.00	7.50	0%
S_300x300x15-67_2000_ISO_2	2012.00	2000.00	2025.00	2000.00	1999.00	1980.00	2000.00	2000.00	2000.00	2001.78	11.95	1%
S_60x60x5-250_500_ ISO _1	500.00	500.00	498.00	520.00	525.00	530.00	500.00	498.00	499.00	507.78	13.18	3%
S_60x60x5-250_500_ ISO _2	596.00	600.00	581.00	550.00	512.00	520.00	515.00	510.00	489.00	541.44	41.55	8%
S_60x60x5-250_1500_ ISO _1	1500.00	1486.00	1500.00	1563.00	1528.00	1500.00	1486.00	1500.00	1500.00	1507.00	24.25	2%
S_60x60x5-250_1500_ ISO _2	1500.00	1500.00	1500.00	1512.00	1500.00	1489.00	1500.00	1521.00	1500.00	1502.44	9.03	1%
S_75x75x10-125_500_ ISO _1	499.00	500.00	500.00	512.00	500.00	525.00	500.00	498.00	500.00	503.78	8.98	2%
S_75x75x10-125_500_ ISO _2	521.00	525.00	546.00	500.00	495.00	498.00	512.00	512.00	500.00	512.11	16.50	3%
S_75x75x10-125_1500_ ISO _1	1498.00	1512.00	1500.00	1500.00	1468.00	1499.00	1512.00	1500.00	1469.00	1495.33	16.13	1%
S_75x75x10-125_1500_ ISO _2	1510.00	1523.00	1500.00	1495.00	1500.00	1496.00	1516.00	1500.00	1546.00	1509.56	16.66	1%
S_135x135x20-67_500_ ISO _1	500.00	500.00	500.00	498.00	500.00	495.00	500.00	489.00	495.00	497.44	3.81	1%
S_135x135x20-67_500_ ISO _1	486.00	495.00	500.00	512.00	512.00	516.00	500.00	500.00	498.00	502.11	9.55	2%
S_135x135x20-67_1500_ ISO _	1500.00	1500.00	1563.00	1500.00	1498.00	1500.00	1589.00	1529.00	1589.00	1529.78	39.81	3%
S_135x135x20-67_1500_ ISO _	1496.00	1512.00	1500.00	1496.00	1496.00	1496.00	1500.00	1520.00	1500.00	1501.78	8.51	1%
S_300x300x4-250_500_SM_1	498.00	500.00	500.00	498.00	495.00	500.00	512.00	498.00	496.00	499.67	4.95	1%
S_300x300x4-250_1000_SM_1	1000.00	999.00	1000.00	1000.00	998.00	1000.00	1024.00	1000.00	1000.00	1002.33	8.15	1%
S_300x300x4-250_1500_SM_1	1512.00	1500.00	1600.00	1450.00	1500.00	1520.00	1500.00	1529.00	1500.00	1512.33	39.55	3%
S_300x300x4-250_2000_SM_1	2012.00	2000.00	2000.00	2000.00	1986.00	1996.00	2000.00	2000.00	2012.00	2000.67	7.87	0%
S_300x300x8-125_500_SM_1	500.00	500.00	512.00	562.00	500.00	512.00	526.00	500.00	500.00	512.44	20.66	4%
S_300x300x8-125_1000_SM_1	1010.00	1000.00	998.00	1000.00	1012.00	1018.00	1000.00	999.00	994.00	1003.44	7.92	1%
S_300x300x8-125_1500_SM_1	1521.00	1496.00	1500.00	1512.00	1521.00	1500.00	1498.00	1500.00	1496.00	1504.89	10.29	1%
S_300x300x8-125_2000_SM_1	2000.00	2000.00	2005.00	2012.00	2000.00	2000.00	1955.00	1900.00	1900.00	1974.67	45.30	2%
S_300x300x15-67_500_ SM _1	485.00	494.00	496.00	500.00	501.00	511.00	546.00	520.00	541.00	510.44	21.26	4%
S_300x300x15-67_1000_ SM _1	1015.00	999.00	1000.00	1000.00	999.00	998.00	1015.00	999.00	1000.00	1002.78	6.96	1%
S_300x300x15-67_1500_ SM _1	1500.00	1496.00	1500.00	1500.00	1499.00	1500.00	1500.00	1510.00	1521.00	1502.89	7.77	1%
S_300x300x15-67_2000_ SM _1	2011.00	2000.00	2015.00	2000.00	2015.00	2011.00	2000.00	1986.00	2000.00	2004.22	9.54	0%

Evaluation of d_{IC} on steel plate samples for cone heater tests

In this case, the dry film thickness, for IC_A, IC_B, IC_C was evaluated through the weight of the sample plate before and after the IC application. The weigh scale is extremely accurate. All the results are contained in table A.2.

While, the IC_C* was applied by manufacturer with airless pump; and the IC thickness was measured again with the thickness gauge; the results are in Table A.3.

Table. A.2- d_{IC} Measurements_cone calorimeter tests (IC_A, IC_B, IC_C).

	ID	L	B	area (A)	Density	t_plaes	Volume	Wt_1	Wt_2	DW	d_{IC}
IC_A	A1	101	100	101	1	6	0.164	476	489	13	1006
	A2	100	100	100	1	6	0.164	474	487	13	1008
	A3	100	100	100	1	6	0.163	473	486	13	1028
	A4	100	99	100	1	6	0.165	470	490	20	1576
	A5	101	99	100	1	6	0.164	470	490	20	1543
	A6	101	99	99	1	6	0.164	465	485	20	1547
IC_B	B1	100	99	99	1	6	0.164	468	481	13	1038
	B2	100	99	99	1	6	0.163	469	483	13	1043
	B3	100	99	99	1	6	0.162	464	478	14	1056
	B4	100	98	99	1	6	0.163	466	486	20	1522
	B5	100	98	98	1	6	0.164	462	480	19	1466
	B6	100	98	99	1	6	0.163	465	484	19	1504
IC_C	C1	100	100	101	1	6	0.163	471	485	15	1048
	C2	100	98	98	1	6	0.163	461	475	14	1051
	C3	101	99	99	1	6	0.163	467	481	14	1042
	C4	100	98	98	1	6	0.165	462	484	21	1569
	C5	100	99	100	1	6	0.163	471	492	21	1506
	C6	100	101	102	1	6	0.162	481	502	21	1508

Table. A.3- d_{IC} Measurements_cone calorimeter tests (IC_C*).

Samples	1	2	3	4	5	6	7	8	9	Mean value	DevST.	CoV
C*2	1002	1000	1000	998	1000	1010	1000	1000	1000	1001	3.28	0%
C*4	1056	1000	1010	1000	1000	999	995	1000	1012	1008	17.73	2%
C*9	1000	1000	998	999	1000	1000	996	999	1015	1001	5.18	1%
C*10	998	952	1000	1015	1000	1000	1000	1000	1000	996	16.32	2%
C*11	1000	1000	995	998	1000	1000	1026	1015	1000	1004	9.44	1%
C*12	1000	1005	1000	1000	1090	1100	1059	1012	1000	1030	39.28	4%

B. Appendix B

Validation of unprotected steel temperatures

In order to verify the acceptability and rationality of the results, the experimental set-ups were validated according to FE models performed in SAFIR. In particular, the two different experiments (gas furnace and cone heater) were performed using unprotected steel samples and the measured and calculated steel temperature curves were compared.

Experiments in furnace

Regarding the experiments in furnace, several tests on unprotected steel samples were conducted, varying the A/V and the shape of the samples:

1- A/V= 250 m^{-1};

2- A/V= 125 m^{-1};

3- A/V= 67 m^{-1};

1a- A/V= 250 m^{-1} (small sample);

2a- A/V= 125 m^{-1} (small sample);

3a- A/V= 67 m^{-1} (small sample).

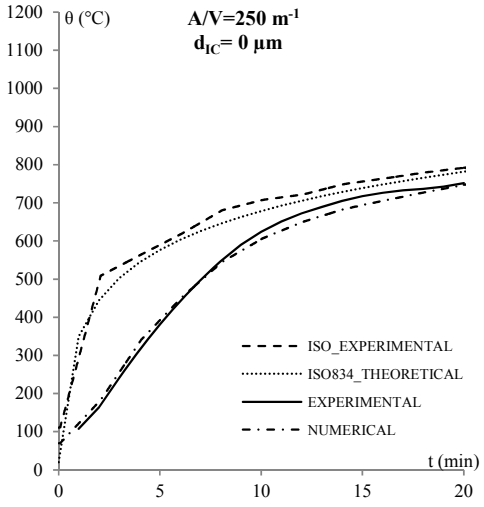

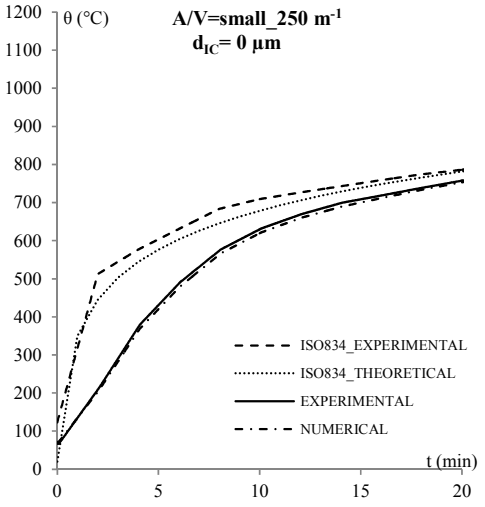

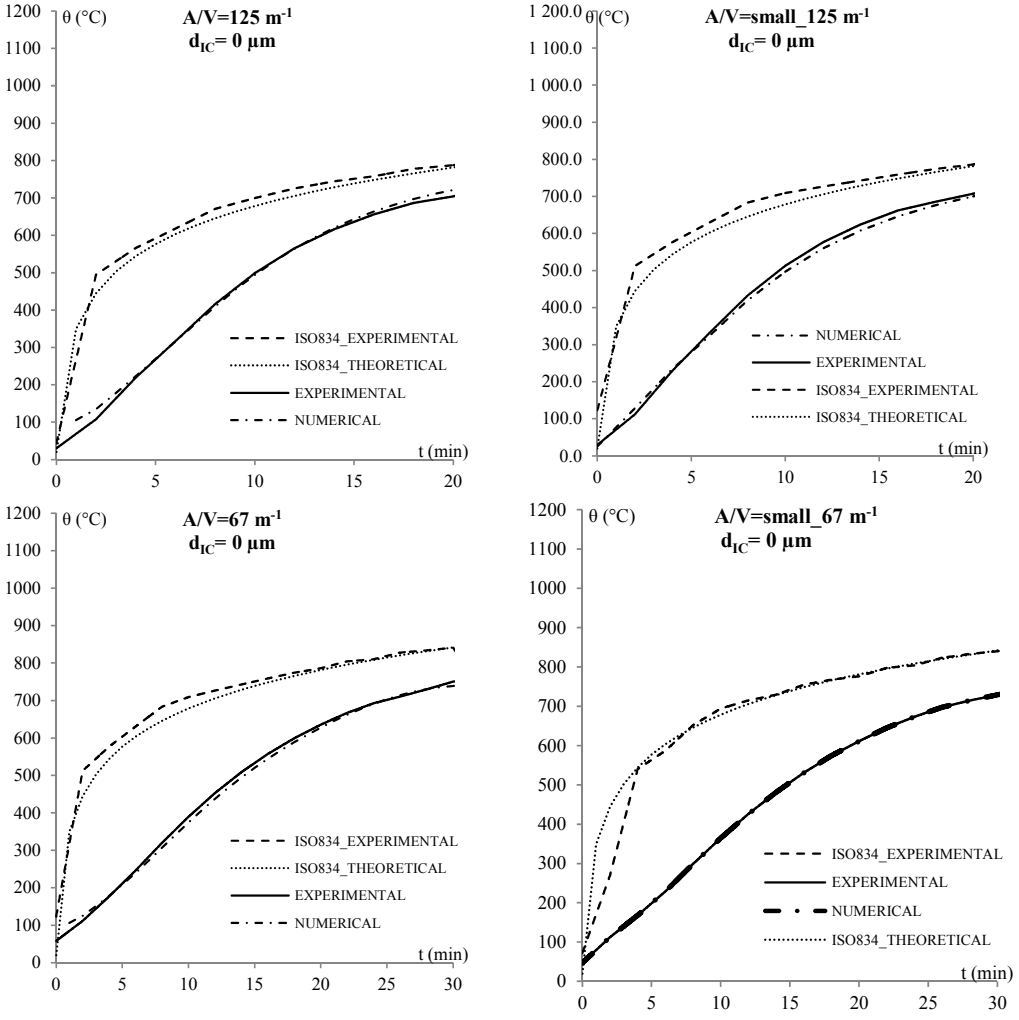

Fig. B.1- Comparison between numerical and experimental unprotected steel samples_furnace.

In the graphs shown in Fig. B.1, the temperature-time curves of the unprotected steel measured during the furnace tests are compared to the numerical curve. Moreover, the two are very similar to each other.

Experiments in cone calorimeter

The mass loss cone calorimeter experimental set-up was validated according to FE models performed in SAFIR, applying directly the heat flux on the exposed plates. Regarding the mass loss cone heater, two different experiments with different heat fluxes (30 and 50 kW/m^2) were carried out in order to understand if the experimental configuration could validate the analytical model:

-steel_30;
-steel_50.

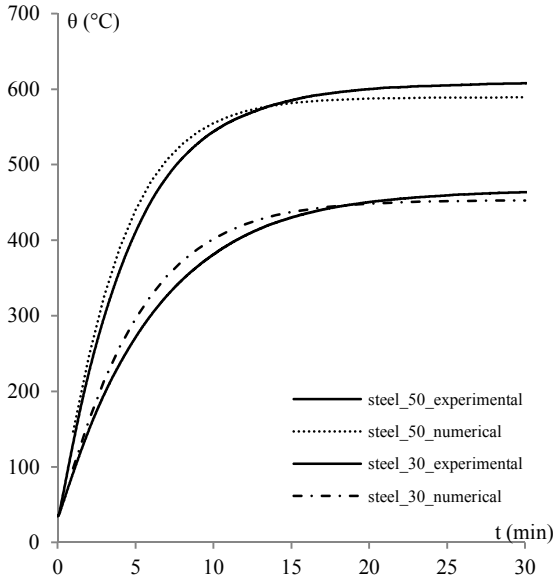

Fig. B.2- Comparison between numerical and experimental unprotected steel samples_cone calorimeter.

In the graphs shown in Fig. B.2, the temperature-time curves of the unprotected steel measured during the furnace tests are compared to the numerical curve. Moreover, the two are very similar to each other.

C. Appendix C

Analytical and numerical results

In this appendix the results of the analytical and numerical models of all the testes which are not included in the body of the thesis tests.

In particular in the following the results are shown for:

- 250_1000_ISO;
- 250_2000_ISO;
- 125_1000_ISO;
- 125_2000_ISO;
- 67_1000_ISO;
- 67_2000_ISO;
- 250_1000_SM;
- 250_2000_ SM;
- 125_1000_ SM;
- 125_2000_ SM;
- 67_1000_ SM;
- 67_2000_ SM.

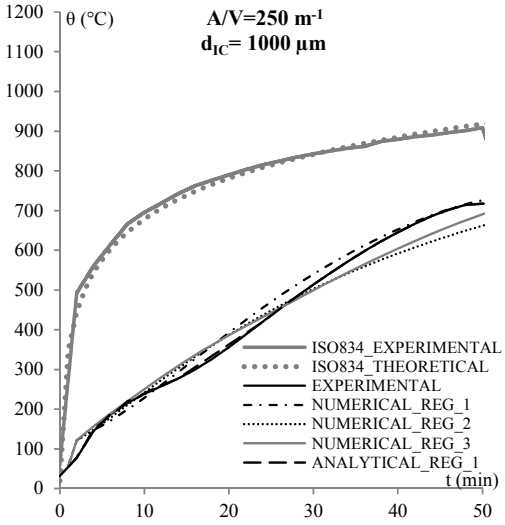

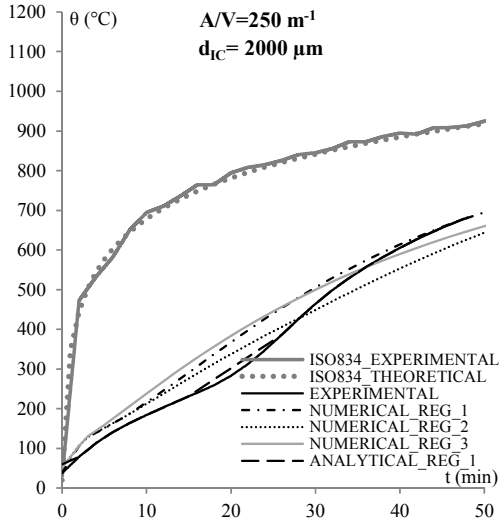

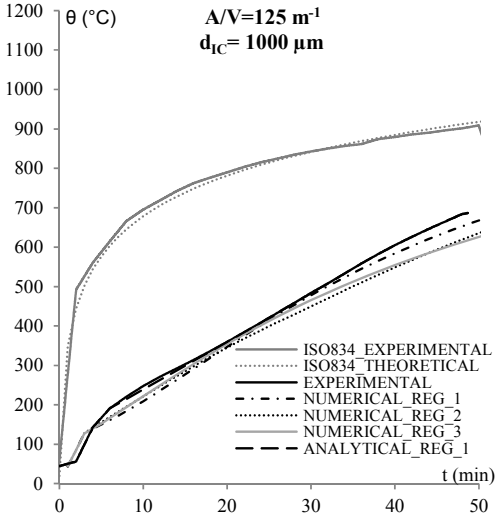
θ (°C)
A/V=125 m-1
dIC= 1000 µm
ISO834_EXPERIMENTAL
ISO834_THEORETICAL
EXPERIMENTAL
NUMERICAL_REG_1
NUMERICAL_REG_2
NUMERICAL_REG_3
ANALYTICAL_REG_1
t (min)

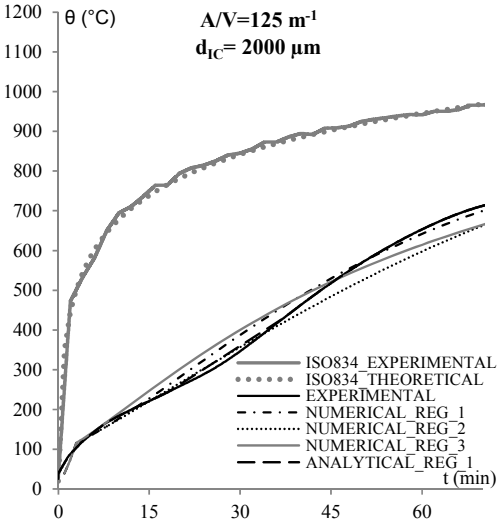
θ (°C)
A/V=125 m-1
dIC= 2000 µm
ISO834_EXPERIMENTAL
ISO834_THEORETICAL
EXPERIMENTAL
NUMERICAL_REG_1
NUMERICAL_REG_2
NUMERICAL_REG_3
ANALYTICAL_REG_1
t (min)

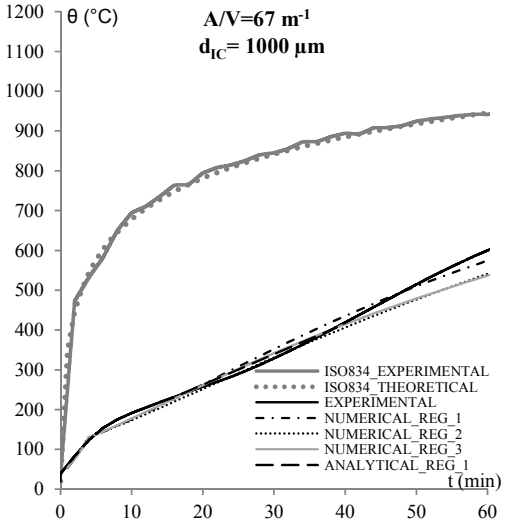
θ (°C)
A/V=67 m-1
dIC= 1000 µm
ISO834_EXPERIMENTAL
ISO834_THEORETICAL
EXPERIMENTAL
NUMERICAL_REG_1
NUMERICAL_REG_2
NUMERICAL_REG_3
ANALYTICAL_REG_1
t (min)

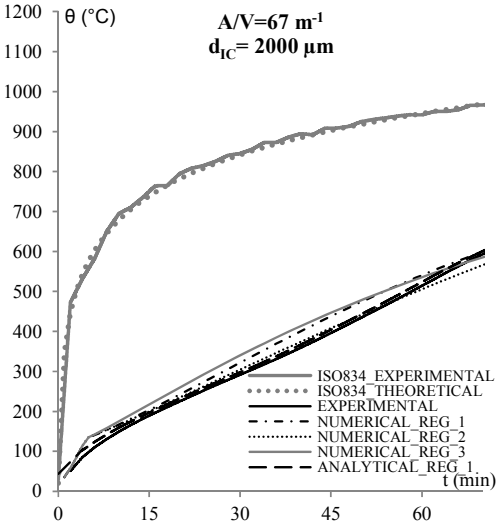
θ (°C)
A/V=67 m-1
dIC= 2000 µm
ISO834_EXPERIMENTAL
ISO834_THEORETICAL
EXPERIMENTAL
NUMERICAL_REG_1
NUMERICAL_REG_2
NUMERICAL_REG_3
ANALYTICAL_REG_1
t (min)

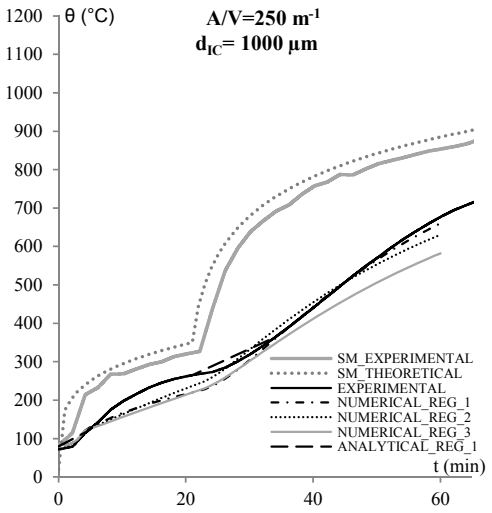
θ (°C)
A/V=250 m-1
dIC= 1000 µm
SM_EXPERIMENTAL
SM_THEORETICAL
EXPERIMENTAL
NUMERICAL_REG_1
NUMERICAL_REG_2
NUMERICAL_REG_3
ANALYTICAL_REG_1
t (min)

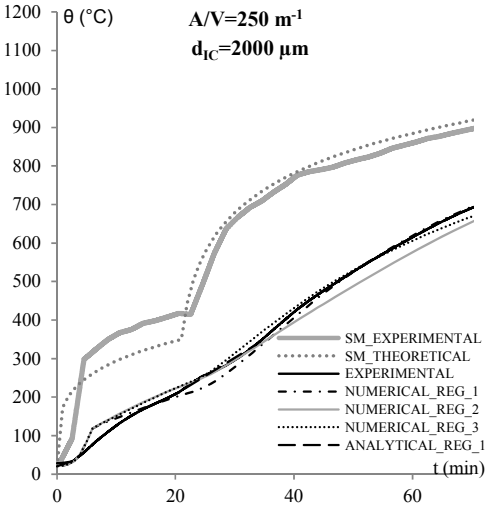
θ (°C)
A/V=250 m-1
dIC=2000 µm
SM_EXPERIMENTAL
SM_THEORETICAL
EXPERIMENTAL
NUMERICAL_REG_1
NUMERICAL_REG_2
NUMERICAL_REG_3
ANALYTICAL_REG_1
t (min)

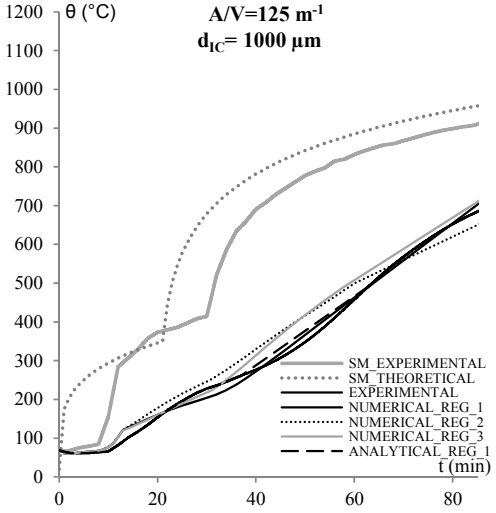
θ (°C)
A/V=125 m-1
dIC= 1000 µm
SM_EXPERIMENTAL
SM_THEORETICAL
EXPERIMENTAL
NUMERICAL_REG_1
NUMERICAL_REG_2
NUMERICAL_REG_3
ANALYTICAL_REG_1
t (min)

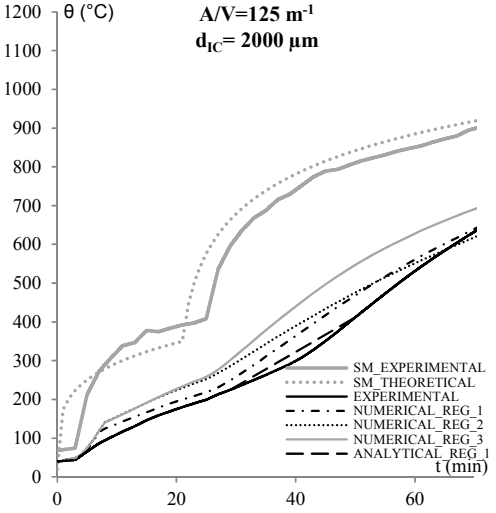
θ (°C)
A/V=125 m-1
dIC= 2000 µm
SM_EXPERIMENTAL
SM_THEORETICAL
EXPERIMENTAL
NUMERICAL_REG_1
NUMERICAL_REG_2
NUMERICAL_REG_3
ANALYTICAL_REG_1
t (min)

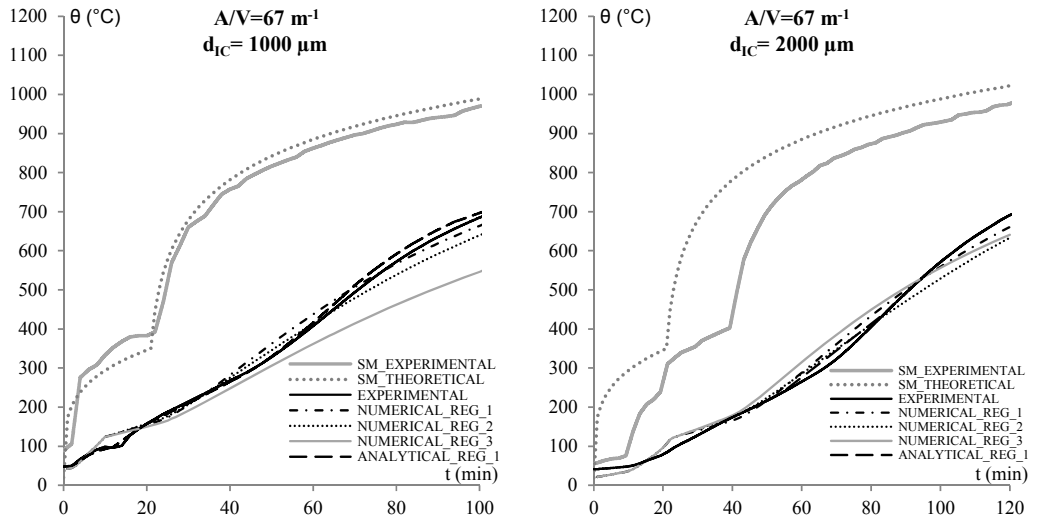

Fig.D.1- Comparison between experimental and simulated results for ISO834 and for Smouldering curves.

The Figure D.1 confirmed the results obtained for 1500 µm samples; in particular there is a good agreement between the experimental curve and the numerical simulation with REG_1; a slight underestimation of the temperature is observed, considering REG_2 and REG_3 in the second phase of the test. A good agreement is also obtained between the experimental and analytical method curves.

Matlab input file for regression

Regress

Multiple linear regression

Syntax

b=regress(y,X)

[b,bint]=regress(y,X)

[b,bint,r]=regress(y,X)

[b,bint,r,rint]=regress(y,X)

[b,bint,r,rint,stats]=regress(y,X)

[...] = regress(y,X,alpha)

Description

b = regress(y,X) returns a p*-by-1 vector b of coefficient estimates for a multilinear regression of the responses in y on the predictors in X. X is an* n*-by-*p *matrix of* p *predictors at each of* n *observations. y is an* n*-by-1 vector of observed responses.*

regress treats NaNs in X or y as missing values, and ignores them.

If the columns of X are linearly dependent, regress obtains a basic solution by setting the maximum number of elements of b to zero.

[b,bint] = regress(y,X) returns a p*-by-2 matrix bint of 95% confidence intervals for the coefficient estimates. The first column of bint contains lower confidence bounds for each of the* p *coefficient estimates; the second column contains upper confidence bounds.*

If the columns of X are linearly dependent, regress returns zeros in elements of bint corresponding to the zero elements of b.

[b,bint,r] = regress(y,X) returns an n*-by-1 vector r of residuals.*

[b,bint,r,rint] = regress(y,X) returns an n*-by-2 matrix rint of intervals that can be used to diagnose outliers. If the interval rint(i,:) for observation i does not contain zero, the corresponding residual is larger than expected in 95% of new observations, suggesting an outlier.*

In a linear model, observed values of y are random variables, and so are their residuals. Residuals have normal distributions with zero mean but with different variances at different values of the predictors. To put residuals on a comparable scale, they are "Studentized," that is, they are divided by an estimate of their standard deviation that is independent of their value. Studentized residuals have t *distributions with known degrees of freedom. The intervals returned in rint are shifts of the 95% confidence intervals of these* t *distributions, centered at the residuals.*

[b,bint,r,rint,stats] = regress(y,X) returns a 1-by-4 vector stats that contains, in order, the R^2 *statistic, the* F *statistic and its* p *value, and an estimate of the error variance.*